

Modelling and predicting properties of polymers in the amorphous glassy state

Citation for published version (APA):

Vleeshouwers, S. M. (1993). *Modelling and predicting properties of polymers in the amorphous glassy state*. [Phd Thesis 1 (Research TU/e / Graduation TU/e), Chemical Engineering and Chemistry]. Technische Universiteit Eindhoven. <https://doi.org/10.6100/IR395494>

DOI:

[10.6100/IR395494](https://doi.org/10.6100/IR395494)

Document status and date:

Published: 01/01/1993

Document Version:

Publisher's PDF, also known as Version of Record (includes final page, issue and volume numbers)

Please check the document version of this publication:

- A submitted manuscript is the version of the article upon submission and before peer-review. There can be important differences between the submitted version and the official published version of record. People interested in the research are advised to contact the author for the final version of the publication, or visit the DOI to the publisher's website.
- The final author version and the galley proof are versions of the publication after peer review.
- The final published version features the final layout of the paper including the volume, issue and page numbers.

[Link to publication](#)

General rights

Copyright and moral rights for the publications made accessible in the public portal are retained by the authors and/or other copyright owners and it is a condition of accessing publications that users recognise and abide by the legal requirements associated with these rights.

- Users may download and print one copy of any publication from the public portal for the purpose of private study or research.
- You may not further distribute the material or use it for any profit-making activity or commercial gain
- You may freely distribute the URL identifying the publication in the public portal.

If the publication is distributed under the terms of Article 25fa of the Dutch Copyright Act, indicated by the "Taverne" license above, please follow below link for the End User Agreement:

www.tue.nl/taverne

Take down policy

If you believe that this document breaches copyright please contact us at:

openaccess@tue.nl

providing details and we will investigate your claim.

**Modelling and Predicting
Properties of Polymers
in the Amorphous Glassy State**

Cover: The upper surface represents the calculated pVT behaviour of an amorphous polymer. The lower surface describes the theoretical equilibrium situation.

Omslag: Het bovenste vlak geeft het berekende pVT-gedrag weer van een amorf polymeer. Het onderste vlak beschrijft de theoretische evenwichtssituatie.

Modelling and Predicting Properties of Polymers in the Amorphous Glassy State

PROEFSCHRIFT

ter verkrijging van de graad van doctor aan de
Technische Universiteit Eindhoven, op gezag van
de Rector Magnificus, prof. dr. J.H. van Lint,
voor een commissie aangewezen door het College
van Dekanen in het openbaar te verdedigen op
dinsdag 11 mei 1993 om 16.00 uur

door

Servatius Maria Vleeshouwers
geboren te Schaesberg

Dit proefschrift is goedgekeurd door

de promotoren : prof. R. Simha
prof. dr. P. J. Lemstra
en de copromotor : dr. E. L. F. Nies

Het in dit proefschrift beschreven onderzoek werd mogelijk gemaakt door ondersteuning door de Stichting Polymer Blends ('SPB').

...Und man siehet die im Lichte
Die im Dunkeln sieht man nicht.

B. Brecht

Contents

1. Introduction	
1.1 The glassy state	1
1.2 Objectives	7
1.3 Survey	8
1.4 References	8
2. The Holey-Huggins equation of state theory: polymer melts and glasses	
2.1 Introduction	11
2.2 The partition function	11
2.3 Thermodynamic properties	13
2.4 Equation of state of glasses	17
2.5 Description of equation of state data	20
2.6 Conclusions	22
2.7 References	23
3. The glass transition and relaxation behaviour in the glassy state	
3.1 Introduction	25
3.2 Theories for the glass transition	26
3.3 Theories for relaxation behaviour	31
3.4 Conclusions	39
3.5 References	40

4.	The mobility of polymer melts	
4.1	Introduction	45
4.2	The pressure dependence of mobility	45
4.3	A modified Fulcher-Tammann-Hesse equation	47
4.4	Applications of the modified FTH	49
4.5	Conclusions	58
4.6	References	59
5.	The stochastic glass formation theory	
5.1	Introduction	61
5.2	The stochastic theory	62
5.3	Basic simulations	69
5.4	Conclusions	73
5.5	References	73
6.	Results of the stochastic glass formation theory	
6.1	Introduction	75
6.2	Temperature and pressure jumps	75
6.3	Cooling and heating experiments	82
6.4	The influence of pressure	90
6.5	The dynamic bulk compressibility	96
6.6	Dynamic light scattering	98
6.7	Enthalpy, entropy and density fluctuations	100
6.8	The molar mass dependence of T_g	106
6.9	The influence of the model parameters	107
6.10	Conclusions	112
6.11	References	114

7.	Positron annihilation spectroscopy	
7.1	Introduction	117
7.2	Positron annihilation spectroscopy	118
7.3	Positron annihilation in polymers	119
7.4	Calculation of cluster size distributions	122
7.5	Analysis of experimental data	130
7.6	Results of calculations	133
7.7	Conclusions	140
7.8	References	142
8.	Outstanding problems	145
	Summary	149
	Samenvatting	153
	Nawoord	157
	Curriculum vitae	159

Chapter 1

Introduction

1.1 The glassy state

The glassy state is in many cases the only state important for applications, especially for amorphous polymers. Mechanical and volumetric properties of the materials are derived from the glassy state. However, it has long been recognized that the conditions under which the glass is formed from the melt, strongly influence the properties of the polymer glass. It is therefore essential to gain understanding on the formation of a glass from the melt. As a consequence, in past years many publications on the subject of polymer glasses have been published (see e.g. ref. 1 and references therein). Except for a fundamental interest in knowledge of parameters that influence the glassy state, also the importance for applications like precision injection moulding and injection moulding simulations is obvious. These latter examples indicate possible applications of the work presented here², moreover because in this work the emphasis will lie on volumetric properties and their relation to formation history.

In the discussion of glasses and the glass transition a few terms play an important role. A *melt* is the state in which equilibrium is attained within the experimental time scale, this in contrast to a *glass*, in which this is not the case. Figure 1.1 illustrates schematically the formation of a glass starting from the melt. If a (polymer) system is cooled from a temperature T_1 in the melt (or isothermally pressurized, which will not be supposed here), then in a certain region the system can not attain (full) equilibrium

any more due to relatively long relaxation times. Further cooling to a temperature T_2 will even further increase the molecular relaxation times, thus enlarging the deviations with equilibrium. The now formed material is a glass. If the trajectory from melt to glass is followed during cooling many properties usually change in a narrow region. This quite sudden transition is called the *glass transition*, at the corresponding *glass transition temperature* T_g . If properties of the glass are monitored e.g. at constant p and T , one can usually observe a slow change in time of these properties. This change is the consequence of the non-equilibrium state, which, by definition, has a higher free energy than the equilibrium state. The system tends to change towards the equilibrium. This process is called *physical aging*. Of course no chemical changes occur during physical aging. Bringing the system back to the temperature T_1 by heating results in a melt with exactly the same properties as at the start of the experiment. Whether the glass can eventually reach the equilibrium state as a result of physical aging (if necessary after an extremely long time) is subject to discussion.

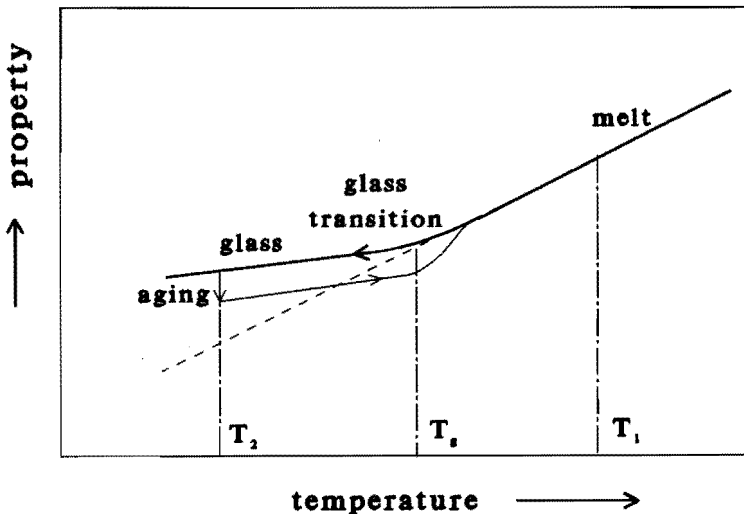


Figure 1.1. Schematic illustration of the formation of a glass and of physical aging.

For a particular polymer, T_g is not fixed. For example, if a glass is formed by cooling, T_g depends on the *cooling rate*, see e.g. ref. 3. Also, if the *pressure* is increased, T_g shifts to higher temperatures, see e.g. ref. 4. The dependence of T_g on pressure and cooling rate already indicates that the particular way in which a glass is formed determines the properties of the glass.

Because many properties change quite suddenly at T_g , the transition temperature can be determined in various ways. One of the most fundamental ways is by observing the *specific volume*. The T_g can be defined, based on dilatometry experiments, as the temperature of the intercept of the tangents at the glass and melt part of the V-T-curve. Volume aging even persists at temperatures far below T_g ⁵⁻⁷. It can also be seen that the above definition of T_g by taking the intercept of the tangents, results in a change of T_g during aging.

The *enthalpy* follows the same general trends as the volume in the case of glass formation. Usually differential scanning calorimetry (DSC) is used to measure the derivative of the enthalpy with respect to time, i.e. a heat flow, which at constant heating rate is proportional to the specific heat c_p . Typically the scanning rates used in DSC experiments are an order of magnitude higher than used in dilatometry (e.g. 10 K/min compared to 1 K/min). T_g 's measured by DSC have no direct correspondence with the dilatometric T_g . For example, the volumetric T_g increases with increasing pressure, whereas the enthalpic T_g is almost independent of formation pressure^{8,9}. DSC data suggest that with increasing pressure $\Delta H = H_{\text{glass}}(p) - H_{\text{glass}}(p=0)$ first shows a slight minimum before it starts increasing with increasing pressure⁸.

Usually, DSC traces are obtained in heating experiments. This is therefore a convenient way to study effects of physical aging on the polymer, because the difference in c_p between a particular glass and the 'reference' melt is measured.

With small-angle X-ray scattering (SAXS), neutron scattering and light scattering *density fluctuations* can be measured. When a polymer is cooled to temperatures below T_g , density fluctuations behave as depicted in figure 1.1. Physical aging has also been studied by SAXS for several polymers¹⁰⁻¹³. It has been noticed that the aging of density fluctuations is not proportional to volume or enthalpy aging^{12,14}.

Using positron annihilation spectroscopy, the glass transition is marked by a sudden change in the temperature dependence of the *o-positronium lifetime* (schematically depicted again in figure 1.1). The behaviour of the *o-positronium intensity* at T_g is different in nature, and generally does not have a clear break at T_g . Positron annihilation spectroscopy is used to study both the (average) size and the concentration of molecular voids. In chapter 7 experimental results are related to the free volume extracted from a hole theory.

Also *mechanical properties*, such as the modulus E , the shear creep compliance $J(t)$, the stress relaxation modulus $G(t)$, the shear viscosity and their temperature coefficients change drastically at T_g . Physical aging can be studied very well by monitoring mechanical properties. Extensive studies have been performed (see e.g. ref. 15). In general the modulus increases and the compliance decreases. Studying aging of a polyimide, Vendetti and Gillham showed that isothermal aging influences only part of the relaxation time spectrum, namely only those relaxation times that, at that temperature, are comparable or shorter than experimental times⁷. Although the issue of aging of mechanical properties is not going to be addressed in this work, an illustration will be presented that shows that the relation between relaxation of different properties is not straightforward. It has been shown that application of large stresses (compression, shear or extension) influences aging processes. Struik¹⁵ showed that large stresses enhance creep, but, at the same time decrease the dependence of mechanical properties, denoted by a_t , on the aging time t_e , i.e. the shift rate = $d(\log a_t)/d(\log t_e)$ decreases ('erasure' of physical aging, or 'rejuvenation').

This behaviour is general for polymers¹⁵ and has been explained by enhanced segmental motion, which is not related to changes in the macroscopic volume occurring during the mechanical experiments¹⁵⁻²⁰. However, Santore et al.²¹ showed that volume aging after a temperature jump ('thermal volume aging') was not influenced by the application of torsional strains. These strains induced a fast-relaxing volume deformation ('mechanical volume aging'), superimposed on the thermal volume aging. Santore et al.²¹ concluded that different mechanisms rule the thermal and mechanical volume aging, and that mechanical stimuli do not influence the thermodynamic state of the glass. Rejuvenation, therefore, was not believed to occur.

The last property mentioned to study the glass transition is *dielectric relaxation* in which the dielectric permittivity is measured. Usually ϵ'' , the loss part, which exhibits a maximum around T_g , is studied. Only sparse aging studies by dielectric relaxation have been reported^{22,23}.

The glass transition, which is related to relaxations and rearrangements of larger parts of the chain is also denoted as the α transition. The β transition has been related to movements of small chain parts (a few segments) or side groups²⁴. The frequency of the β transition has an Arrhenius like temperature dependence. It has been found that at high frequencies both the α and the β transition shift to higher temperatures, the β transition at a faster rate. At a certain temperature (and frequency) the α transition merges with the β transition²⁴. Due to the nature of the β transition, aging effects loose their importance at temperatures below the β transition. It has been shown^{7,15} that aging both above and below the β transition temperature does not influence the position of the β transition.

In case of blends, the location of the glass transition(s) depends on composition. In immiscible blends two T_g 's are found, (practically) equal to the T_g 's of the pure components. If miscibility improves, the T_g 's shift towards each other. In complete miscible blends one T_g is observed which can be, however, very broad²⁵. This is related to the presence of composi-

tion fluctuations that are always present as can be shown from a thermodynamic point of view. The presence of concentration fluctuations can be considered to result in a whole range of T_g 's. Care has to be taken to draw conclusions about (im)miscibility of a particular system. Depending on the used technique different results can be obtained. For example the system polystyrene / poly(2,6-dimethyl phenylene oxide) is found to have one T_g using differential scanning calorimetry (DSC), and two T_g 's using dynamic mechanical testing^{26,27}. The scales of the processes studied can determine whether or not one finds two T_g 's.

For miscible blends the composition dependence of T_g has been studied extensively (see for a review ref. 28). To describe this dependence several phenomenological equations have been proposed. Theories have been proposed to link T_g to molecular parameters in the blend, such as the Flory-Huggins interaction parameter χ^{29} , to entropy^{30,31}, to enthalpy³² or to molecular interaction contacts³³.

The existence of the glass transition has been explained by several, sometimes (seemingly) contradictory, theories. By one group of theories the glass transition has been considered to be (related to) a phase transition (see e.g. Gibbs and DiMarzio^{34,35}, Cohen and Grest^{36,37}). By other theories the T_g was thought to be the result of a gradual increase of relaxation times (see e.g. Jäckle³⁸, Palmer³⁹, Leuthusser⁴⁰ and Bengtzelius et al.⁴¹). Besides the location of the T_g , also the occurrence of relaxation effects in the glass (physical aging) is an important issue and has drawn extensive attention. The relaxation behaviour of polymer glasses has been analyzed with several theories. In these relaxation theories especially the methods for description of mobility and for the representation of a relaxation time distribution are important aspects. In phenomenological theories the *description* of the relaxation behaviour in non-equilibrium glassy systems is being pursued. First the *dependence of relaxation times on temperature and/or actual structure* has to be defined. For an accurate description of complex relax-

ation behaviour also a *distribution of relaxation times* has to be adopted. In molecular kinetic theories the relaxation behaviour is related to molecular processes underlying the relaxation behaviour and often theoretical justification for the phenomenological equations can be found. Parameters in these theories usually have a physical meaning. However, in applications the values of the parameters are not extracted from the physical meaning but are fitted to experimental data, thus making these theories equal to phenomenological theories. In this work we approach the phenomena of the glass transition and physical aging from a description of the melt. This allows us to use parameters determined in the melt, which from a thermodynamic point of view, is characterized unambiguously. Furthermore, the influence of formation history can be included in a natural way. The RSC theory⁴² (after Robertson, Simha and Curro) is considered to form a promising basis and is also appealing since the input parameters are derivable from independent measurements. It has been extended and modified in this work to simulate polymer glasses and relaxation processes with special attention to the dependence on formation history, retracing the glass to the equilibrium melt state. Except for scientific importance, a theory that correlates the properties of the glassy state to the polymer melt is also of great importance in applications for e.g. injection moulding simulation and the study of dimensions and dimensions stability in precision injection moulding.

1.2 Objectives

The objectives of this thesis are a theoretical analysis of the glass transition and the glassy state, starting from the equilibrium. We want to relate (the properties of) the glassy state to the melt with the formation history as an important factor determining the nature of the glass. Furthermore, we also want to include physical aging effects.

1.3 Survey

In chapter 2 the description of the equation of state of polymer melts with the HH-theory will be recapitulated. The free volume and free volume fluctuations defined in this theory are input parameter for the glass formation theory. Also a quasi-equilibrium approach of the polymer glass with the HH-theory will be presented. In chapter 3 a survey will be given of theories that describe and predict the glass transition and relaxation phenomena in glasses. In chapter 4 the relation between mobility and free volume, temperature and pressure is closely examined and a new relation is presented covering extensive data sets. This relation is also necessary input for the glass formation theory. In chapter 5 the development of the glass formation theory from the RSC theory is presented. In chapter 6 results, obtained with the glass simulation theory are presented. Finally, in chapter 7, the presence of molecular voids and their size distribution is approached from two opposite sides: theoretically, based on the HH-theory, and experimentally, using positron lifetime spectroscopy.

1.4 References

1. G. B. Kenna, in *Comprehensive Polymer Science*, vol. 2, Pergamon Press, Oxford, 1989.
2. G. G. J. Schennink, *On the dimensional stability of injection moulded, amorphous thermoplastic products*, report, Eindhoven, 1992.
3. R. Greiner and F. R. Schwarzl, *Rheol. Acta*, **23**, 378 (1984).
4. K. H. Hellwege, W. Knappe and P. Lehmann, *Kolloid.-Z. u. Z. Polym.*, **183**, 110 (1962).
5. A. J. Kovacs, *J. Polym. Sci.*, **30**, 131 (1958).
6. H. H. D. Lee and F. J. McGarry, *J. Mac. Sci.-Phys.*, **29**, 11 (1990).

7. R. A. Venditti and J. K. Gillham, *J. Appl. Polym. Sci.*, **45**, 1501 (1992).
8. A. Weitz and B. Wunderlich, *J. Polym. Sci., Polym. Phys. Ed.*, **12**, 2473 (1974).
9. I. G. Brown, R. E. Wetton, M. J. Richardson and N. G. Savill, *Polymer*, **19**, 659 (1978).
10. J. H. Wendorff, *J. Polym. Sci., Polym. Lett.*, **17**, 765 (1979).
11. J. J. Curro and R.-J. Roe, *J. Polym. Sci., Polym. Phys. Ed.*, **21**, 1785 (1983).
12. J. J. Curro and R.-J. Roe, *Polymer*, **25**, 1424 (1984).
13. R.-J. Roe and J. J. Curro, *Macromolecules*, **18**, 1603 (1985).
14. R.-J. Roe and J. J. Curro, *Macromolecules*, **16**, 428 (1983).
15. L. C. E. Struik, *Physical Ageing in Amorphous Polymers and Other Materials*, Elsevier, Amsterdam, 1978.
16. T. T. Wang, H. M. Zupko, L. A. Wyndon and S. Matsuoka, *Polymer Comm.*, **23**, 1407 (1982).
17. R. Pixa, B. Grisoni, T. Gay and D. Froelich, *Polym. Bull.*, **16**, 381 (1986).
18. T. L. Smith, G. Levita and W. K. Moonan, *J. Polym. Sci., Polym. Phys. Ed.*, **26**, 875 (1988).
19. J. Bartos, J. Müller and J. H. Wendorff, *Polymer*, **31**, 1678 (1990).
20. A. Lee and G. B. McKenna, *Polymer*, **31**, 423 (1990).
21. M. M. Santore, R. S. Duran and G. B. McKenna, *Polymer*, **32**, 2377 (1991).
22. E. Schlosser and A. Schönhals, *Polymer*, **32**, 2135 (1991).
23. A. Alegría, L. Goitlandia, I. Tellería and J. Colmenero, *J. Non-Cryst. Sol.*, **131-133**, 457 (1991).
24. J. Heijboer, in *Physics of Non-Crystalline Solids*, J. A. Prins, ed, North-Holland Publishing Company, Amsterdam, 1965, p. 231; J. Koppelmans, *ibid*, p. 255; G. P. Mihailov, *ibid*, p. 270.

25. H. A. Schneider, H.-J. Cantow, C. Wendland and B. Leikauf, *Makromol. Chem.*, **191**, 2377 (1990).
26. J. Stoelting, F. E. Karasz and W. J. MacKnight, *Polym. Eng. Sci.*, **10**, 133 (1970).
27. W. M. Prest and R. S. Porter, *J. Polym. Sci.: A2*, **10**, 1639 (1972).
28. H. A. Schneider, *Polymer*, **30**, 771 (1989).
29. X. Lu and R. A. Weiss, *Macromolecules*, **25**, 3242 (1992).
30. P. R. Couchman, *Polym. Eng. Sci.*, **27**, 618 (1987).
31. E. A. Di Marzio, *Polymer*, **31**, 2294 (1990).
32. P. C. Painter, J. F. Graf and M. M. Coleman, *Macromolecules*, **24**, 5630 (1991).
33. M.-J. Brekner, H. A. Schneider and H.-J. Cantow, *Polymer*, **29**, 78 (1988).
34. J. H. Gibbs and E. A. DiMarzio, *J. Chem. Phys.*, **28**, 373 (1958).
35. E. A. DiMarzio and J. H. Gibbs, *J. Chem. Phys.*, **28**, 807 (1958).
36. M. H. Cohen and G. S. Grest, *Phys. Rev. B*, **20**, 1077 (1979).
37. G. S. Grest and M. H. Cohen, *Phys. Rev. B*, **21**, 4113 (1980).
38. J. Jäckle, *Phil. Mag. B*, **44**, 533 (1981).
39. R. G. Palmer, *Adv. Phys.*, **31**, 669 (1982).
40. E. Leutheusser, *Phys. Rev. A*, **29**, 2765 (1984).
41. U. Bengtzelius, W. Götze and A. Sjölander, *J. Phys. C*, **17**, 5915 (1984).
42. R. E. Robertson, R. Simha and J. G. Curro, *Macromolecules*, **17**, 911 (1984).

Chapter 2

The Holey-Huggins equation of state theory: polymer melts and glasses

2.1 Introduction

For the development of the glass formation theory (chapter 5), the description of the equation of state (EoS) is necessary. To model the EoS of polymers a successful theory has been developed by Simha and Somcynsky¹. This SS theory is an example of a hole theory; it combines compressibility of lattice cells with the introduction of empty lattice sites. In this work the Holey-Huggins (HH) theory, related to the SS theory², is used. From a thermodynamic point of view the treatment of polymer melts is unambiguous. For the description of polymer glasses, additional assumptions have to be made due to the non-equilibrium state of glasses. Here, a treatment of glasses using a quasi-equilibrium approach due to McKinney and Simha³ will be presented. In this framework, instantaneous glasses (with no time dependence) can be treated.

2.2 The partition function

The HH theory² is a modification of the SS theory¹. In both theories a polymer (with volume V) has been modelled by a partly filled lattice. A

fraction y of all lattice sites is occupied by the segments of the total N molecules. A polymer molecule is considered to be a chain consisting of s segments, each occupying one lattice site. Of the total of $3s$ degrees of freedom per molecule, $3c$ are assumed to be external. So each segment has $3c/s=3c_s$ external or volume dependent degrees of freedom. It is assumed that c_s is a constant for a particular polymer.

The interaction between neighbouring segments on the lattice is described by a 6-12 Lennard-Jones potential⁴

$$\varepsilon(r) = \varepsilon^* \left[\left(\frac{r^*}{r} \right)^{12} - 2 \left(\frac{r^*}{r} \right)^6 \right] = \varepsilon^* \left[\left(\frac{v^*}{\omega} \right)^4 - 2 \left(\frac{v^*}{\omega} \right)^2 \right] \quad (2.1)$$

with ε^* , v^* and r^* the characteristic energy, volume and radius, respectively, belonging to the minimum in the potential curve, r the radius and ω the cell volume

$$\omega = \frac{yV}{Ns} \quad (2.2)$$

For the cell partition function instead of the sum of Lennard-Jones potentials a square well potential has been adopted⁴ with an infinite potential at $r > 2^{1/6} r^*$. As a modification of the SS theory, the HH theory² does not use the occupied fraction y as a structure parameter, but q , a measure for the number of external contacts a segment can make

$$q = \frac{(1-\alpha)y}{1-\alpha y} \quad \text{with} \quad \alpha = \frac{2}{z} \left[1 - \frac{1}{s} \right] \quad (2.3)$$

and the lattice coordination number $z=12$. The HH version reduces to the SS version for monomers ($s=1$) and for $q \rightarrow 1$ (high densities).

The volume available to a segment, i.e. the cell free volume v_f , depends on q via a linear averaging of the free length which is proportional to $\omega^{1/3}$

$$v_f = [q(\omega^{1/3} - 2^{-1/6}(v^*)^{1/3}) + (1-q)\omega^{1/3}]^3 \tag{2.4}$$

Now the configurational partition function Z reads

$$Z = g \cdot (v_f)^{cN} \cdot \exp\left[-\frac{E_0}{kT}\right] \tag{2.5}$$

with T the temperature, g a combinatorial term and E₀, the lattice energy of the system. For g one can write

$$g = (1-\alpha y)^{(1-\alpha y)/\gamma y} 2^{-N} N^N N_h^{Nh} [(z-1)/e]^{(s-1)Nh} \cdot (sN+N_h)^{N+N_h} y^{-N-Nh} (1-y)^{-(1-y)(sN+N_h)/y} \tag{2.6}$$

The relation of this combinatorial term to the expression for g by Huggins and Flory^{5,6} has been discussed in ref. 2. The expression for E₀ reads

$$E_0 = \frac{1}{2} q N ((z-2)s+2)\epsilon^* \left[A \left[\frac{v^*}{\omega} \right]^4 - 2B \left[\frac{v^*}{\omega} \right]^2 \right] \tag{2.7}$$

with A=1.011 and B=1.2049, evaluated for a face centred cubic lattice.

2.3 Thermodynamic properties

From the partition function the free energy A can be obtained:

$$A = -kT \ln Z \tag{2.8}$$

$$\begin{aligned} \frac{A}{NskT} &= \frac{\ln y}{s} + \frac{1-y}{y} \ln(1-y) - \frac{1-\alpha y}{\gamma y} \ln(1-\alpha y) - c_s \ln[v^* y \bar{V} (1-\eta)^3] \\ &+ \frac{(1-\alpha)yc_s}{2\bar{T}(1-\alpha y)} \left[\frac{A}{(y\bar{V})^4} - \frac{2B}{(y\bar{V})^2} \right] - \frac{3}{2} c_s \ln \left[\frac{2\pi M_0 RT}{(N_a h)^2} \right] \end{aligned} \tag{2.9}$$

with \bar{T} , \bar{V} the reduced temperature and volume respectively, which will be defined below. In general, for N particles, the pressure $p = -(\partial A / \partial V)_T$ can be written as:

$$p = - \left[\frac{\partial A}{\partial V} \right]_{T,y} - \left[\frac{\partial A}{\partial y} \right]_{T,V} \left[\frac{\partial y}{\partial V} \right]_T \quad (2.10)$$

At equilibrium it is assumed that the Helmholtz free energy is minimized with respect to the structure parameter y

$$\left[\frac{\partial A}{\partial y} \right]_{T,V} = 0 \quad (2.11)$$

Equation 2.10 then reduces to:

$$p = - \left[\frac{\partial A}{\partial V} \right]_{T,y} \quad (2.12)$$

In reduced form the equation of state (EoS) and minimization condition deduced from eqs. 2.11 and 2.12 obey a practical principle of corresponding states and are defined by

$$\frac{\bar{p}\bar{V}}{\bar{T}} = \frac{1}{(1-\eta)} + \frac{2(1-\alpha)y}{(1-\alpha y)\bar{T}(y\bar{V})^2} \left[\frac{A}{(y\bar{V})^2} - B \right] \quad (2.13)$$

and

$$1 - \frac{1}{s} + \frac{1}{y} \ln(1-y) - \frac{z}{2y} \ln(1-\alpha y) - \frac{\alpha z}{2} = \quad (2.14)$$

$$c_s \left[\frac{(3\eta-1+\alpha y)}{(1-\eta)(1-\alpha y)} + \frac{(1-\alpha)y}{2\bar{T}(1-\alpha y)^2(y\bar{V})^2} \left\{ 2B - \frac{3A}{(y\bar{V})^2} + 4\alpha y \left[\frac{A}{(y\bar{V})^2} - B \right] \right\} \right]$$

with $\eta = \frac{2^{-1/6}(1-\alpha)y}{(y\bar{V})^{1/3}(1-\alpha y)}$, $\bar{p} = \frac{p}{p^*}$, $\bar{V} = \frac{V}{V^*}$, $\bar{T} = \frac{T}{T^*}$. The scaling quantities p^*

(bar), V^* (cm^3/g) and T^* (K) can be expressed in ε^* (J/mol segment), v^* (m^3/mol segment), s (-) and c (-), with M_0 (kg/mol segment)

$$\begin{aligned} V^* &= \frac{v^*}{M_0} \cdot 10^3 \\ T^* &= \frac{((z-2)s+2)\varepsilon^*}{cR} \\ p^* &= \frac{((z-2)s+2)\varepsilon^*}{sv^*} \cdot 10^5 \end{aligned} \quad (2.15)$$

with R the gas constant and M_0 the molar mass of the segment. In the HH approach the number of segments s per molecule is set equal to the number of monomer units per molecule, resulting in the occupation of a lattice site by one monomer unit.

To obtain the scaling parameters volume data $V(T,p)$ of the equilibrium liquid are used. With the use of a multi parameter fitting program⁷ the scaling parameters are obtained by simultaneously solving eqs. 2.13 and 2.14 while minimizing the total sum of errors. Once the scaling parameters are known, other thermodynamic quantities can be derived from the free energy A , e.g.:

$$S = -(\partial A/\partial T)_V = -(\partial A/\partial T)_{y,v} - (\partial A/\partial y)_{v,T} (\partial y/\partial T)_V \quad (2.16)$$

$$U = A + TS \quad (2.17)$$

$$H = U + pV = A - T(\partial A/\partial T)_{y,v} - T(\partial A/\partial y)_{v,T} (\partial y/\partial T)_V + pV \quad (2.18)$$

$$p_i = (\partial U/\partial V)_T \quad (2.19)$$

$$c.e.d. = -U/V \quad (2.20)$$

$$\mu = (\partial A / \partial N)_{T,V} \quad (2.21)$$

$$\langle \delta N^2 \rangle / \langle N \rangle = \frac{kT}{N^2 (\partial \mu / \partial N)_{T,V,aff}} = -\frac{kT}{V^2} \left\{ \left[\frac{\partial p}{\partial V} \right]_{T,N,y} + \left[\frac{\partial y}{\partial V} \right]_{T,N,aff} \left[\frac{1}{V} \left[\frac{\partial A}{\partial y} \right]_{T,V,N} + \left[\frac{\partial p}{\partial y} \right]_{T,V,N} \right] \right\}^{-1} \quad (2.22)$$

$$\begin{aligned} \langle (\delta y_{eq})^2 \rangle &= \frac{kT}{(\partial^2 A / \partial y^2)_{N,T,V}} = \\ &= \frac{1}{Nsy^2} \left\{ 1 - \frac{1}{s} + \frac{1}{1-y} + \frac{2}{y} \ln(1-y) - \frac{\alpha z}{2} \left[1 + \frac{1}{(1-\alpha y)} \right] - \frac{z}{y} \ln(1-\alpha y) \right. \\ &\quad \left. + c_s \left[1 + \frac{\eta \{ 3\alpha y(1-\eta) + \frac{1}{3}(2+\alpha y)^2 \}}{(1-\alpha y)^2(1-\eta)^2} - \frac{(2+\alpha y)\eta}{(1-\alpha y)(1-\eta)} \right] \right\}^{-1} \\ &\quad \left. + \frac{y(1-\alpha)}{(1-\alpha y)^3 \tilde{T}(y\tilde{V})^2} \left[\frac{(10\alpha^2 y^2 - 15\alpha y + 6)A}{(y\tilde{V})^2} + 2(-3\alpha^2 y^2 + 3\alpha y - 1)B \right] \right\}^{-1} \quad (2.23) \end{aligned}$$

with S the entropy, U the energy, H the enthalpy, p_i the internal pressure, c.e.d. the cohesive energy density, μ the chemical potential, $\langle \delta N^2 \rangle / \langle N \rangle$ the density fluctuations, *aff* the affinity⁸, here defined as⁹ affinity $\equiv (\partial A / \partial y)_{T,V}$, and finally $\langle (\delta y_{eq})^2 \rangle$ the fluctuations in the occupied fraction y in a volume element containing $N_s = Ns$ segments. In equilibrium the minimization of A with respect to y has been performed. This results in the omission the factors containing $(\partial A / \partial y)_{V,T}$ in eqs. 2.16 and 2.18 and $(\partial A / \partial y)_{V,T,N}$ in eq. 2.22. The above equations will be used in the following chapters to discuss the formation of polymer glasses.

It has been shown that numerical differences between SS and HH are small regarding the description of EoS of state behaviour². Both theories successfully describe the EoS of polymer melts. Generally the values for y in the HH theory are smaller than in the SS theory². But although numerical values for y in the two theories are slightly different, general results and conclusions can be translated between SS and HH.

We now can define an order parameter h

$$h = 1-y \quad (2.24)$$

which is a measure for the structural disorder and can be identified with the free volume. The use of h to quantify the free volume is the basis for the work which will be presented in further chapters. It must be noted that by this definition the concept of free volume is defined unambiguously within the SS or within the HH theory.

2.4 Equation of state of glasses

In contrast to the equilibrium state, in the glass the minimization of A with respect to y is not applicable. Instead the complete equation, eq. 2.10 has to be used. Simha and Wilson¹⁰ have analyzed the glass transition within the scope of the SS theory, to investigate possible links between the T_g and scaling parameters. Trends with the reduced \hat{T}_g and h_{T_g} have been found. The reduced \hat{T}_g does not obey a corresponding state principle but increases with increasing T^* and T_g^{10} . Also the equilibrium free volume h_{T_g} at the glass transition temperature T_g , obtainable from the equilibrium conditions, increases with increasing T_g and T^* .

If the EoS of a glass is being considered, the equilibrium approach does not suffice. Nevertheless, in first approximation eq. 2.13 can be used to describe the glass. Analysing the contributions of cell volume and free lattice site volumes to a macroscopic thermal expansion, Simha et al.¹¹

concluded that both contributions play an important role, comparable to that in the equilibrium state. Only at extremely low temperatures the macroscopic volume expansion can be related to only cell expansion. Just below T_g the importance of cell and free lattice site volumes can be expressed in the frozen fraction F.F.:

$$F.F. = 1 - \frac{(dy/dT)_g}{(dy/dT)_l} \quad (2.25)$$

the subscripts g and l referring to the glass and the equilibrium liquid, respectively. In equilibrium $F.F.=0$, in a completely frozen glass $F.F.=1$. The frozen fraction $F.F.$ decreases with increasing T_g : for low- T_g polymers $F.F.$ is close to unity, for high- T_g polymers $F.F.$ reaches values less than 0.5.

From an analysis of poly(vinyl acetate) (PVAC) glasses with different formation histories, McKinney and Simha¹² have concluded that the free volume in the glassy state h_g is not constant and depends on pressure. For a glass which is a 'single physical substance' (for which any point in the glass can be reached from any other point without leaving the glassy state), it has been shown that h_g is independent of pressure¹².

An extensive analysis of the EoS of a glass has been given by McKinney and Simha³, using the more consistent approach based on the full EoS (eq. 2.10). In obtaining the results mentioned so far for glasses in this paragraph, the EoS (eq. 2.12) was used and y was estimated from p , T and the particular value of V . In this manner y is treated as an adjustable parameter, hence the name A.P. method. The more consistent approach is the use of eq 2.10 (which is derived from the partition function: the P.F. method). The requisite derivatives of A can be evaluated. The derivative $(\partial y/\partial V)_T$ can only be obtained if an explicit relation between y and V is assumed. McKinney and Simha³ used a second order polynomial $y=f(V, T)$, including cross terms. Using a set of experimental volume data $V(p, T)$ in the glass, the polynomial coefficients could be extracted by applying eq.

2.10. It is important to notice that the P.F. method can only be used for 'instantaneous' glasses, that is, for glasses in which no time dependency is relevant. The glass is treated as a quasi-equilibrium state: changes in p and/or T cause reversible changes in y and V . To apply the P.F. method, it is necessary to have volume data for several pressures and temperatures. This forms a serious restriction for the application of the P.F. method. To study e.g. aging with the P.F. method, the complete behaviour $V(p,T,t)$ of a particular aging glass must be known.

It is clear that the use of the P.F. method is restricted to cases where sufficient $V(T,p)$ data are available. For several PVAC glasses McKinney and Simha have extensively discussed the differences between the A.P. and P.F. method for e.g. S , H and p_i^3 . They concluded that in most cases a satisfying correspondence between the two methods is obtained. Both methods have also been applied to analyze theoretically simulated glasses (see chapters 5 and 6). In this case the goal is to obtain the volume V from y . Differences in volume calculated with the A.P. and P.F. methods are very small ($\Delta V < 10^{-5}$ cm³/g). This justifies the use of the A.P. method (eq. 2.12 or 2.13) instead of the laborious P.F. method to determine $V=f(y,T,p)$ in the framework of the stochastic theory presented in chapter 5. Furthermore, McKinney and Simha³ noted that in the hole theories for energy and related quantities only the configurational part is counted for, resulting in significantly too low values for both melt and glass.

Not only for instantaneous glasses, but also for the analysis of changes of e.g. V , H and density fluctuations during aging, the A.P. method has been used. Jain and Simha¹³ have applied this method to the aging of PVAC. From the experimental values of V during aging, using eq. 2.13 the value for y was calculated. Then, using the pertinent equations, the enthalpy and density fluctuations were calculated.

2.5 Description of equation of state data

For different polymers the scaling parameters of the HH theory are extracted from a selection of experimental pVT data. The scaling parameters are summarized in table 2.1. In all cases presented here the experimental data are described within the experimental accuracy.

Table 2.1. Scaling parameters of the HH theory, obtained from eqs. 2.13 and 2.14, for poly(vinyl acetate) (PVAC), polystyrene (PS), bisphenol-A polycarbonate (PC) and poly(methyl methacrylate) (PMMA).

	p^* (bar)	V^* (cm ³ /g)	T^* (K)	ϵ^* (J/mol)	$10^5 v^*$ (m ³ /mol)	c_s	range data	ref
PVAC	8954.8	0.80627	7988.0	2467.7	2.7559	0.37156	0-80MPa 328-373K	14
PS	6796.5	0.94679	9438.0	6689.6	9.8466	0.85284	0-160MPa 389-469K	15
PC	10004.7	0.79675	7928.5	20209.	20.237	3.07144	0-180MPa 417-610K	16
PMMA	8881.7	0.81985	8531.9	7280.2	8.1985	1.02650	0-120MPa 398-432K	17

McKinney and Simha³ and Jain and Simha¹³ have performed calculations on static and aging polymer glasses, respectively, using the SS theory and the A.P. as well as the P.F. method. In this work these calculations have been repeated for the HH theory to check the correspondence between SS and HH. As expected, similar results have been obtained as those of McKinney and Simha³ on non-aging PVAC glasses. However, repeating the calculations for PVAC during aging in ref. 13 (with the use of eq. 2.13 and eqs. 2.16, 2.18 and 2.22) yielded deviating results. In contrast to ref.

13, exactly the same reduced aging rate for H, S and density fluctuations as for V was obtained. This is illustrated in figure 2.1. Similar results were also obtained for PVAC at other temperatures and also for polystyrene (PS).

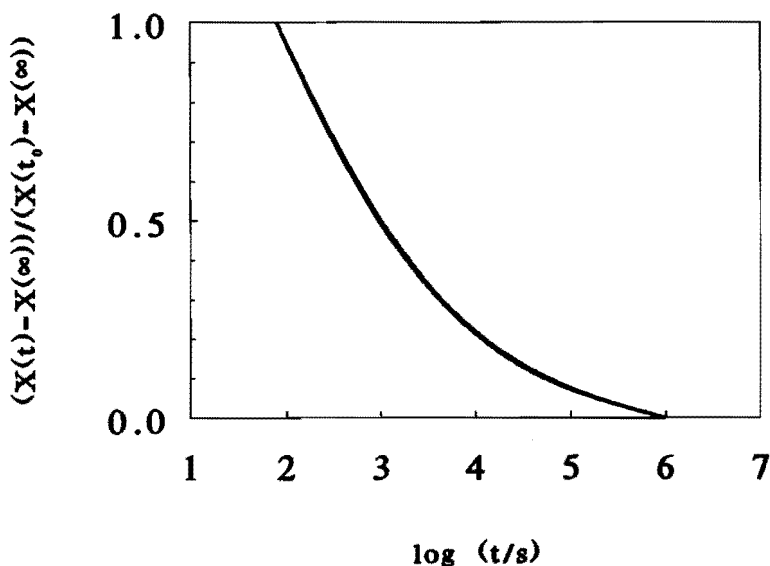


Figure 2.1. Calculations for PVAC at 25°C. Comparison of $(X(t) - X(\infty)) / (X(t_0) - X(\infty))$ versus time for X equal to V, S, H and density fluctuations, calculated from eq. 2.13 and eqs. 2.16, 2.18 and 2.22, respectively. All curves coincide. The absolute differences $X(t_0) - X(\infty)$ equal 0.0025 cm³/g, $8 \cdot 10^{-3}$ J/K mol, 2.44 J/mol, for V, S, H, respectively. The relative difference $(X(t_0) - X(\infty)) / X(t_0)$, with X the density fluctuations, equals 0.0046.

In the discussion of these discrepancies several remarks are pertinent. First, differences are not due to differences between SS and HH, because they are also found for the SS case. Second, the reported agreement with experiments of the slow aging of density fluctuations by Wendorff¹⁸ is open

to question. Jain and Simha express the aging of a quantity X as $R(t) = (X(t) - X(\infty)) / (X(t_0) - X(\infty))$. Wendorff uses the ratio $X(t)/X(t_0)$ to describe the aging of density fluctuations, which is expected to decrease only about 3% during the complete aging process. Thus the reported experimental data might not be detailed enough to allow comparison with theory. As a final point, similar calculations relating aging of V and H have been performed by Cowie et al.¹⁹. From experimental H data on PVAC the order parameter h was extracted, using the A.P. method. From the free volume h , the corresponding V was calculated. The same aging rate $R(t)$ for V and H was observed. Comparison of these calculations with experimental volume aging of PVAC^{20,21}, with the equilibrium value $V_{eq}(30^\circ\text{C}) = 0.8417 \pm 0.0001 \text{ cm}^3/\text{g}$ (figure 15, ref. 20), yields within experimental accuracy the same aging rate for V as for H . The use of the calculated theoretical equilibrium volume at 30°C ($0.8412 \text{ cm}^3/\text{g}$) led the authors to opposite conclusions¹⁹. This example shows that one has to be very careful when comparing data from different sources and extrapolating values to equilibrium. The difference between the theoretical and experimental equilibrium volume is smaller than the experimental accuracy with which the volume can be measured! It can be caused by only a very small difference between the samples but nevertheless result in completely different conclusions.

2.6 Conclusions

The HH theory (like the SS theory) successfully describes the configurational properties of the polymer melt^{2,10}. Generally in the glassy state the use of the equilibrium EoS (A.P. method) gives results which are in good agreement with results obtained from the more consistent method (P.F.) based on the full EoS. To describe the EoS of polymer glasses the occupied fraction y must be assumed temperature and pressure dependent.

In contrast to calculations shown in refs. 13 and 19, it was shown that the calculated aging of several quantities occurs at the same rate. Experimentally, differences in aging rates have been found (see chapter 1). This seems to indicate that the description of aging with only one parameter is not sufficient. In the frame of the free volume approach, this might indicate that except for the *average* free volume fraction y , also details of the free volume distribution might play a role in the hole theory, as was already pointed out by Olabisi and Simha¹⁷. This point of view is elaborated in the discussion of relaxation processes in chapter 5 and 6 and of positron annihilation spectroscopy in chapter 7.

2.7 References

1. R. Simha and T. Somcynsky, *Macromolecules*, **2**, 341 (1969).
2. E. Nies and A. Stroeks, *Macromolecules*, **23**, 4088 (1990).
3. J. E. McKinney and R. Simha, *Macromolecules*, **9**, 430 (1976).
4. I. Prigogine, *The Molecular Theory of Solutions*, North-Holland Publishing Company, Amsterdam, 1957
5. M. L. Huggins, *Ann. N. Y. Acad. Sci.*, **43**, 1 (1942).
6. P. J. Flory, *J. Chem. Phys.*, **10**, 51 (1942).
7. L. T. M. E. Hillegers, *The Estimation of Parameters in Functional Relationship Models*, thesis, Eindhoven, 1986
8. J. H. Wendorff and E. W. Fischer, *Kolloid-Z. u. Z. Polym.*, **251**, 876 (1973).
9. C. M. Balik, A. M. Jamieson and R. Simha, *Colloid Polym. Sci.*, **260**, 477 (1982).
10. R. Simha and P. S. Wilson, *Macromolecules*, **6**, 908 (1973).
11. R. Simha, J. M. Roe and V. S. Nanda, *J. Appl. Phys.*, **43**, 4312 (1972).
12. J. E. McKinney and R. Simha, *Macromolecules*, **7**, 894 (1974).

13. S. C. Jain and R. Simha, *Macromolecules*, **15**, 1522 (1982)
14. J. E. McKinney and M. Goldstein, *J. Res. Nat. Bur. Stand.-A. Phys. Chem.*, **78A**, 331 (1974).
15. A. Quach and R. Simha, *J. Appl. Phys.*, **42**, 4592 (1971).
16. P. Zoller, *J. Polym. Sci., Polym. Phys. Ed.*, **20**, 1453 (1982).
17. O. Olabisi and R. Simha, *Macromolecules*, **8**, 206 (1975).
18. J. H. Wendorff, *J. Polym. Sci., Polym. Lett.*, **17**, 765 (1979).
19. J. M. G. Cowie, S. Elliot, R. Ferguson and R. Simha, *Polym. Comm.*, **28**, 298 (1987).
20. A. J. Kovacs, R. A. Stratton and J. D. Ferry, *J. Phys. Chem.*, **67**, 152 (1963).
21. A. J. Kovacs, *Fortschr. Hochpol.-Forsch.*, **3**, 394 (1963).

Chapter 3

The glass transition and relaxation behaviour in the glassy state

3.1 Introduction

In the previous chapter we have discussed the equation of state (EoS) and other related thermal properties of polymer melts and glasses. So far the physical origin of the existence of a polymer glass has not been addressed. The onset of the glassy state, starting from the melt, is signalled by the position of the glass transition temperature. Furthermore a typical property of polymer glasses is the occurrence of physical aging or relaxation. In this chapter the start of the glassy state, i.e. the location of the glass transition temperature, and the relaxation in the glassy state will be discussed from a theoretical point of view. The reader is reminded of a few terms that play an important role in the discussion of glasses and the glass transition. A *melt* is the state in which equilibrium is attained in the experimental relevant time scale, this in contrast to the *glass*, in which this is not the case. In a certain region the system can not attain (full) equilibrium any more due to relatively long relaxation times. If the trajectory from melt to glass is followed during cooling many properties usually change in a narrow region. This quite sudden transition is called the *glass transition*, at the corresponding *glass transition temperature* T_g . If properties of the glass are monitored e.g. at constant p and T , one can usually observe a slow change in time of these properties. The system tends to change towards the equilibrium. This process is called *physical aging*.

3.2 Theories for the glass transition

The glass transition has been explained by several, sometimes contradictory, theories. The question whether the glass transition is a thermodynamic transition has been given much attention. It was proposed that there is a phase transition underlying the glass transition, which, theoretically, can be reached by infinitely slow cooling^{1,2}. Careful analysis of volume data left Rehage et al.^{3,4} no other choice than to conclude that the glass transition is not a true thermodynamic phase transition. In another approach the glass transition was regarded as a gradual freeze-in of molecular motions⁵, without relations to a thermodynamic transition. These different points of view are presented in more detail later in this paragraph.

The question of thermodynamics will be dealt with first. One can immediately conclude that the glass transition is not a first order transition. At such a transition the first derivatives of the free energy G with respect to p and T , i.e. V and S , show a discontinuity. That this is not the case is obvious from e.g. figure 1.1. Whether a second order transition is observed has been analyzed extensively (see e.g. refs. 3 and 4). According to Ehrenfest⁶ the following relations must hold along the transition line at a second order transition

$$\left[\frac{dp}{dT} \right]_{tr} = \frac{\Delta\alpha^*}{\Delta\kappa^*} \quad (3.1)$$

$$\left[\frac{dp}{dT} \right]_{tr} = \frac{\Delta c_p}{T\Delta\alpha^*} \quad (3.2)$$

with $\Delta\alpha^* = \alpha_l^* - \alpha_g^*$, $\Delta\kappa^* = \kappa_l^* - \kappa_g^*$, $\Delta c_p = c_{p,l} - c_{p,g}$, α^*/V , κ^*/V and c_p the thermal expansion, compressibility and specific heat, respectively. The subscripts l and g refer to the melt and glass state, respectively.

Equations 3.1 and 3.2 are often combined to

$$\frac{\Delta c_p \Delta \kappa^*}{T(\Delta \alpha^*)^2} = 1 \quad (3.3)$$

known as the Prigogine-Defay ratio. Equations 3.1 and 3.2 express that states on the transition line $T_{tr}(p_{tr})$ can be reached along a path through the melt or through the glass. Both trajectories should result in the same values for the volume V (eq. 3.1) and for the entropy S (eq. 3.2), since on both sides thermodynamic equilibrium is supposed. Breuer and Rehage³ show that in the case of atactic polystyrene, the most extensively studied polymer, along the transition line the value of the ordering parameter changes^{3,4} (surprisingly eq. 3.3 still holds due to the fact that the right hand side of eqs. 3.1 and 3.2 give the same values, however not the value for $(dp/dT)_{tr}$ found experimentally). This led to the assumption that the glass transition is governed by an extra internal parameter or order parameter. This approach results in equations similar to those of Ehrenfest

$$\left[\frac{dp}{dT} \right]_{tr} = \frac{\Delta \alpha^*}{\Delta \kappa^*} - \frac{1}{\Delta \kappa^*} \left[\frac{\partial V}{\partial \zeta} \right]_{T,p} \left[\frac{d\zeta}{dT} \right]_{tr} \quad (3.4)$$

$$\left[\frac{dp}{dT} \right]_{tr} = \frac{\Delta c_p}{T \Delta \alpha^*} - \frac{1}{\Delta \alpha^*} \left[\frac{\partial S}{\partial \zeta} \right]_{T,p} \left[\frac{d\zeta}{dT} \right]_{tr} \quad (3.5)$$

It is clear that if the ordering parameter ζ is constant along the transition line, viz. $(d\zeta/dT)_{tr}=0$, eqs. 3.4 and 3.5 reduce to eqs. 3.1 and 3.2. So one cannot distinguish between a second order transition and a freeze-in of the ordering parameter along the transition boundary. If the glass transition is described by more than one ordering parameter, the Prigogine-Defay ratio (eq. 3.3) changes in the inequality^{7,8}

$$\frac{\Delta c_p \Delta \kappa^*}{TV(\Delta \alpha^*)^2} \geq 1 \quad (3.6)$$

It was concluded from the analysis of relaxation experiments that the vitrification of polystyrene has to be described with more than one ordering parameter ζ .

The consequences of this Ehrenfest analysis for the treatment of glass formation with a hole theory have been thoroughly discussed by Quach and Simha⁹ and later by McKinney and Simha¹⁰. The reader is reminded that in the hole theory the polymer is modelled on a lattice with vacant lattice sites. The fraction of empty lattice sites, called the free volume fraction h , plays the role of the order parameter. For instance the glass transition cannot be considered to be an iso-free volume state, since the ordering parameter h is not found to be constant along the transition boundary. The inadequate description of the glass transition as an event governed by a single ordering parameter is also supported by the non-validity of the first Ehrenfest relation (eq. 3.1) at T_g for a variety of polymers (see e.g. Goldstein¹¹).

Already earlier Simha and Boyer¹² had argued that, based on the free volume concept $f=(V-V_0)/V$, with V the volume and V_0 the occupied volume ($=V(T=0K)$), and assuming that the glass transition is an iso-free volume transition, the value for $(\alpha_1-\alpha_g) \cdot T_g$ should be constant for different polymers and equal to the free volume fraction f_g at the glass transition. Although one should take into account the sensitivity of thermal expansion coefficients and also experimental accuracy, discrepancies between the experimental value for $(\alpha_1-\alpha_g) \cdot T_g$ and the calculated free volume were found. And furthermore the term $(\alpha_1-\alpha_g) \cdot T_g$ was found not to be constant. The authors concluded that this might be due to the assumed complete freeze-in of the free volume in the glass, and the use of only one order parameter to describe the glass.

Based on a lattice consisting of polymer segments and empty lattice sites, Gibbs and DiMarzio^{1,2} predicted for polymer chains a second order phase transition, which was identified with the glass transition at infinitely slow cooling. They showed that the phase transition temperature T_2 increases with increasing chain stiffness and chain length, and decreasing free volume. The vanishing entropy S at T_2 also clarified the apparent Kauzmann paradox¹³. According to Kauzmann the entropy of the liquid phase obtained by extrapolation to temperatures below T_g , threatens to become negative, which is of course not possible. Later DiMarzio et al. showed that the transition at T_2 obeys as expected the Ehrenfest relations¹⁴ (eqs. 3.1 and 3.2). The transition temperature T_2 was shown to increase with increasing pressure to an asymptotic value at high pressures. Oels and Rehage¹⁵ concluded that the approach of Gibbs and DiMarzio was not contradicted by their analysis of the glass transition in the spirit of the Ehrenfest relations. They concluded that there are no objections to consider a phase transition at T_2 , corresponding to the lowest possible T_g .

Based on molecular dynamic simulations Cohen and Grest¹⁶ postulated the presence of liquid- and solid-like clusters as basic units in a free volume model. Surprisingly they concluded that the glass transition is most probably a first order transition. The fraction of liquid- and solid-like clusters was obtained from percolation theory. Below a critical value p_c , isolated clusters are found whereas above p_c the liquid-like clusters form a cluster from infinite size. In this way the communal entropy (the entropy associated with the accessibility of the total configurational volume) of the amorphous phase was determined. Later they developed a kinetic theory based on the cluster model¹⁷, stating that the observed T_g is a consequence of non equilibrium, which softens the sharp first order glass transition. The fraction liquid-like clusters is assumed to relax via a single relaxation time. Instead of the sharp changes that can be expected at a first order transition, a gradual transition, as found experimentally, was predicted. Similar con-

clusions concerning the existence of a phase transition were drawn by Kirkpatrick et al.¹⁸. with their droplet model, in which a typical size, or coherence length ξ of glassy droplets, is defined. This length ξ was found to diverge at an 'ideal structural glass transition' (compare with T_2) and to scale as $(T-T_\infty)^{-\nu}$. Donth¹⁹ estimated ξ , depending on the nature of the glass former, to be 1-2 nm.

In the mode coupling theory the glassy state is considered to be essentially an non-ergodic state. This can be thought of as the occurrence of relaxation times that are far longer than the experimental time scale^{20,21}. The breakdown of ergodicity arises from the strong correlation between density fluctuations^{22,23}. Using the mode-coupling theory (reviewed in ref. 5), the following features resembling experimentally found behaviour were predicted: a non-Arrhenius type of viscosity; a strongly non-exponential type of relaxation; a freeze-in of a large part of the density fluctuations at the glass transition; and both a fast and a slow relaxation process in the glass²⁴. Although agreement with computer simulation data was obtained²⁵, only qualitative agreement with experiments was established⁵. Especially the occurrence of a very sharp glass transition has led to a further modification of the theory²⁶.

A way of studying the glass transition that is still limited but has much potential is analysis of computer simulated glasses. One advantage is the possibility of getting microscopic information about the glass, such as a radial distribution function and chain conformations. Using the Monte Carlo method, only very small numbers of particles can be simulated, and no time evolution is possible (see, for example, Abraham²⁷ and Wittmann et al.²⁸). A glass transition, manifested by a sudden change of several quantities, has been observed. Rigby and Roe have simulated polymer chains using molecular dynamics²⁹⁻³¹. This method allows the study of the time evolution, but is restricted to very short times (in the simulations of Rigby

and Roe a time span in the order of 10^9 s was covered). They found a glass transition temperature, which increased with increasing chain length to an asymptotic value. No structural changes between the polymer below and above T_g were found.

In chapter 5 we treat the glass transition as the consequence of a gradual freeze-in of molecular mobility. No assumption about a phase transition at a temperature $T_2 < T_g$ is made.

3.3 Theories for relaxation behaviour

The relaxation behaviour in the glassy state has many different aspects, which can be described more or less successfully by different theories, such as phenomenological and molecular kinetic theories. Especially the methods for description of mobility and for the representation of a relaxation time distribution are important features of a theory. Often similar expressions appear in the phenomenological as well as in molecular dynamic theories.

In phenomenological theories only the *description* of the relaxation behaviour in non-equilibrium glassy systems is being pursued. The relaxation can be described with a time and temperature dependent relaxation function $\phi(t, T)$ that initially has a value $\phi(0, T) = 1$ and finally, after the new equilibrium has been obtained, $\phi(\infty, T) = 0$. The parameters which enter the equations of phenomenological theories do not necessarily have a physical meaning.

Two basic aspects characterize phenomenological relaxation theories. First the *dependence of relaxation times on temperature and/or actual structure* has to be defined. A relation that only includes structure dependence (via the free volume f) is the Doolittle equation³²

$$\tau = \tau_g \exp \left[\frac{B}{f} - \frac{B}{f_g} \right] \quad (3.7)$$

with B , f_g and τ_g constants. The relaxation time τ_g equals the relaxation time at reference state $T=T_g$, where $f=f_g$. The free volume f is defined by

$$f = \frac{V-V_0}{V_\infty} \quad (3.8)$$

with V the actual volume, V_0 the occupied volume and V_∞ the equilibrium volume. The value for V_0 does usually not depend on temperature and is determined via extrapolation. Several possible definitions of V_0 give rise to different values for the free volume. Thus the definition of free volume by eq. 3.8 is not always unambiguous. An equation that describes the relaxation time τ as a function of only temperature is the Fulcher³³-Tamman-Hesse³⁴ equation

$$\log \tau = A + \frac{B}{T-T_\infty} \quad (3.9)$$

This relation can be easily transformed to the well known relation proposed by Williams, Landel and Ferry^{35,36}

$$\tau = \tau_r \exp \frac{-c_1^g(T-T_g)}{c_2^g + T-T_g} \quad (3.10)$$

with τ_r , T_g , c_1^g and c_2^g constants. This equation, known as the WLF equation, is used to describe relaxation times in the equilibrium polymer. It can be derived from the Doolittle equation (eq. 3.7) with the extra assumption that at a temperature T_∞ the equilibrium free volume vanishes according to

$$f = f_g + \alpha_f(T - T_g) \tag{3.11}$$

and $T_\infty = T_g - f_g/\alpha_f$. Here α_f is the free volume thermal expansion coefficient. The WLF equation then reads

$$\tau = \tau_r \exp \left[\frac{-(B/f_g)(T - T_g)}{(f_g/\alpha_f) + T - T_g} \right] \tag{3.12}$$

with B a constant, usually set to unity. In the scope of the WLF theory it has been argued^{35,36} that at the glass transition temperature the free volume $f_g \approx 0.025$ is a typical value for different polymers although closer inspection reveals that this value is certainly not universal. The free volume expansion coefficient can be calculated from $\alpha_f \approx \alpha_l - \alpha_g$ and is typically $5 \cdot 10^{-4} \text{ K}^{-1}$, with α_l and α_g the thermal expansion coefficients in the melt and the glass, respectively. Combining the WLF equation, eq. 3.12, with the free volume as defined by the order parameter from the SS theory, Curro et al.³⁷ had to lift the assumption $B=1$.

A combined temperature- and structure-dependence of relaxation times has been found to be necessary to improve the description of the relaxation behaviour of non equilibrium systems. This was first proposed by Tool³⁸. The structure dependence was described in terms of the 'fictive temperature' T_f which was defined as the temperature of the equilibrium state that corresponds with the actual non-equilibrium state. Ritland³⁹ showed that one limitation of this assumption is formed by the postulated correspondence between the glassy state and a single equilibrium state. He observed that depending on the property (e.g. refractive index or volume), different fictive temperatures were obtained. Narayanaswamy⁴⁰ combined Tool's concept of fictive temperature with a memory effect which was related to the history of the glass.

The second basic aspect in phenomenological theories for the description of relaxation behaviour is the assumption of a *distribution of relaxation times*. Kovacs and coworkers^{41,42} have described the isothermal volume and enthalpy relaxation behaviour of poly(vinyl acetate) and polystyrene using a single relaxation time. For example, for volume relaxation

$$-\frac{d\delta}{dt} = \Delta\alpha q + \frac{\delta}{\tau} \quad (3.13)$$

with $\Delta\alpha = \alpha_l - \alpha_g$ and δ the deviation from equilibrium. The relaxation time τ was given by a Doolittle expression. By solving the differential eq. 3.13, Kovacs et al.^{41,42} have described isothermal volume and enthalpy aging after a single temperature jump. Furthermore the presence of a glass transition temperature during cooling (with a reasonable rate dependence) and a strong hysteresis during heating has been described. However, the extreme in volume after multiple temperature steps or the self accelerating process during a jump from a low to a higher temperature was not predicted. From this it was pointed out that a relaxation time distribution is necessary to describe such more complex behaviour.

In the KAHR model^{43,44} (after Kovacs, Aklonis, Hutchinson and Ramos) a discrete set of N relaxation times is used. Equation 3.13 then converts for each subsystem i into

$$-\frac{d\delta_i}{dt} = \Delta\alpha_i q + \frac{\delta_i}{\tau_i} \quad 1 \leq i \leq N \quad (3.14)$$

where $\sum_N \delta_i = \delta$ and $\sum_N d\delta_i = d\delta$. For example, in the description of poly(vinyl acetate)^{43,44}, a four decade wide two-block distribution was assumed, with $N=33$. To describe the relaxation time distribution all values $\tau_{i,r}$ ($1 \leq i \leq N$) at a reference temperature T_r have to be defined. Furthermore, the relaxation times τ_i were assumed to depend on temperature and actual free

volume. Both relaxation after single and multiple temperature steps and after finite heating and cooling rates have been discussed^{43,44}. The extreme after multiple jumps, non-linearity and asymmetry of relaxation has been described. An extension of the theory for combined pressure and temperature relaxation has also been presented⁴⁵. In the KAHR model an arbitrary distribution is defined. Alternatively the relaxation function $\phi(t,T)$ can be given by a Kohlrausch-Williams-Watts relation⁴⁶

$$\phi(t,T) = \exp \left[- \left[\frac{t}{\tau_r(T)} \right]^\beta \right] \tag{3.15}$$

with $\tau_r(T)$ a characteristic relaxation time, and β a constant, $0 < \beta \leq 1$. The width of the distribution of relaxation times is expressed by the exponent β . It is clear from eq. 3.15 that a single relaxation time governs the relaxation for $\beta=1$. Adapting smaller values for β a distribution of relaxation times is obtained. Keeping β constant during relaxation implies thermorheologically simple behaviour. The average relaxation time is

$$\langle \tau \rangle = \frac{\tau_r}{\beta} \Gamma \left[\frac{1}{\beta} \right] \tag{3.16}$$

with $\Gamma(x)$ the gamma function. Use of the KWW equation circumvents the necessity of an explicit definition of a distribution of relaxation times. It is known that the KWW equation can describe the distribution function in many different experiments.

The KAHR model is probably the best known phenomenological model. However, many other phenomenological models exist such as the models of Narayanaswamy⁴⁰, Moynihan⁴⁷, Struik⁴⁸, Matsuoka⁴⁹, Abe and Kakizaki^{50,51} and Tribone⁵². In these models, often more or less comparable assumptions are made.

In molecular kinetic theories the relaxation behaviour is related to molecular processes underlying the relaxation behaviour. Parameters in these theories can be attributed a physical meaning and in many cases the basic equations of phenomenological theories, i.e. expressions for relaxation times and distributions, can be derived from theory. In applications the values of the parameters are usually not extracted from independent experiments but are fitted to experimental data, thus making these theories in this respect equal to phenomenological theories. Subsequently, however, predictions can be extended to other properties.

Chow⁵³ has derived Moynihan's phenomenological equations, starting from a distribution of holes on a lattice⁵⁴, taking into account the entropy of mixing holes and polymer molecules. He showed⁵⁵ that relaxation following temperature up and down jumps and also following multiple temperature jumps for poly(vinyl acetate) could be described very well. By introducing a term for the work done by pressure or tension on the system a (nonlinear) pressure dependence was calculated. Interestingly, he also showed⁵³ that the rates of decay for density fluctuations and for volume relaxation are not the same. Density fluctuations were expected to relax slower than the free volume.

Adam and Gibbs⁵⁶ proposed a molecular kinetic theory based on the assumption of a phase transition at T_2 and derived an equation closely related to the WLF equation. They assumed that molecular relaxations are based on cooperative rearrangements of small regions (CRR's), containing z molecules, which can rearrange without influencing the surrounding regions. The value for z can change with temperature and generally increases with decreasing temperature. At T_2 , the lowest temperature at which configurational rearrangements are possible, z becomes equal the size of the whole sample. Based on this model an equation for the shift factor a_T ensues, closely related to the widely valid WLF equation. A functional dependence of the relaxation time on temperature as suggested

by the WLF equation was derived by Angell and Sichina⁵⁷ starting from the theory of Adam and Gibbs with the additional assumption that the configurational entropy vanishes at a temperature T_2 . The derivation of the WLF equation with this assumption was considered⁵⁶ to be in favour of the validity of the second order phase transition theory. Adam and Gibbs showed that the ratio T_g/T_2 is remarkably constant for a wide range of substances. This also verified the connection between T_g and T_2 . However, identifying T_2 with the temperature at which the WLF equation diverges, has to be done with care because of the uncertainty of such a far extrapolation.

Also Ngai and Rendell's coupling theory⁵⁸ is based on the Adam-Gibbs theory. By incorporating interactions between the CRR's Ngai et al. showed that the relaxation function of the KWW could be derived, with the strength of coupling $n=1-\beta$, β the KWW-parameter, and τ_r , the experimentally observable relaxation time, a function of n and temperature. The theory was used successfully for different systems⁵⁹⁻⁶², with n fitted to experimental relaxation curves, sometimes including a temperature dependence. The coupling model is possibly⁶² the only theory so far that can successfully describe the 'gap' in effective relaxation times close to equilibrium in temperature jump experiments from low to high temperature. Although the theory is based on molecular rearrangements, no physical quantities are used that can possibly be determined by independent techniques. In applications of the coupling theory n is treated as a fitting parameter. On a case-by-case basis the dependency of n on temperature and pressure is examined⁵⁹.

Matsuoka et al.⁶³ modified the Adam-Gibbs theory by introducing a size distribution of cooperative domains, which resulted in a better description of dielectric relaxation data at short times, compared to using a KWW equation. Equations that are practically equal to the KWW-equation have also been derived, starting from hierarchically constraint dynamics of molecular species (Palmer et al.⁶⁴).

Glarum⁶⁵ proposed to model relaxation behaviour as a diffusion process. Relaxation was assumed to be possible at spots where certain defects are present, due to diffusion of these defects. The results of this theory could only correspond to a KWW equation (with $\beta=1/2$) if physically unrealistic assumptions were made. Curro et al.⁶⁶ also proposed a diffusion process as a basis for relaxation processes. The diffusivity was given, via a Doolittle equation, by the local free volume, which was obtained from the Simha-Somcynsky (SS) theory⁶⁷. Curro et al. assumed that the relaxation process is governed by one diffusion mechanism. Only one parameter had to be defined. Although single temperature steps were described reasonably well, the magnitude of the extreme in volume, following two consecutive temperature steps was underestimated by this model. The authors themselves also pointed out that the necessary introduction of an arbitrary length scale for diffusion was unsatisfying. Finally the correspondence of relaxation and diffusion was explored by Perez⁶⁸. According to this author relaxation can be compared to diffusion of 'defects' (negative and positive fluctuations of enthalpy and entropy). Strong correlations between molecular movements were incorporated. By taking parameters from a set of independent experiments, most features of volume and enthalpy relaxation of poly(vinyl acetate) could be reproduced.

Robertson et al.⁶⁹ based a stochastic theory (the RSC theory, after Robertson, Simha and Curro) on the occurrence of local relaxations. A minimum size V for a region was defined⁷⁰, necessary to enable conformational changes in V . The average free volume $f(T,p)$, and fluctuations in free volume were calculated with the SS theory⁶⁷. These two quantities were used⁶⁹ to define a discrete binomial free volume distribution. Assuming equilibrium on segmental scale the WLF relation was written with τ depending on free volume instead of temperature. Later instead of the WLF equation, two WLF terms were used in different temperature regions⁷¹ and also a fictive temperature term was introduced⁷². Successful

quantitative description of relaxation after single⁶⁹ and multiple⁷² temperature steps and also after pressure⁷³ steps was obtained. The RSC theory will be used later on to discuss the formation and the properties of glasses.

Brawer⁷⁴ presented a relaxation theory comparable to the RSC theory. Brawer used a set of quasi equilibrium structures, and a master equation to give transitions between structures. An exact kinetic equation was derived.

3.4 Conclusions

Since the important experimental work by Kovacs⁴¹, it has become clear that a successful theory must be able to describe at least the following features: the extreme in volume after two consecutive temperature steps, the non-linearity of relaxation with respect to the size of deviation from equilibrium $\delta=(V-V_{\infty})/V_{\infty}$ (the relaxation behaviour is not proportional to the size of the deviation from equilibrium); and finally the asymmetry with respect to the sign of δ (the relaxation rates in experiments from T_1 to T_2 and vice versa).

In this chapter phenomenological theories have been recapitulated, successful in describing relaxation behaviour of e.g. volume, enthalpy and dielectric loss permittivity for a wide range of materials, and in particular polymers. However, due to the phenomenological nature of these theories the description obtained for a particular experiment can not be transferred to predict the behaviour of other properties.

On the other hand, successful molecular theories should be able to explain or predict relaxation behaviour. It turns out that equations (almost equal to those) used in the phenomenological theories, can be derived from molecular kinetics. However, the particular physical meaning of the molecular parameters in these equations makes them in many cases inaccessible via independent experiments. In applications these molecular

parameters are treated as fitting parameters, thus practically removing differences with phenomenological theories. This is also the case for theories based on molecular diffusion processes.

A positive exception forms the RSC theory, for which most input parameters can be determined independently from the polymer equilibrium state. Practically, only one adjustable parameter remains which must be derived from a relaxation experiment. If this parameter is fixed, a whole set of experiments can be predicted. This will be shown in chapter 5, where a modified RSC theory will be presented.

3.5 References

1. E. A. DiMarzio and J. H. Gibbs, *J. Chem. Phys.*, **28**, 807 (1958).
2. J. H. Gibbs and E. A. DiMarzio, *J. Chem. Phys.*, **28**, 373 (1958).
3. H. Breuer and G. Rehage, *Kolloid-Z. u. Z. Polym.*, **216**, 159 (1967).
4. G. Rehage and W. Borchard, in *The Physics of Glassy Polymers*, R. N. Haward, ed., Applied Science Pub. Ltd., London, 1973.
5. J. Jäckle, *J. Phys.: Condens. Matter*, **1**, 267 (1989).
6. P. Ehrenfest, *Proc. Kon. Akad. Wetensch. Amsterdam*, **36**, 153 (1933).
7. J. Meixner, *Changements des Phases*, Société de Chimie Physique, Paris, 1952, p. 432.
8. R. O. Davies and G. O. Jones, *Adv. Physics*, **2**, 370 (1953).
9. A. Quach and R. Simha, *J. Phys. Chem.*, **76**, 416 (1972).
10. J. E. McKinney and R. Simha, *J. Res. Nat. Bur. Stand.-A. Phys. Chem.*, **81A**, 283 (1977).
11. M. Goldstein, *J. Chem. Phys.*, **39**, 3369 (1963).
12. R. Simha and R. F. Boyer, *J. Chem. Phys.*, **37**, 1003 (1962).
13. W. Kauzmann, *Chem. Revs.*, **43**, 219 (1948).

14. E. A. DiMarzio, J. H. Gibbs, P. D. Fleming and I. C. Sanchez, *Macromolecules*, **9**, 763 (1976).
15. H.-J. Oels and G. Rehage, *Macromolecules*, **10**, 1036 (1977).
16. M. H. Cohen and G. S. Grest, *Phys. Rev. B*, **20**, 1077 (1979).
17. G. S. Grest and M. H. Cohen, *Phys. Rev. B*, **21**, 4113 (1980).
18. T. R. Kirkpatrick, D. Thirumalai and P. G. Wolynes, *Phys. Rev. B*, **40**, 1045 (1989).
19. E. Donth, *J. Non-Cryst. Solids*, **53**, 325 (1982).
20. J. Jäckle, *Phil. Mag. B*, **44**, 533 (1981).
21. R. G. Palmer, *Adv. Phys.*, **31**, 669 (1982).
22. E. Leutheusser, *Phys. Rev. A*, **29**, 2765 (1984).
23. U. Bengtzelius, W. Götze and A. Sjölander, *J. Phys. C*, **17**, 5915 (1984).
24. U. Bengtzelius, *Phys. Rev. A*, **34**, 5059 (1986).
25. U. Bengtzelius, *Phys. Rev. A*, **33**, 3433 (1986).
26. W. Götze and L. Sjögren, *Z. Phys. B*, **65**, 415 (1987).
27. F. F. Abraham, *J. Chem. Phys.*, **72**, 359 (1980).
28. H.-P. Wittmann, K. Kremer and K. Binder, *J. Chem. Phys.*, **96**, 6291 (1992).
29. D. Rigby and R. J. Roe, *Macromolecules*, **23**, 5312 (1990).
30. D. Rigby and R. J. Roe, *J. Chem. Phys.*, **87**, 7285 (1987).
31. R. J. Roe, D. Rigby, H. Furuya and H. Takeuchi, *Comput. Polym. Sci.*, **2**, 32 (1992).
32. A. K. Doolittle, *J. Appl. Phys.*, **22**, 1471 (1951).
33. G. S. Fulcher, *J. Am. Chem. Soc.*, **8**, 339, 789 (1925).
34. G. Tammann and G. Hesse, *Z. Anorg. Allg. Chem.*, **156**, 245 (1926).
35. M. L. Williams, R. F. Landel and J. D. Ferry, *J. Am. Chem. Soc.*, **77**, 3701 (1955).
36. J. D. Ferry, *Viscoelastic Properties of Polymers*, Wiley & Sons, New York, 1980.

37. J. G. Curro, R. R. Lagasse and R. Simha, *J. Appl. Phys.*, **52**, 5892 (1981).
38. A. Q. Tool, *J. Amer. Ceram. Soc.*, **29**, 240 (1946).
39. H. N. Ritland, *J. Amer. Ceram. Soc.*, **39**, 403 (1956).
40. O. S. Narayanaswamy, *J. Amer. Ceram. Soc.*, **54**, 491 (1971).
41. A. J. Kovacs, *Fortschr. Hochpolym. Forsch.*, **3**, 394 (1963).
42. J. M. Hutchinson and A. J. Kovacs, *J. Polym. Sci., Polym. Phys. Ed.*, **14**, 1575 (1976).
43. A. J. Kovacs, J. M. Hutchinson and J. J. Aklonis, *The Structure of Non-crystalline Materials*, P. H. Gaskell, ed, Taylor & Francis, London, 1977, p153.
44. A. J. Kovacs, J. J. Aklonis, J. M. Hutchinson and A. R. Ramos, *J. Polym. Sci., Polym. Phys. Ed.*, **17**, 1097 (1979).
45. A. R. Ramos, A. J. Kovacs, J. M. O'Reilly, J. J. Tribone and J. Greener, *J. Polym. Sci., Polym. Phys. Ed.*, **26**, 501 (1988).
46. R. Kohlrausch, *Ann. Phys. (Leipzig)*, **12**, 393 (1847); G. Williams and D. C. Watts, *Trans. Faraday Soc.*, **66**, 80 (1970).
47. M. A. DeBolt, A. J. Eastreal, P. B. Macebo and C. T. Moynihan, *J. Amer. Ceram. Soc.*, **59**, 16 (1976).
48. L. C. E. Struik, *Physical Aging in Amorphous Polymers and Other Materials*, Elsevier, Amsterdam, 1978.
49. S. Matsuoka, G. Williams, G. E. Johnson, E. W. Anderson and T. Furukawa, *Macromolecules*, **18**, 2652 (1985).
50. Y. Abe, M. Kakizaki and T. Hideshima, *Jap. J. Appl. Phys.*, **24**, 1074 (1985).
51. M. Kakizaki, Y. Abe and T. Hideshima, *Jap. J. Appl. Phys.*, **25**, 485 (1986).
52. J. J. Tribone, J. M. O'Reilly and J. Greener, *Macromolecules*, **19**, 1732 (1986).
53. T. S. Chow, *J. Chem. Phys.*, **79**, 4602 (1983).
54. N. Hirai and H. Eyring, *J. Pol. Sci.*, **37**, 51 (1959).

55. T. S. Chow, *Pol. Eng. Sci.*, **24**, 1079 (1984).
56. G. Adam and J. H. Gibbs, *J. Chem. Phys.*, **43**, 139 (1965).
57. C.A. Angell and W. Sichina, *Ann. N. Y. Acad. Sci.*, **279**, 53 (1976).
58. K. L. Ngai, *Comments Solid State Phys.*, **9**, 127 (1979); **9**, 141 (1980).
59. D. J. Plazek, K. L. Ngai and R. W. Rendell, *Pol. Eng. Sci.*, **24**, 1111 (1984).
60. K. L. Ngai, R. W. Rendell and D. J. Plazek, *J. Chem. Phys.*, **94**, 3018 (1991).
61. K. L. Ngai and A. F. Yee, *J. Polym. Sci., Polym. Phys. Ed.*, **29**, 1493 (1991).
62. R. W. Rendell, K. L. Ngai, G. R. Fong and J. J. Aklonis, *Macromolecules*, **20**, 1070 (1987).
63. S. Matsuoka and X. Quan, *Macromolecules*, **24**, 2770 (1991).
64. R. G. Palmer, D. L. Stein, E. Abrahams and P. W. Anderson, *Phys. Rev. Letters*, **53**, 958 (1984).
65. S. H. Glarum, *J. Chem. Phys.*, **33**, 639 (1960).
66. J. G. Curro, R. R. Lagasse and R. Simha, *Macromolecules*, **15**, 1621 (1982).
67. R. Simha and T. Somcynsky, *Macromolecules*, **2**, 342 (1969).
68. J. Perez, *Polymer*, **29**, 483 (1988).
69. R. E. Robertson, R. Simha and J. G. Curro, *Macromolecules*, **17**, 911 (1984).
70. R. E. Robertson, *J. Polym. Sci., Polym. Phys. Ed.*, **17**, 597, (1979).
71. R. E. Robertson, *Macromolecules*, **18**, 953 (1985).
72. R. E. Robertson, R. Simha and J. G. Curro, *Macromolecules*, **21**, 3216 (1988).
73. R. E. Robertson, R. Simha and J. G. Curro, *Macromolecules*, **18**, 2239 (1985).
74. S. A. Brawer, *J. Chem. Phys.*, **81**, 954 (1984).

Chapter 4

The mobility of polymer melts

4.1 Introduction

It is clear that the description of the relaxation times as a function of structure, temperature and other variables such as pressure is of great importance. In the previous work the influence of pressure was not considered explicitly although it was discussed earlier in the case of aging, e.g. by Ramos et al¹. In these considerations it was tacitly assumed that the influence of pressure was properly taken care of by the equations only depending on temperature or structure. However it is well known that the influence of pressure is not well described by these equations. In the discussion it will become clear that a good description of the relaxation times as a function of pressure is needed. The efforts to describe the pressure dependence discussed in literature will be summarized and a new empirical equation is presented. This equation by itself is of practical value to describe e.g. the influence of pressure on viscosity.

4.2 The pressure dependence of mobility

Ferry and Stratton proposed an equivalent of the usual WLF equation to describe the influence of pressure on relaxation times. Expressed in a shift factor, this reads²

$$\log a_p = \log \frac{\tau_p}{\tau_{p_0}} = \frac{c_1''(p-p_0)}{c_2'' + p - p_0} \quad (4.1)$$

with $c_1'' = B/(2.3f_0)$ and $c_2'' = f_0/\beta_f$. Combined with temperature dependence this becomes³

$$\log a_{\tau,p} = \frac{c_1'''(T-T_0-\Theta(p))}{c_2''' + T - T_0 - \Theta(p)} \quad (4.2)$$

with $c_2''' = f_0/\alpha_f(p)$ and $\Theta(p)$ a function of pressure. It was shown^{4,5} that eq. 4.2 describes the effect of temperature and pressure on stress relaxation.

If one wants to explain relaxation times solely as a function of free volume f , then one has to assume⁶

$$f(T,p) = f_g + \alpha_f(T-T_g) - \beta_f p \quad (4.3)$$

with β_f the isothermal compressibility of the free volume. Now α_f and β_f have to obey

$$\left[\frac{\partial T}{\partial p} \right]_{\tau} = \left[\frac{\partial T}{\partial p} \right]_f = \frac{\beta_f}{\alpha_f} \quad (4.4)$$

with the index τ referring to states at constant mobility. Values for $(\partial T/\partial p)_{\tau}$ have been listed⁶. In this way, the free volume is chosen to obey eq. 4.4.

Utracki⁷ showed that for n-alkanes with 5 to 18 C-atoms the free volume h (according to the SS theory, see chapter 2) uniquely determines the temperature and pressure dependence of the viscosity, however not via a Doolittle relation $\log(\eta) \propto 1/f$. He found that for most polymers this simple relation breaks down.

4.3 A modified Fulcher-Tammann-Hesse equation

To model the shift factor, based on viscosity or other viscoelastic properties, as a function of temperature *at atmospheric pressure* a WLF like relation, based on free volume instead of temperature⁸ is adopted in this work. The expression of a shift factor as function of the order parameter h in a hole theory was first utilized by Curro et al.⁹, using a Doolittle expression. This gave satisfactory results in the small temperature trajectory considered^{9,10}. Combining this with linearity between h and T resulted in a WLF equation. Proceeding along similar lines, in this work the free volume is identified with the order parameter h from the Holey Huggins (HH) theory¹¹ (see chapter 2). The temperature dependence of the shift factor a_T is

$$\log a_T = -\frac{c_1(h(T)-h(T_0))}{c_2+h(T)-h(T_0)} \quad (4.5)$$

with $h(T)$ and $h(T_0)$ the free volume at T and T_0 , respectively, and c_1 and c_2 constants. Equation 4.5 can be written as

$$\log a_T = \frac{B}{h-A} + D \quad (4.6)$$

with $D=-c_1$, $B=c_1c_2$, $A=h(T_0)-c_2$ and omitting the explicit dependence of h on temperature. Equation 4.6 resembles the Fulcher-Tammann-Hesse (FTH) equation, eq. 3.9, with h instead of T . In general, the description by eq. 4.6 is excellent over the complete temperature range where experimental data are available, as will be shown in paragraph 4.4. When describing the data over an extended temperature range, the value for A must be allowed to have a finite value. Thus a Doolittle expression can not satisfactorily describe the complete temperature interval. It will be illustrated in paragraph 4.4 that eq. 4.6 does not describe the *pressure* dependence of the shift factors. From this it can be concluded that the free volume (described

by the order parameter h from the HH theory) does not solely describe the mobility in the polymer.

Choosing a function to describe both the temperature and pressure dependence of mobility, several considerations can be made. From a physical point of view, it is natural to take h and T as parameters to describe mobility. (Choosing p and h leads to an apparent contradiction: at constant h and increasing pressure the mobility *increases*, i.e. the shift factor decreases, which seems difficult to rationalize). Several empirical equations have been investigated. Of those that describe all experimental data quantitatively, one was chosen for further analysis

$$\log a_{T,p} = \frac{B}{h+CT-A} + D \quad (4.7)$$

with A , B , C and D constants. As explained below, the parameter D is not a physically important parameter but only serves to shift experimental data derived from different sources. For $C=0$, eq. 4.7 reduces to eq. 4.6. The dependence of $\log a_{T,p}$ on h and T is symmetric, because eq. 4.7 can also be written as

$$\log a_{T,p} = \frac{B'}{T+C'h-A'} + D \quad (4.8)$$

with $B'=B/C$, $C'=1/C$ and $A'=A/C$.

At constant pressure the free volume parameter h is approximately a linear function of T , reducing eq. 4.7 to eq. 4.6. If $CT \gg h-A$, eq. 4.7 reduces to an Arrhenius equation. If h is constant, which is approximately the case in the glass, eq. 4.7 reduces to a FTH equation, or to an Arrhenius equation if $h_g \approx A$. And finally, if T is constant, e.g. during isothermal aging, eq. 4.7 reduces again to eq. 4.6. All these examples show that eq. 4.7 has, in principle, the ability to describe different observed behaviour. Because of the resemblance of eq. 4.8 with the original FTH equation (eq. 3.9) and

with eq. 4.6, which on its turn has the same structure as the FTH equation, we have chosen the name 'modified FTH' for eqs. 4.7 and 4.8.

4.4 Applications of the modified FTH

In the present paragraph the description of experimental data with eqs. 4.6 and 4.7 is examined. For poly(vinyl acetate) (PVAC) relaxation time data at atmospheric pressure derived from different measurements have been reported: dielectric data by Williams and Ferry¹² and O'Reilly¹³, creep data by Plazek¹⁴ and stress relaxation data by Ninomiya¹⁵. Dynamic light scattering (DLS) data have been reported by Tribone et al.¹⁶. Compared to the other data, DLS shows a smaller temperature dependence (a smaller activation energy). All these experimental data except the DLS data have been used to fit the parameters A, B and D in eq. 4.6. In the fitting procedure only experimental data obtained in the equilibrium melt have been used. Several sets of shift factors, derived from different experimental techniques, are used simultaneously and each set has been allowed to have a different value for D. Thus, D shifts the different data sets relative to each other. For the fitting a multi-parameter fitting program is used¹⁷. Whereas the value for D depends on e.g. the particular property under consideration or the choice of the reference state, the constants A and B are characteristic for the polymer. For this reason we prefer the form of eq. 4.6 over that of eq. 4.5, where all parameters depend on e.g. the particular property considered. We now define the mobility μ as

$$\mu \equiv -\log a_{T,p} + D \quad (4.9)$$

with $\log a_{T,p}$ given by eq. 4.6 or 4.7.

Table 4.1 lists the results from fitting eq. 4.6 to the experimental data measured at atmospheric pressure. This is illustrated for PVAC in figure 4.1b. For PVAC also pressure dependence of viscosity¹⁸ and dielec-

tric relaxation¹³ has been reported. In figure 4.2a these pressure data are plotted versus the order parameter h . It is clear that eq. 4.6 does not describe the pressure dependence. If data measured both at atmospheric and higher pressure are fitted to eq. 4.7, a good description is obtained, as is shown in figure 4.2b. Parameters obtained from the fit to eq. 4.7 are listed in table 4.2.

Table 4.1. Parameters obtained from the fit to eq. 4.6 of shift factors a_T as a function of temperature measured at atmospheric pressure for several polymers. Simultaneous description of different sets of experimental data is obtained by allowing for a different value of D for each set of experimental data. Since D is not a characteristic parameter of the polymer, values for D are not shown.

	A	B	experimental data used for fit ^a	ref.
PVAC	0.0581	0.392	dielectric	12
			creep	14
			stress relaxation	15
PS	0.0518	0.156	viscosity	19
			creep	20
			creep	21
PC	0.0797	0.358	viscosity	19
			viscosity	22
			stress relaxation	23
PMMA	0.0646	0.309	viscosity	19
			creep	21

^a Only data in equilibrium and at atmospheric pressure have been used.

Table 4.2. Parameters obtained from the fit to eq. 4.7 of the temperature and pressure dependence of shift factors $a_{T,P}$ for several polymers. Simultaneous description of different sets of experimental data is obtained by allowing for a different value of D for each set of experimental data. Since D is not a characteristic parameter of a polymer, values for D are not shown.

	A	B	$C \cdot 10^4$	experimental pressure data used for fit ^a	ref.
PVAC	0.201	0.785	5.52	dielectric	13
				viscosity	18
PS	0.140	0.315	2.70	viscosity	19
				viscosity	24
PC	0.183	0.558	2.93	viscosity	19
PMMA	0.211	0.561	4.25	viscosity	19
				viscosity	25

^a Except these data, also the atmospheric pressure data listed in table 4.1 are used in the fit of eq. 4.7.

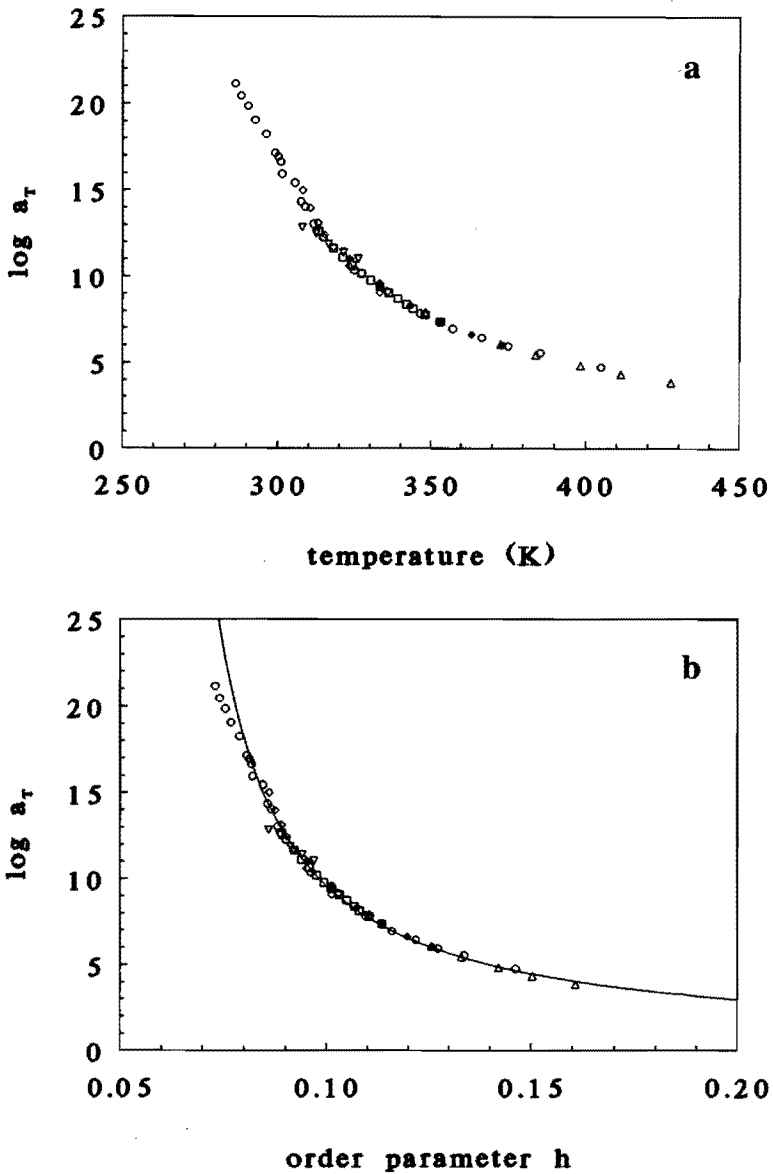


Figure 4.1. Shift factors for poly(vinyl acetate) at atmospheric pressure (a) versus temperature and (b) versus the order parameter h ; Symbols: experimental data (\square , ref. 12; \blacklozenge , ref. 13; \diamond , ref. 14 (creep); \triangle , ref. 14 (viscosity); \circ , ref. 15; ∇ , ref. 16). Line: fit of eq. 4.6. The systematic deviations at low h values are due to the non-equilibrium state in some measurements.

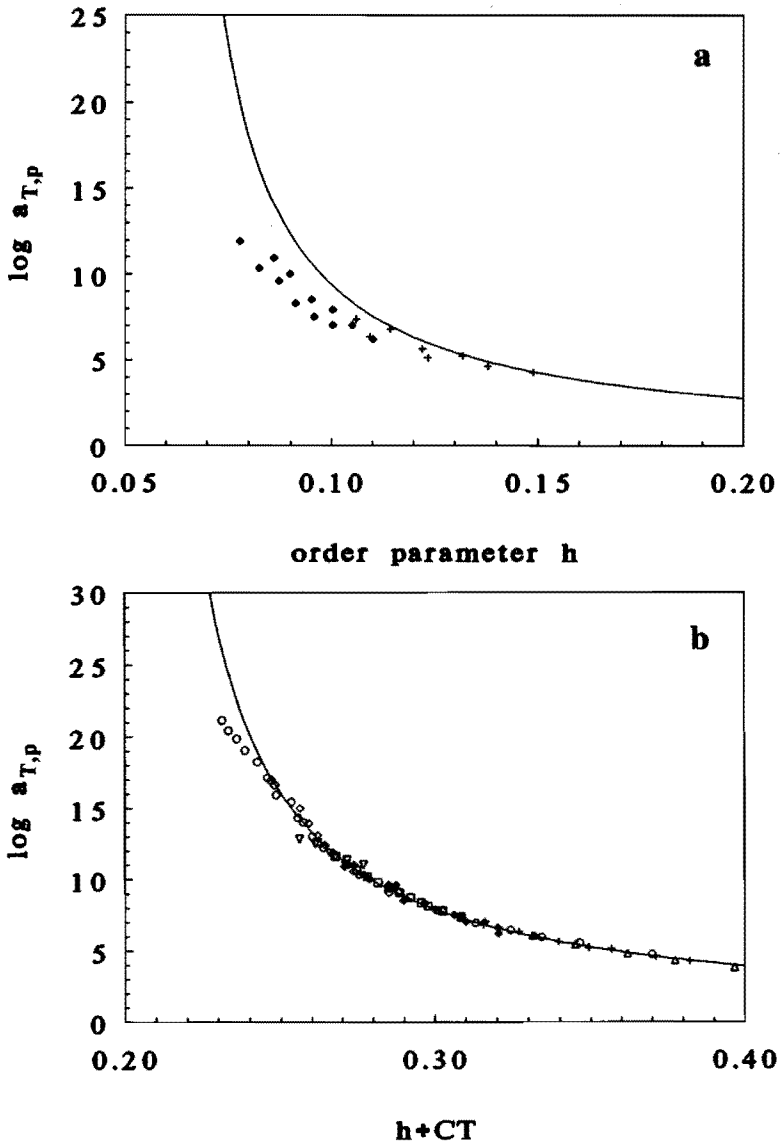


Figure 4.2. Shift factors for poly(vinyl acetate) (a) at different temperatures and elevated pressure versus the order parameter h . Symbols: experimental data (\blacklozenge , ref. 13; $+$, ref. 18); line: representation of atmospheric pressure data by eq. 4.6. (b) measured at different temperatures and pressures versus $h+CT$. Symbols: experimental data (\square , ref. 12; \blacklozenge , ref. 13; \blacklozenge , ref. 14 (creep); \triangle , ref. 14 (viscosity); \circ , ref. 15; ∇ , ref. 16; $+$, ref. 18); line: eq. 4.7.

Also for polystyrene (PS) many atmospheric pressure data are available. Creep data, both above and below T_g , have been reported by Schwarzl and Zahradnik²¹ and above T_g by Plazek²⁰. DLS data have been reported by Lee et al.²⁶, and Lindsey et al.²⁷. These two sets of DLS data do not agree very well. According to Patterson²⁸ this discrepancy is due to artifacts of the graphical fitting procedure of Lee et al. Also in this case the temperature dependence of DLS data is different from that of mechanical data. This can be seen in figure 4.3, where the fit of atmospheric pressure data to eq. 4.6 is shown. Due to these discrepancies, the DLS data are not used in the fitting procedures. Each set of experimental data is allowed to have a different value for D . Parameters of this fit are listed in table 4.1.

Pressure viscosity data are reported by Cogswell and McGowan¹⁹ and by Kadijk and Brule¹⁸. The unsatisfying description of pressure data by eq. 4.6, and the description of both pressure and temperature dependence by eq. 4.7, are shown in figures 4.4a and 4.4b, respectively. Parameters of the fit to eq. 4.7 are listed in table 4.2.

Shear creep data on bisphenol-A polycarbonate (PC) have been reported by Wimberger-Friedl²², viscosity data by Cogswell and McGowan¹⁹, and stress relaxation data by Maurer et al.²³. Pressure data on viscosity have been reported by Cogswell and McGowan¹⁹. Results of fitting atmospheric pressure data to eq. 4.6 are reported in table 4.1, and of fitting also pressure data to eq. 4.7 in table 4.2. Again, atmospheric pressure data are described well by eq. 4.6, pressure and temperature data by eq. 4.7.

For poly(methyl methacrylate) (PMMA) creep data in melt and glass at atmospheric pressure have been reported by Schwarzl and Zahradnik²¹, viscosity data at several pressures by Cogswell and McGowan¹⁹ and by Christmann and Knappe²⁵. Again, results of fitting temperature dependence at atmospheric pressure to eq. 4.6, and pressure and temperature dependence to eq. 4.7, are listed in tables 4.1 and 4.2, respectively.

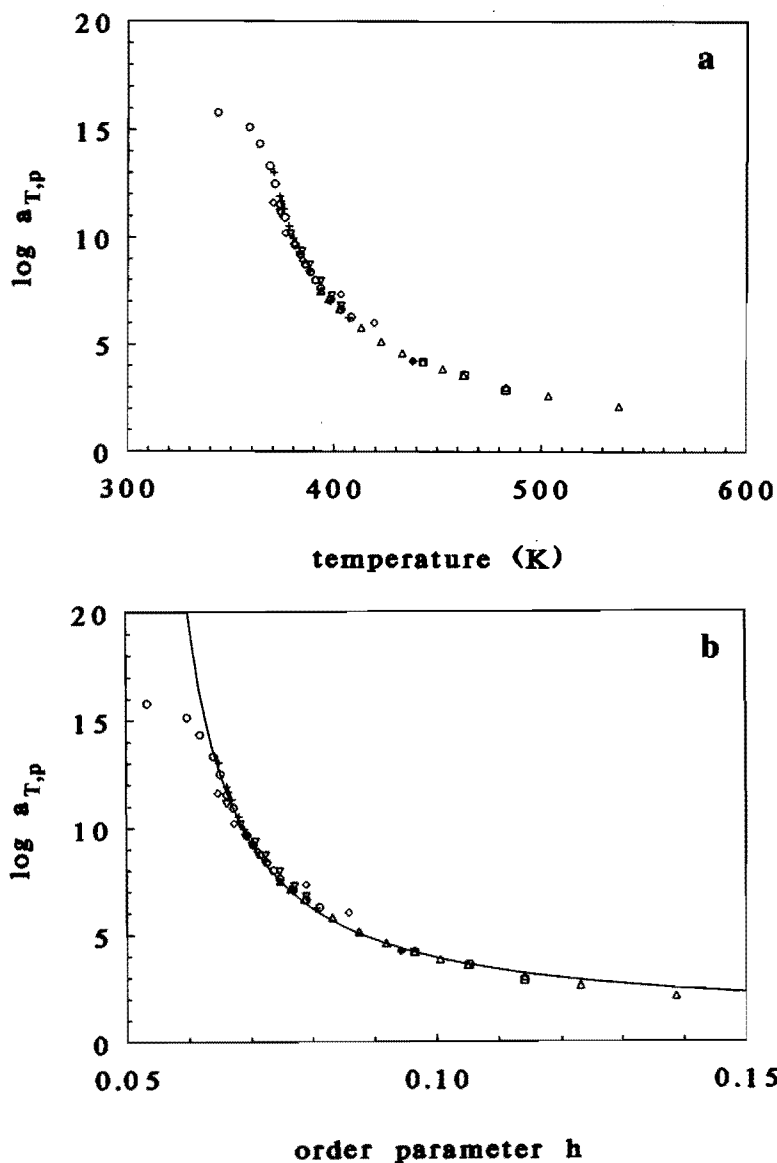


Figure 4.3. Shift factors for polystyrene measured at atmospheric pressure (a) versus temperature and (b) versus the order parameter h . Symbols: experimental data (\square , ref. 19; $+$, ref. 20; \circ , ref. 21; \blacklozenge , ref. 24; \diamond , ref. 26; ∇ , ref. 27; \triangle , ref. 29). Line: fit of eq. 4.6. The systematic deviations at low h values are due to the non-equilibrium state in some measurements.

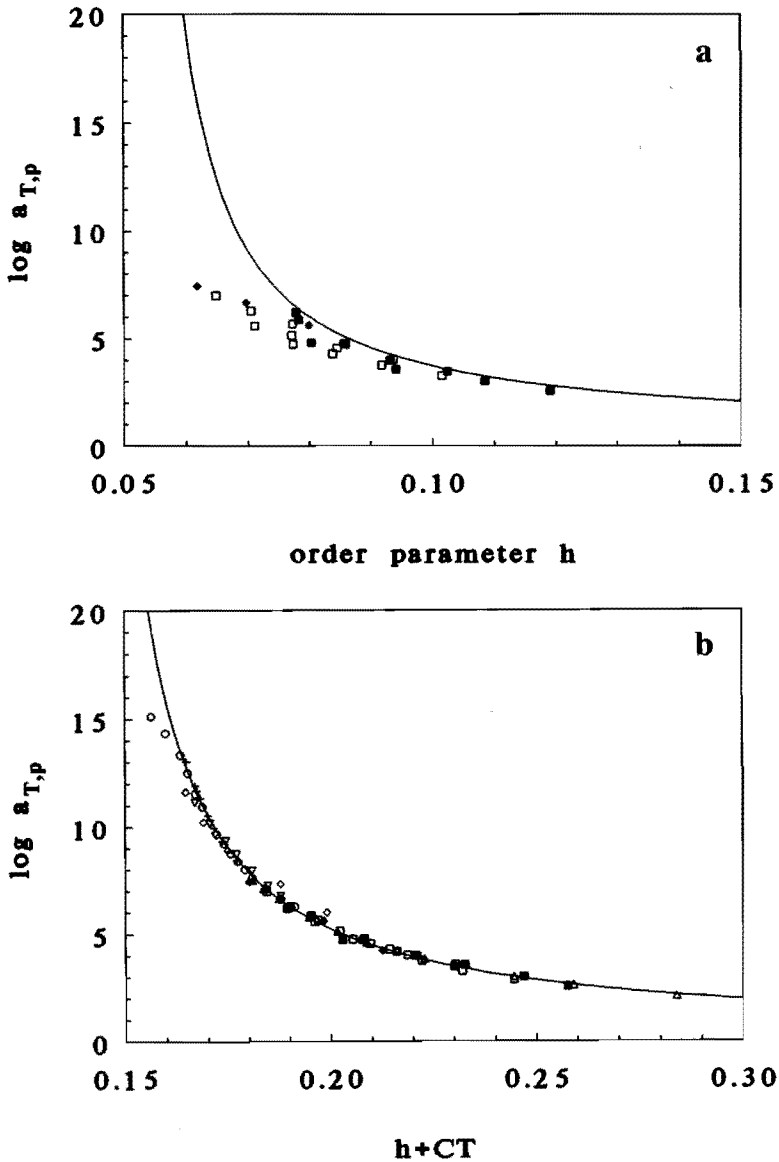


Figure 4.4. Shift factors for polystyrene (a) measured under pressure versus the order parameter h . Symbols: experimental data (\blacksquare , ref. 18; \square , ref. 19; \blacklozenge , ref. 24); line: representation of atmospheric pressure data by eq. 4.6. (b) measured at different temperatures and pressures versus $h+CT$. Symbols: experimental data (\blacksquare , ref. 18; \square , ref. 19; $+$, ref. 20; \circ , ref. 21; \blacklozenge , ref. 24; \blacklozenge , ref. 26; \blacktriangledown , ref. 27; \blacktriangle , ref. 29); line: eq. 4.7.

It is interesting to notice that in contrast to the examined polymers, both temperature and pressure dependence of viscosity based shift factors in low molar mass liquids, e.g. benzene³⁰ and cyclohexane³¹, are described well by solely the free volume h , and eq. 4.6. This is illustrated in figure 4.5.

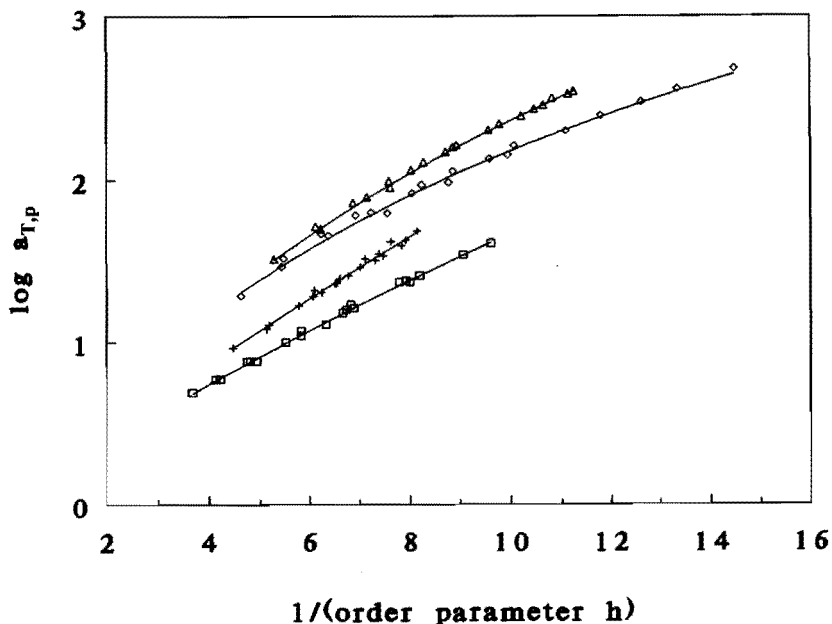


Figure 4.5. Shift factors for low molar mass liquids, measured at different temperatures and pressures, versus the reciprocal free volume h . Symbols, experimental data (\square , benzene³⁰; +, cyclohexane³¹; \diamond , n-dodecane^{32,33}; Δ , n-octadecane^{33,34}); lines: fit by eq. 4.6.

As previously mentioned Utracki⁷ found similar results for a series of n-alkanes. The difference in the description of polymers and the low molar mass benzene may be due to the fact that in the regime where data are available for the low molar mass liquids generally the free volume content is larger than for polymers. Describing the temperature and pressure

dependence of mobility with eq. 4.7, the constant C can therefore be undetermined. We have

$$\frac{d \log a}{dh} = \left. \frac{d \log a}{dh} \right]_{\tau} + \left. \frac{d \log a}{dT} \right]_{h} \cdot \frac{dh}{dT} \approx \left. \frac{d \log a}{dh} \right]_{\tau} \quad (4.10)$$

because

$$\left. \frac{d \log a}{dT} \right]_{h} = -\frac{C}{B} \mu^2 \quad (4.11)$$

The value of the latter equation decreases rapidly with increasing free volume h , and is therefore negligible compared to $(d \log(a)/dh)_{\tau}$ in the case of low molar mass liquids such as benzene. For these conditions, the influence of pressure coincides with that of temperature. Some intermediate behaviour has also been observed¹⁸, supporting the above mentioned reduction of eq. 4.7 to eq. 4.6 for large values of h .

4.5 Conclusions

In this chapter an expression has been presented (eq. 4.6) to describe the *temperature* dependence of relaxation times at atmospheric pressure. This expression, related to the WLF equation, yields a quantitative description of shift factors as a function of the order parameter h from the HH theory, which is identified with the free volume.

For the simultaneous description of the *pressure and temperature* dependence of relaxation times, an empirical equation (eq. 4.7) has been presented in which the shift factor is a function of both temperature and the order parameter h . This is comparable to the use of temperature and fictive temperature in many phenomenological theories.

4.6 References

1. A. R. Ramos, A. J. Kovacs, J. M. O'Reilly, J. J. Tribone and J. Greener, *J. Polym. Sci., Polym. Phys. Ed.*, **26**, 501 (1988).
2. J. D. Ferry and R. A. Stratton, *Kolloid.-Z. u. Z. Polym.*, **171**, 107 (1960).
3. R. W. Fillers and N. W. Tschoegl, *Trans. Soc. Rheol.*, **21**, 51 (1977).
4. W. F. Moonan and N. W. Tschoegl, *Macromolecules*, **16**, 55 (1983).
5. W. F. Moonan and N. W. Tschoegl, *J. Polym. Sci., Polym. Phys. Ed.*, **23**, 623 (1985).
6. J. D. Ferry, *Viscoelastic Properties of Polymers*, Wiley & Sons, New York, 1980.
7. L. A. Utracki, *Can. J. Chem. Eng.*, **61**, 753 (1983).
8. R. E. Robertson, R. Simha and J. G. Curro, *Macromolecules*, **17**, 911 (1984).
9. J. G. Curro, R. R. Lagasse and R. Simha, *J. Appl. Phys.*, **52**, 5892 (1981).
10. R. R. Lagasse and J. G. Curro, *Macromolecules*, **15**, 1559 (1982).
11. E. Nies and A. Stroeks, *Macromolecules*, **23**, 4088 (1990).
12. M. L. Williams and J. D. Ferry, *J. Colloid Sci.*, **9**, 479 (1954).
13. J. M. O'Reilly, *J. Polym. Sci.*, **57**, 429 (1962).
14. D. J. Plazek, *Polym. J. (Tokyo)*, **12**, 43 (1980).
15. K. Ninomiya and H. Fujita, *J. Colloid Sci.*, **12**, 204 (1957).
16. J. Tribone, A. M. Jamieson and R. Simha, *J. Polym. Sci., Polym. Symp.*, **71**, 231 (1984).
17. L. T. M. E. Hillegers, *thesis*, Eindhoven University of Technology, 1986.
18. S. E. Kadijk and B. H. A. A. van den Brule, to be published (1992).

19. F. N. Cogswell and J. C. McGowan, *Br. Polym. J.*, **4**, 183 (1972).
20. D. J. Plazek, *J. Phys. Chem.*, **69**, 3480 (1965).
21. F. R. Schwarzl and F. Zahradnik, *Rheol. Acta*, **19**, 137 (1980).
22. R. Wimberger-Friedl, *thesis*, Eindhoven University of Technology, 1991.
23. F. H. J. Maurer, J. H. M. Palmen and H. C. Booij, *Rheol. Acta*, **24**, 243 (1985).
24. K.-H. Hellwege, W. Knappe, F. Paul and V. Semjonow, *Rheol. Acta*, **6**, 165 (1967).
25. L. Christmann and W. Knappe, *Colloid Polym. Sci.*, **252**, 705 (1974).
26. H. Lee, A. M. Jamieson and R. Simha, *Colloid Polym. Sci.*, **258**, 545 (1980).
27. C. P. Lindsey, G. D. Patterson and J. R. Stevens, *J. Polym. Sci., Polym. Phys. Ed.*, **17**, 1547 (1979).
28. G. D. Patterson, *Adv. Polym Sci.*, **48**, 125 (1983).
29. W. F. Zoetelief, unpublished (1990).
30. H. J. Parkhurst and J. Jonas, *J. Chem. Phys.*, **63**, 2705 (1975).
31. J. Jonas, D. Hasha and S. G. Huang, *J. Phys. Chem.*, **84**, 109 (1980).
32. J. H. Dymond, J. Robertson and J. D. Isdale, *J. Chem. Thermodyn.*, **14**, 51 (1982).
33. D. L. Hogenboom, W. Webb and J. A. Dixon, *J. Chem. Phys.*, **46**, 2586 (1967).
34. W. G. Cutler, R. H. McMickle, W. Webb and R. W. Schliessler, *J. Chem. Phys.*, **29**, 727 (1958).

Chapter 5*

The stochastic glass formation theory

5.1 Introduction

In contrast to polymer liquids the same limited set of macroscopic variables does not suffice to fix the thermodynamic state of polymer glasses. Instead, the formation history of the glass influences the equation of state and other properties. It may be clear that the unambiguously defined melt state can serve as a good starting point for the simulation of glasses. A stochastic theory has been developed to describe the influence of formation history on the equation of state of polymer glasses and on the glass transition temperature. The theory is based on the RSC theory^{1,2}. The assumption of a spatial distribution of free volume and hence mobility in the polymer system is made. Because the equilibrium is chosen as a reference state, this allows one to define both the free volume (distribution) and the mobility in a well defined way. The free volume is identified with the order parameter h in the Holey Huggins theory. The response of the system to a change in pressure and/or temperature is formed by a change of the actual free volume distribution to the new equilibrium.

* Reprinted in part from: S. Vleeshouwers and E. Nies, *Macromolecules*, **25**, 6921 (1992)

5.2 The stochastic theory.

It is assumed that the relaxation behaviour governing the glass transition region can be described by the approach to equilibrium of the conformational degrees of freedom of the polymer backbone. Vibrational and side group rotational degrees of freedom are assumed to be sufficiently fast and thus to respond almost instantaneously to variations in thermodynamic variables.

Consider now a change of temperature and/or pressure in the system from an initial to a final state. The thermodynamic properties change accordingly. It is our aim to monitor the kinetics of the changes. On a microscopic level this change in macroscopic properties is caused by rearrangements in the polymer chains. A discussion of the interrelation between microscopic and macroscopic changes has been given by Robertson in the context of the relaxation behaviour in polymer glasses³. The importance of the segmental rearrangements in the isolated chain and the influence of the surrounding segments in the dense disordered state have been explained. Furthermore the rate of change in the small volume element, containing the rearranging segments, is not only determined by the local segmental mobility but also by the possibility of the environment to assimilate the necessary changes.

However, our main interest are the kinetics of macroscopic properties and it is hoped that less detailed information concerning the microscopic state of the system should suffice to discuss these relaxation phenomena. It was suggested by Robertson³ that the local free volume is an appropriate parameter to describe the local segmental mobility and thus the rate of rearrangements. The system is thought to be subdivided into small volume elements, each with its (local) free volume. The sample is thus characterised by a (time dependent) free volume distribution. For mathematical convenience it is assumed that this distribution is a set of n discrete levels $\{w_i(t), i = 1, n\}$:

$$w(t) = \{w_i(t), i=1,n\} = [w_1(t) \dots w_i(t) \dots w_n(t)] \quad (5.1)$$

with the local free volume in level w_i given by $(i-1)\beta$, and β , the width of the free volume level, defined later.

Changes in the occupation of the levels occur by transitions between the different levels and can be regarded as a stochastic process known as a Markov chain, which has the following important properties

1. The no-memory property; transitions and transition rates between different states are independent of earlier transitions.
2. The Chapman-Kolmogorov condition; the transition probability P_{ij} that the system changes from state i to state j in the time $(t+s)$ is equal to:

$$P_{ij}(t+s) = \sum_{k=1}^n P_{ik}(t)P_{kj}(s), \quad 1 \leq i,j,k \leq n \quad (5.2)$$

The time derivative of this equation with respect to s yields a set of coupled differential equations which can be written in matrix form

$$\dot{P}(t) = P(t) \cdot A \quad (5.3)$$

with $P(t)$ the transition probability and A the generator matrix respectively

$$P(t) = \begin{bmatrix} P_{11}(t) & P_{12}(t) & \dots & P_{1n}(t) \\ P_{21}(t) & \dots & \dots & P_{2n}(t) \\ \dots & \dots & \dots & \dots \\ P_{n1}(t) & \dots & \dots & P_{nn}(t) \end{bmatrix} \quad \text{with } \sum_{j=1}^n P_{ij}=1 \quad (5.4)$$

$$A = \begin{bmatrix} A_{11} & A_{12} & \dots & A_{1n} \\ A_{21} & \dots & \dots & \dots \\ \dots & \dots & \dots & \dots \\ A_{n1} & \dots & \dots & A_{nn} \end{bmatrix} \quad \text{with } A_{ij} = \lim_{s \rightarrow 0} \frac{d P_{ij}(s)}{ds} \quad (5.5)$$

In an infinitesimal time interval ($s \rightarrow 0$), only transitions between adjacent levels can occur. Then the transition probabilities can be written in terms of transition rates

$$\begin{aligned} P_{i,i-1} &= s\lambda_{i,i-1} + O(s) \\ P_{i,i+1} &= s\lambda_{i,i+1} + O(s) \\ P_{i,i} &= 1 - s(\lambda_{i,i-1} + \lambda_{i,i+1}) + O(s) \\ P_{ij} &= O(s) \quad \text{for } j \neq (i, (i-1), (i+1)) \end{aligned} \quad (5.6)$$

where $\lambda_{i,i-1}$ and $\lambda_{i,i+1}$ are the downward and upward transition rates from state i to state $(i-1)$ and state $(i+1)$, respectively, and $O(s)$ a quantity that approaches zero faster than s . Combining eqs. 5.5 and 5.6 the generator matrix A becomes tridiagonal:

$$A = \begin{bmatrix} -\lambda_{1,2} & \lambda_{1,2} & 0 & \dots & \dots & \dots & 0 \\ \lambda_{2,1} & -\lambda_{2,1} - \lambda_{2,3} & \lambda_{2,3} & 0 & \dots & \dots & \dots \\ 0 & \lambda_{3,2} & -\lambda_{3,2} - \lambda_{3,4} & \lambda_{3,4} & 0 & \dots & 0 \\ \dots & \dots & \dots & \dots & \dots & \dots & \lambda_{n-1,n} \\ 0 & \dots & \dots & \dots & 0 & \lambda_{n,n-1} & -\lambda_{n,n-1} \end{bmatrix} \quad (5.7)$$

The formal solution of eq. 5.3 is given by

$$P(t) = P(0)e^{At} \quad (5.8)$$

where $P(0)$ is the initial transition probability matrix, in all applications set equal to the identity matrix I . Equation 5.8 can be solved by an eigenvalue analysis described in many textbooks⁴. It is numerically more efficient to first transform A into a symmetric matrix Z by

$$Z = C^{-1}AC \tag{5.9}$$

with C a diagonal matrix. After substitution of A in eq. 5.3 by Z

$$P(t) = P(0)C e^{Zt} C^{-1} \tag{5.10}$$

Because the exponent in the right hand term of eq. 5.10 can be written as

$$e^{Zt} = QEQ^{-1} \tag{5.11}$$

with Q the matrix of the eigenvectors of Z , and E a diagonal matrix with the elements $E_{ii} = \exp(\zeta_i t)$, with ζ_i the i -th eigen value of Z . Now we obtain

$$P(t) = P(0)CQEQ^{-1}C^{-1} \tag{5.12}$$

Once the transition probability $P(t)$ is known, the calculation of the occupation levels is straightforward:

$$w(t+s) = w(t) \cdot P(s) \tag{5.13}$$

Equation 5.13 defines the time evolution of the occupation of the free volume levels. It can be shown that at sufficiently long times the Markov chain evolves to a stationary distribution $\xi \{ \xi_i, i=1, n \}$

$$\lim_{t \rightarrow \infty} w(t) = [\xi_1 \ . \ . \ \xi_i \ . \ . \ \xi_n] \tag{5.14}$$

Furthermore, for this stationary distribution, the up and downward transition rates are related by the balance equations

$$\lambda_{i,i+1} \xi_i = \lambda_{i+1,i} \xi_{i+1}, \quad 1 \leq i \leq (n-1) \tag{5.15}$$

This stationary distribution can be identified with the equilibrium condition for the system since it has been assumed a priori that the relaxation beha-

viour of the system is due to the approach to the equilibrium state. It is important to note that according to this theory the system will definitely reach the equilibrium state if the system is left for sufficiently long time. Information about this equilibrium state can be derived from equilibrium thermodynamics and statistical mechanics.

The stochastic theory was applied by Robertson, Simha and Curro to study the volume relaxation behaviour of polymers subjected to single and combined temperature and pressure jumps in the glass transition region^{1,5,6}. The authors identified the free volume parameter, appearing in the stochastic model, with the order parameter h defined in the SS theory. It is emphasized that by this assumption the free volume has been defined consistently. In this work the HH theory (chapter 2) is used to extract information concerning the order parameter h in the equilibrium state of the polymer system. In the equilibrium y and V are given by p and T by eqs. 2.13 and 2.14. The equilibrium fluctuations are given by eq. 2.22.

For sufficiently small fluctuations it can be shown that the fluctuations have a Gaussian distribution with mean and variance given by $\langle h \rangle_{eq}$ and $\langle (\delta h_{eq})^2 \rangle = \langle (\delta y_{eq})^2 \rangle$, respectively. For numerical convenience the continuous distribution is approximated by n discrete levels. It is trivial that the distribution should be zero for $h < 0$ and $h > 1$. Keeping in mind that the normal distribution is practically zero for deviations larger than four times the variance, these boundary conditions will not cause any problems in the discrete representation if the continuous distribution is divided in n levels with the width of a free volume level β :

$$\beta = \frac{\langle h \rangle_{eq} + 4\sqrt{\langle (\delta h_{eq})^2 \rangle}}{n-1} \quad (5.16)$$

In this work the value for n is kept constant to $n=20$, resulting in an accurate representation of the distribution, but also in acceptable computation times. According to this scheme the following free volume distribution is obtained

$$\begin{aligned}\xi_i &= \Gamma\{\beta(i-\frac{1}{2})\} - \Gamma\{\beta(i-\frac{3}{2})\}, \quad i=2, n-1 \\ \xi_1 &= \Gamma\{\beta(\frac{1}{2})\} \\ \xi_n &= 1 - \Gamma\{\beta(n-\frac{1}{2})\}\end{aligned}\tag{5.17}$$

with $\Gamma(x)$ the cumulative normal distribution⁷ with mean $\langle h \rangle_{eq}$, variance $\langle (\delta h_{eq})^2 \rangle = \langle (\delta y_{eq})^2 \rangle$, evaluated at x .

In order to use the stochastic theory the upward and downward transition rates $\lambda_{i,i+1}$ and $\lambda_{i+1,i}$, $1 \leq i \leq (n-1)$, respectively, must be defined. It was argued³ that the rate of change in a small volume element is not only determined by the local segmental mobility but also by the possibility for the neighbouring volume elements to assimilate these changes. Although at equilibrium correlations in the free volume content between neighbouring volume elements are absent, this may not be true away from equilibrium. However, it is assumed that the correlations remain small and that the free volume of the neighbours can be set equal to the average free volume $\langle h \rangle$ of the system. Hence the transition rates in a central element out of state i depend on the regional free volume \hat{h}_i

$$\hat{h}_i = \frac{(i-1)\beta + (z_n-1)\langle h \rangle}{z_n}, \quad i=1, n\tag{5.18}$$

where z_n is the number of regions necessary to liberate or absorb the free volume changes in the central region. In agreement with literature¹, z_n is put equal to $z_n=13$ in all applications.

Finally the functional dependence of the local transition rates on regional free volume h_i is assumed to be identical with the dependence of the global mobility μ defined by eq. 4.9 on the equilibrium overall free volume $\langle h \rangle_{\text{eq}}$. The global mobility of a system with free volume h is expressed e.g. by a FTH or WLF type of equation. On a local level this reads for the mobility

$$\mu_i \equiv -\frac{B}{h_i - A} \quad (5.19)$$

or, alternatively, by

$$\mu_i \equiv -\frac{B}{h_i + CT - A} \quad (5.20)$$

It is restated that eq. 5.19 is not capable of describing the influence of pressure, in contrast to eq. 5.20. The consequence of the different functional dependencies given by eqs. 5.19 and 5.20 will become clear in chapter 6 when the theory is compared to experiments. For the local transition rates the following expressions are used

$$\lambda_{i,i-1} = \frac{R}{\beta^2} 10^{\mu_i} \sqrt{\frac{\xi_{i-1}}{\xi_i}} \quad (5.21)$$

$$\lambda_{i,i+1} = \frac{R}{\beta^2} 10^{\mu_i} \sqrt{\frac{\xi_{i+1}}{\xi_i}}$$

where R (s^{-1}) contains a characteristic rate and a compensation for differences in global and local mobilities and the occurrence of ξ_i 's assures detailed balancing (eq. 5.15). The factor β^{-2} arises from the random walk representation.

5.3 Basic simulations

We are now in a position to study the dynamics of free volume relaxation. The following procedure is followed.

1. At a given T and p , well in the equilibrium liquid state, the corresponding V , $\langle h \rangle_{eq}$ and $\langle (\delta h_{eq})^2 \rangle$ are computed (eqs. 2.13, 2.14 and 2.23).
2. These thermodynamic data are used to specify the complete Gaussian distribution $\{\xi_i, i=1,n\}$ (eqs. 5.16 and 5.17).
3. The actual distribution $\{w_i(t), i=1,n\}$ is set equal to the equilibrium distribution.

After preparation of the initial distribution, the actual simulation of e.g. a cooling, a pressurizing or a combined experiment is started. First the general procedure will be illustrated for a temperature jump experiment and for a cooling experiment, and then the detailed simulation scheme will be illustrated for a cooling experiment.

In a 'temperature jump' experiment the temperature is changed instantaneously. The value of the equilibrium free volume changes accordingly. Now the time evolution of the actual free volume distribution is monitored towards the new equilibrium. In figure 5.1 both the equilibrium and the actual average free volume and their time dependence are given schematically. A cooling experiment is considered to be a series of small instantaneous changes of the temperature. Again, the equilibrium free volume changes in pace. This is illustrated in figure 5.2. At high temperatures, the relaxation is sufficiently fast to allow the actual distribution to relax to equilibrium on a timescale faster than the cooling process (see figure 5.2a). At lower temperatures the time needed for complete relaxation becomes comparable to the timescale of cooling, and even longer (figure

5.2b). Now, complete relaxation during the cooling can not be reached. This can be viewed as the onset of the glass transition.

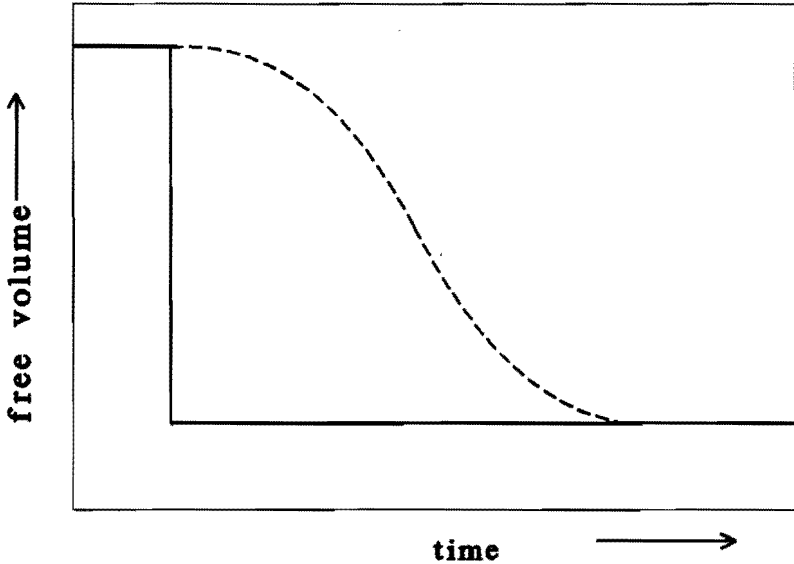


Figure 5.1. A schematic representation of the equilibrium free volume (drawn line) and the actual free volume (dashed line) in an experiment in which the temperature is changed instantaneously (a 'temperature jump' experiment).

The numerical simulation of this real time experiment proceeds along the following scheme. The specified cooling rate assures the existence of a one to one correspondence between time and temperature. According to the following procedure the stochastic process is performed:

1. Calculate the equilibrium properties (V , $\langle h \rangle_{eq}$, $\langle (\delta h_{eq})^2 \rangle$) at T and p corresponding to a time $t + \Delta t$.
2. Calculate the equilibrium distribution $\{\xi_i, i=1, n\}$ at $t + \Delta t$.
3. Compute the transition rates using the equilibrium distribution and the actual distribution $\{w_i(t), i=1, n\}$ at time t .

4. Determine the transition probabilities $P(t)$ (eq. 5.12).
5. Update the actual distribution $\{w_i(t+\Delta t), i=1,n\}$ (eq. 5.13) at time $t+\Delta t$.
6. Increment the time with Δt , and repeat steps 1-6.

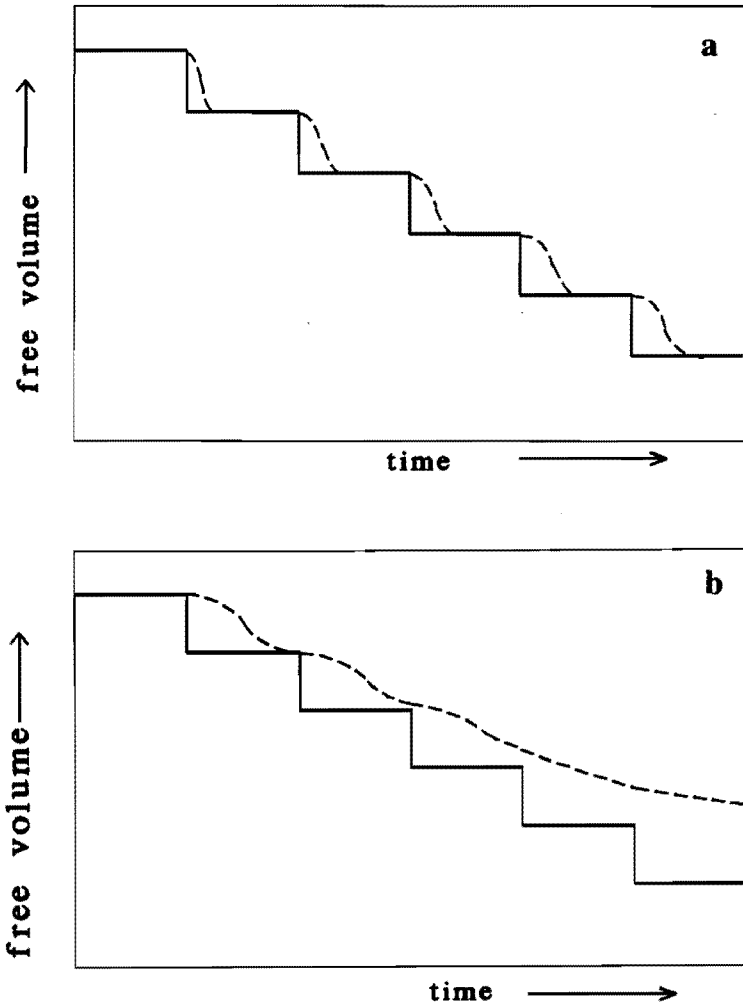


Figure 5.2. A schematic representation of the equilibrium free volume (solid line) and the actual free volume (dashed line) in a cooling experiment, at a relatively high temperature (a) and at a lower temperature (b).

The time step Δt is chosen sufficiently small to assure that the equilibrium free volume changes only approximately $5 \cdot 10^{-4}$. Typically this corresponds to a temperature change of 1K or a pressure change of 2 MPa. The matrix A (eq. 5.7) will not change significantly during Δt , and the process between t and $t + \Delta t$ can be treated as a Markov chain.

A similar experiment can be done by e.g. specifying a pressurizing rate p' or by a simultaneous change in T and p . Furthermore T' and p' can be changed at will during the simulation. E.g. at a given T and p in the glassy state one can set $T' = 0$ and $p' = 0$ and from that time on monitor the physical aging. It is thus possible to simulate the complete formation history of a polymer glass and study the influence of these parameters on the resulting thermal properties.

The thermodynamic scaling parameters p^* , V^* and T^* are estimated from experimental pVT data in the liquid state and are summarized in chapter 2. The parameters A , B and C describing the correlation between global mobility and free volume are obtained from experimental viscosimetric shift factors (chapter 4). The only parameter that must be obtained from dynamical information is the constant R in eq. 5.21. It will become clear in chapter 6 that this parameter can be estimated from different kinds of experiments.

The theory presented is based on the RSC theory, which has been extended to enable analysis of kinetic processes governing the glass transition. However, in the part that both theories have in common, several modifications have been introduced, compared to the RSC theory: the use of HH instead of SS, the description of mobility (compare with refs. 6 and 8), the use of a gaussian distribution (compare with ref. 1), the temperature independence of R and the inability of h to change instantaneously (compare with ref. 1).

5.4 Conclusions

The theory presented enables the treatment of kinetics that influence the equation of state of a glass. Most parameters can be obtained from independent measurements in the equilibrium state. Only one parameter, R , presently must be obtained from a non-equilibrium experiment.

5.5 References

1. R. E. Robertson, R. Simha and J. G. Curro, *Macromolecules*, **17**, 911 (1984).
2. R. E. Robertson, in *Computer Modeling of Polymers*, J. Bicerano, ed., Marcel Dekker Inc., New York, 1992.
3. R. E. Robertson, *J. Polym. Sci., Polym. Phys. Ed.*, **17**, 597 (1979).
4. R. Goodman, *Introduction to Stochastic Models*, Benjamin/Cummings, Menlo Park, 1988, p 127.
5. R. E. Robertson, R. Simha and J. G. Curro, *Macromolecules*, **18**, 2239 (1985).
6. R. E. Robertson, R. Simha and J. G. Curro, *Macromolecules*, **21**, 3216 (1988).
7. M. Abramowitz and I. A. Stegun, *Handbook of Mathematical Functions*, Dover Publications, New York, 1965.
8. R. E. Robertson, *Macromolecules*, **18**, 953 (1985).

Chapter 6*

Results of the stochastic glass formation theory

6.1 Introduction

In this chapter, the glass formation theory presented in chapter 5 will be mainly used to investigate the equation of state behaviour of polymer glasses, depending on formation history. In addition, relaxation behaviour and oscillatory dynamic phenomena are described. Finally the influence of thermodynamic parameters on the glass transition temperature T_g will be discussed. All computations in this chapter have been performed with the equation of state (EoS) parameters from table 2.1, the mobility parameters from table 4.1 and 4.2 and finally the additional parameters which will be listed in this chapter in table 6.1.

6.2 Temperature and pressure jumps

The most basic experiment that can be described is the volume relaxation following an instantaneous change in temperature or pressure (a jump experiment). In this application the theory presented in this work almost reduces to the RSC theory, except for the points mentioned earlier: the use of HH to describe the EoS, the description of mobility, the use of a

* Reprinted in part from: S. Vleeshouwers and E. Nies, *Macromolecules*, **25**, 6921 (1992).

Gaussian free volume distribution, the temperature independence of R and finally the inability of h to change instantaneously. In this first application we use the relaxation in a temperature jump experiment to obtain a value for R for poly(vinyl acetate) PVAC ($40^\circ\text{C}\rightarrow 37.5^\circ\text{C}^1$), as is also done by Robertson et al². The single temperature jump experiment can be described by the stochastic process. A change in the value of R basically shifts the relaxation pattern horizontally, i.e. along the time axis, see figure 6.1.

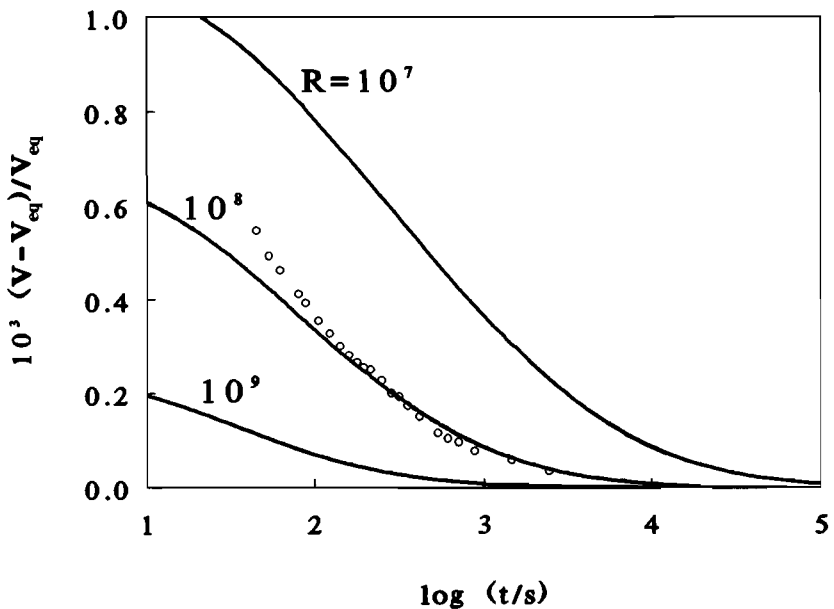


Figure 6.1. Volume relaxation for poly(vinyl acetate) after a temperature jump from 40°C to 37.5°C . Symbols, experimental¹; lines, calculations with R as indicated.

Due to the assumed finite cooling rate (in this case 0.1K/s , to mimic the reported 72s needed to obtain thermal equilibrium¹) also the shape of the curves has changed slightly. The best description of these experiments yields the value for the constant R . For polystyrene (PS) the value for R has been obtained similarly, using a temperature jump experiment from $91.82^\circ\text{C}\rightarrow 90.7^\circ\text{C}^3$. By the lack of volume relaxation data after a temperature jump for bisphenol-A polycarbonate (PC) and poly(methyl metha-

crylate) (PMMA), the constant R has been determined by fitting simulations to the experimental T_g (see paragraph 6.3). It should be noted that the numerical value of R is not attributed physical significance but is merely an adjustable parameter. The values of R for the different polymers are given in table 6.1. In these and all subsequent simulations not only the value of R , but also of N_s is kept fixed. For PS and PVAC, N_s is put equal to 50 and 26, respectively². For PMMA and PC N_s is put equal to the value for PVAC. It must be noted that changes in simulation results due to the choice of different numerical values for N_s and/or z_n are relatively small and can be compensated by a change in the effective R value. The overall shape of e.g. a relaxation curve only changes slightly. In paragraph 6.9 the sensitivity of results for N_s and z_n is discussed in detail.

Table 6.1. Parameters R used in the simulations for different polymers.

	R with use of $\mu(h)$	R with use of $\mu(h,T)$
PVAC	10^8	10^8
PS	$3 \cdot 10^8$	10^8
PC	10^{10}	$3 \cdot 10^7$
PMMA	$3 \cdot 10^{11}$	$2 \cdot 10^{13}$

In figure 6.2 the computed volume relaxation behaviour of PVAC brought about by single temperature jumps is compared to experimental results. In the simulations cooling and heating rates are put equal to 0.1 K/s, to mimic the finite experimental rates, which result in thermal equilibrium within 72s¹. The differences between the use of an expression $\mu(h)$ or $\mu(h,T)$ for mobility are also shown. It is clear that including a temperature term to describe mobility strongly changes the shape of the relaxation curves.

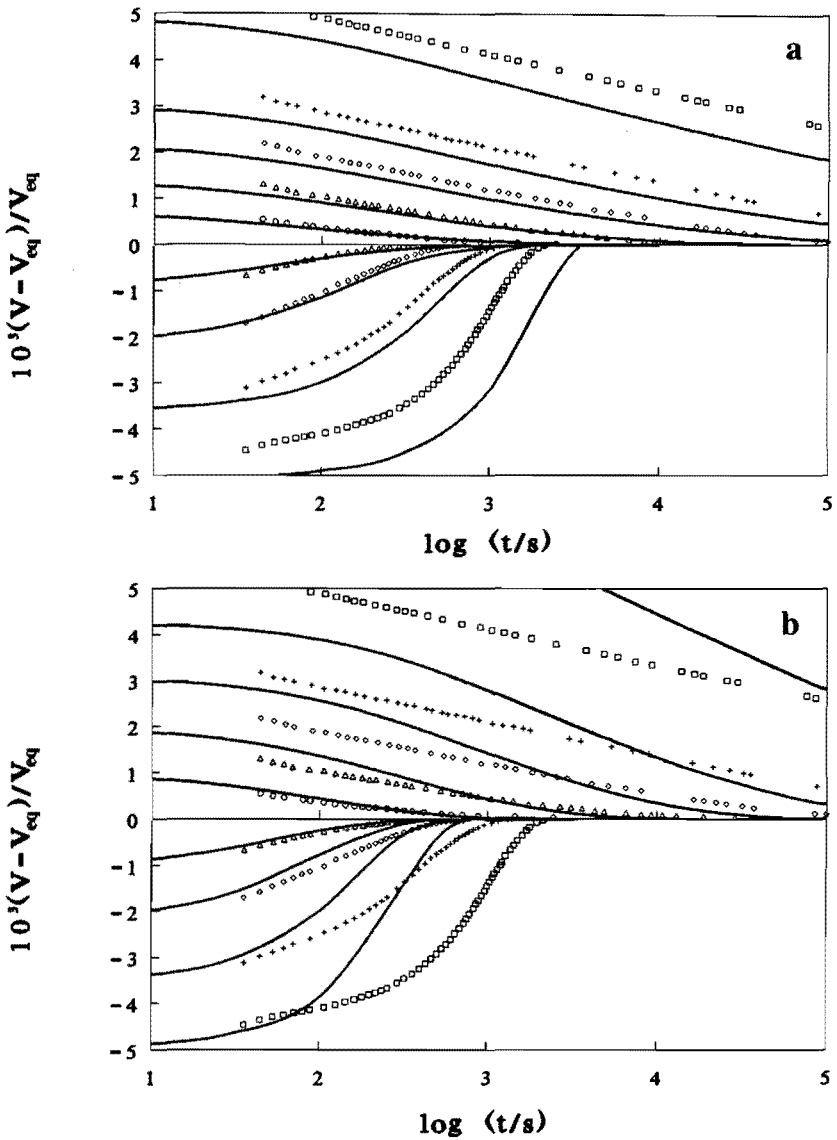


Figure 6.2. Volume departure from equilibrium versus time after single temperature jumps for PVAC. Symbols, experimental data (Kovacs⁴): $(V - V_{eq})/V_{eq} > 0$ jumps from 40°C to 37.5°C (\circ), 35°C (Δ), 32.5°C (\diamond), 30°C ($+$) and 25°C (\square); (b) jumps to 40°C $(V - V_{eq})/V_{eq} < 0$ from 37.5°C (Δ), 35°C (\diamond), 32.5°C ($+$) and 30°C (\square). Solid lines, calculated with use of (a) eq. 4.6, $\mu(h)$; (b) eq. 4.7, $\mu(h, T)$.

As discussed earlier, the typical features, i.e. non-linearity, non-uniformity and non-symmetry, can be recognized in both cases. However, the 'gap' in the effective relaxation times which is found experimentally close to equilibrium⁴, is predicted in neither case. Also the relaxation after two consecutive temperature jumps, showing an extreme, has been calculated, see figure 6.3. In such an experiment first a jump is made from a high temperature T_0 to a low temperature T_1 . After a time t_{T_1} at this temperature a second jump is made to a temperature T_2 , with $T_1 < T_2 < T_0$. The volume relaxation is monitored as a function of the time at T_2 . In the simulations, the aging time at the lowest temperature has been chosen to yield approximately the equilibrium volume immediately after the second temperature jump.

Pressure jump experiments have been published by Rehage and Goldbach³ for PS. In figure 6.4 the simulation of these volume relaxation experiments is shown. It is again emphasized that the simulation was performed with fixed R , derived from a temperature jump experiment by the same authors. The agreement shown so far is typical for the present implementation of the stochastic theory as observed earlier by Robertson et al.², who subsequently demonstrated that the agreement can be improved by adopting a temperature dependent R and more refined functions correlating the macroscopic mobility and free volume^{2,5-7}. If one wants to quantitatively describe relaxation experiments one has to keep in mind that also differences in relaxation behaviour are found between experimental data from different literature sources. Compare for example relaxation data from refs. 3 and 8-11. For the present purpose we will accept the observed deviations, bearing in mind how some of them can be resolved, and proceed with other simulation results. A more detailed analysis of the relaxation simulations shows that the range of linearity for PS for temperature jumps is $\Delta T \leq 0.25\text{K}$ and for pressure jumps $\Delta p \leq 0.5\text{ MPa}$. This has to be compared to experimental data of Rehage³, in which the linear range was found to be $\Delta T \leq 0.6\text{K}$ and $\Delta p > 2.2\text{ MPa}$.

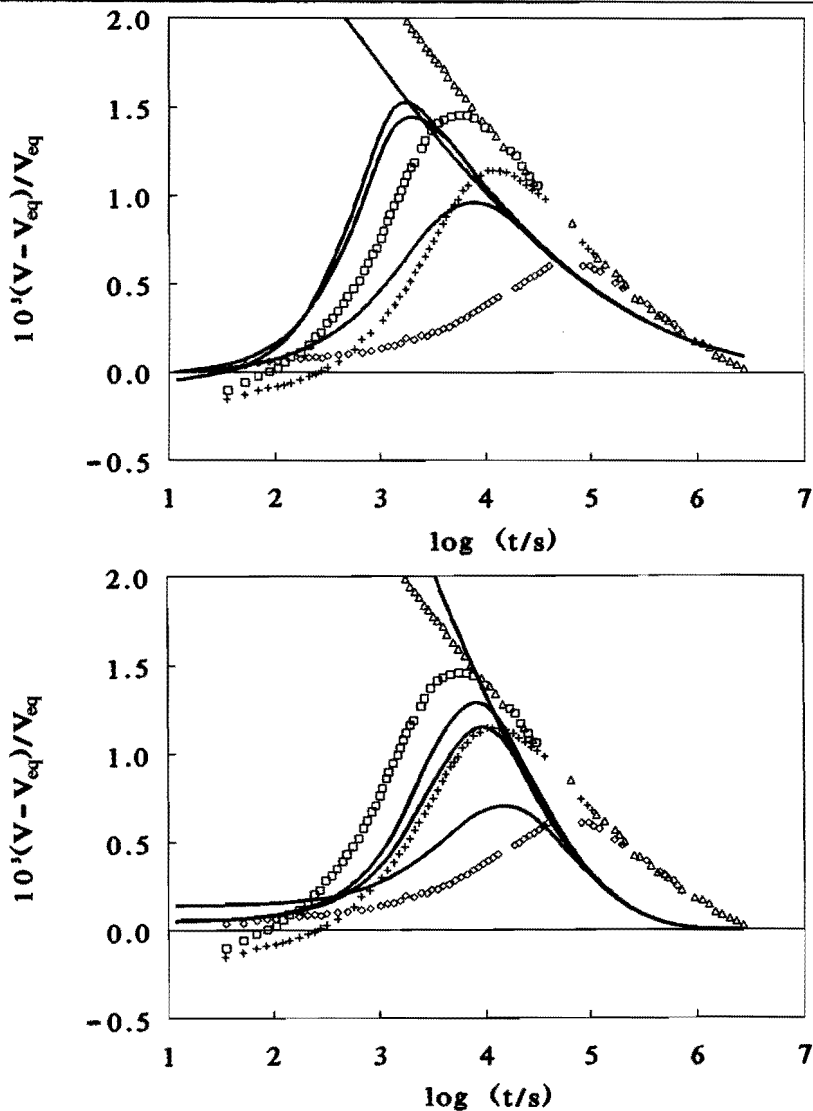


Figure 6.3. Volume departure from equilibrium versus time after two consecutive temperature jumps for PVAC. Symbols, experimental data (Kovacs⁴): jumps from 40°C to 10°C, and after $t_{10^\circ\text{C}} = 5.8 \cdot 10^5 \text{ s}$ to 30°C (\square); to 15°C, and after $t_{15^\circ\text{C}} = 5 \cdot 10^5 \text{ s}$ to 30°C ($+$); to 25°C, and after $t_{25^\circ\text{C}} = 3.2 \cdot 10^5 \text{ s}$ to 30°C (\diamond), directly to 30°C (Δ). Solid lines, calculated with use of (a) eq. 4.6, $\mu(h)$ with $t_{10^\circ\text{C}} = 900 \text{ s}$, $t_{15^\circ\text{C}} = 1500 \text{ s}$ and $t_{25^\circ\text{C}} = 1.3 \cdot 10^4 \text{ s}$; (b) eq. 4.7, $\mu(h, T)$, with $t_{10^\circ\text{C}} = 5 \cdot 10^7 \text{ s}$, $t_{15^\circ\text{C}} = 4 \cdot 10^6 \text{ s}$ and $t_{25^\circ\text{C}} = 1.1 \cdot 10^5 \text{ s}$.

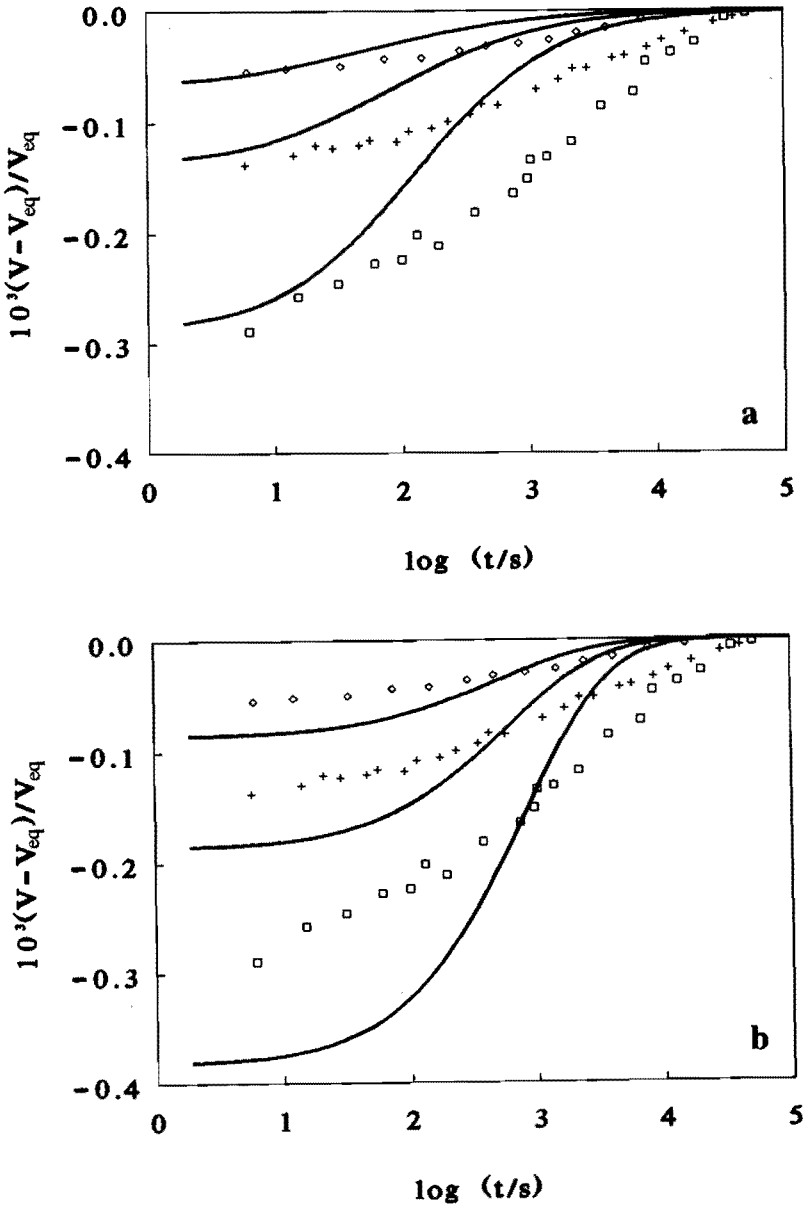


Figure 6.4. Volume departure from equilibrium versus time after single pressure jumps for PS. Symbols, experimental data³: jumps to 0.1 MPa from 2.2 MPa (\square), 1.1 MPa ($+$) and 0.56 MPa (\diamond). Solid lines, calculated with use of (a) eq. 4.6, $\mu(h)$; (b) eq. 4.7, $\mu(h, T)$.

6.3 Cooling and heating experiments

We now proceed to the simulations of more complex experiments, related to the formation of a glass. If a polymer is first cooled at a fixed rate and subsequently heated at the same rate, different results are predicted in the simulation if one uses $\mu(h)$ or $\mu(h,T)$. This is illustrated in figure 6.5. In case of $\mu(h)$, significant aging occurs during the short time (a few hours) that the polymer is in the glassy state. This results in two distinct curves for cooling and heating, due to the earlier aging. By the time the polymer is heated to temperatures around T_g , relaxation times have increased so far that a large overshoot is observed before equilibrium is obtained. If $\mu(h,T)$ is used, simulation results resemble experimental data very well. An important observation is that the best R value derived from the jump experiment gives predictions of T_g at atmospheric pressure within a few degrees of the experimental values (see table 6.3 for PS). This suggests that also the volumetric glass transition temperature, which is more commonly available than volume relaxation experiments, can be used to estimate the parameter R, which enables prediction of the volume relaxation behaviour for a given polymer under different conditions. In fact, this procedure has been followed for PC and PMMA.

In figure 6.6 the simulated glass transition temperatures T_g of PVAC and PS at ambient pressure are presented as a function of cooling rate. In the simulations T_g is identified with the intercept of the extrapolated glass and liquid like volume traces. The simulated cooling rate dependence of T_g is not linear and increases with increasing cooling rate (illustrated in figure 6.6b). Simulated values are in quite good agreement with experimental data, especially if one keeps in mind that no parameters have been adjusted for these simulations. The particular choice of eq. 4.6 or 4.7 to describe mobility has only minor influence on the predicted T_g and on the cooling rate dependence. Results for PS and PVAC are summarized in tables 6.2 and 6.3, respectively.

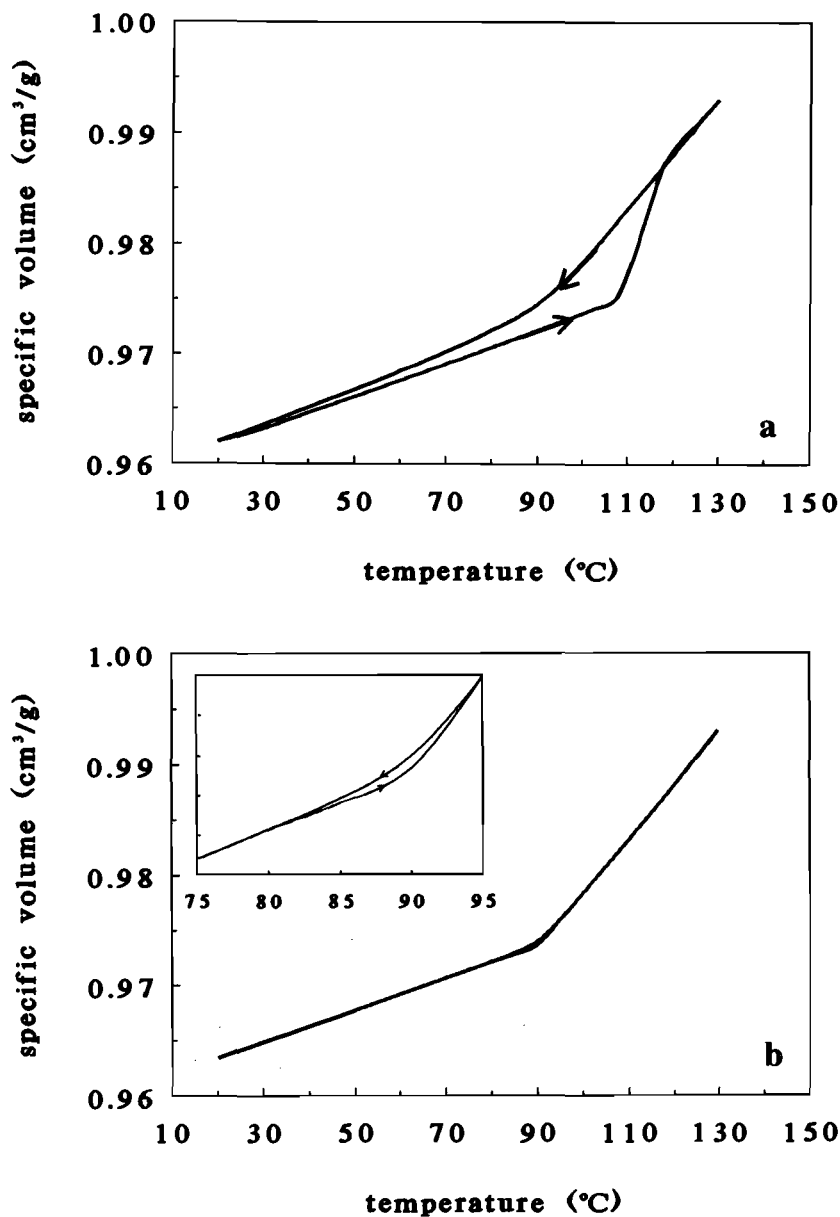


Figure 6.5. Volume versus temperature for PS during a simulation of cooling and subsequently heating, both at 10K/h: (a) $\mu(h)$; (b) $\mu(h,T)$. The inset shows the transition region.

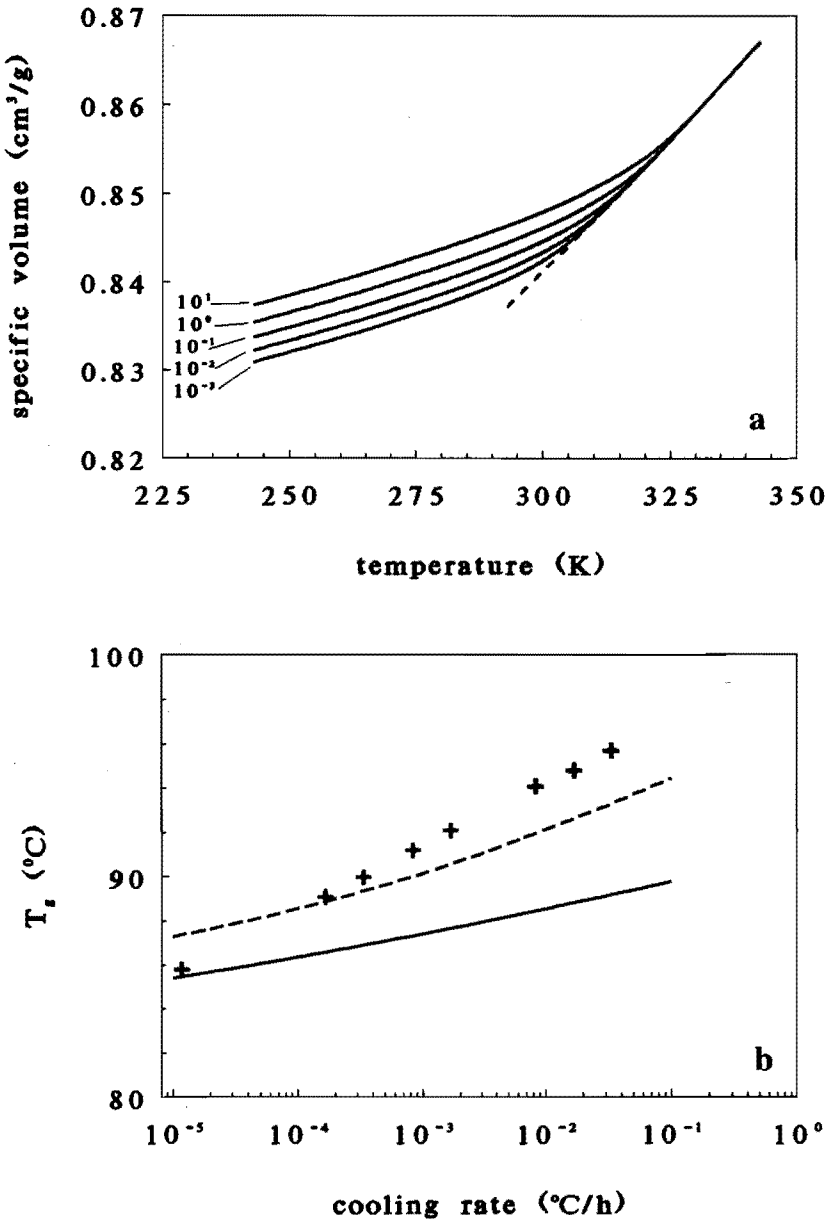


Figure 6.6. (a) Calculated volume versus temperature for indicated cooling rates for PVAC. (b) The glass transition temperature T_g for PS for indicated cooling rates; symbols, experimental; solid line, $\mu(h)$; dotted line $\mu(h,T)$.

Table 6.2. Comparison of calculated quantities with experimental data for PVAC.

property	exper.	calculated,		formation history		fig.
		using $\mu(h)$	using $\mu(h,T)$	p MPa	cooling rate q K/s	
T_g (K)		314.5	319.2	0.1	10	6.6a
		310.0	314.9	0.1	1	6.6a
		306.2	310.8	0.1	10^{-1}	6.6a
		303.1	306.3	0.1	10^{-2}	6.6a
		300.7	304.0	0.1	10^{-3}	6.6a
$dT_g/d(\log q)$ (K)	2.9^{12}	3.5	3.8	0.1	10^{-3} -10	6.6a
T_g (K)	304.7^1	301.0	304.4	0.1	$1.39 \cdot 10^{-3}$	6.8
	309.7^1	306.3	309.0	20	$1.39 \cdot 10^{-3}$	6.8
	314.2^1	314.0	312.4	40	$1.39 \cdot 10^{-3}$	6.8
	321.6^1	326.1	319.1	80	$1.39 \cdot 10^{-3}$	6.8
dT_g/dp (K MPa $^{-1}$)	0.212^1	0.33	0.185	0.1-80	$1.39 \cdot 10^{-3}$	6.8
α (0.1MPa-glass, 273K) (10^{-4} K $^{-1}$)	2.86^1	2.24	1.58	0.1	$1.39 \cdot 10^{-3}$	6.10
	2.59^1	2.03	1.41	80	$1.39 \cdot 10^{-3}$	6.10
β (0.1MPa-glass, 273K) (10^{-4} MPa $^{-1}$)	2.75^1	2.64	2.64	0.1	$1.39 \cdot 10^{-3}$	6.10
	2.54^1	2.32	2.33	80	$1.39 \cdot 10^{-3}$	6.10
α (80MPa-glass, 273K) (10^{-4} K $^{-1}$)	2.94^1	1.96	1.64	0.1	$1.39 \cdot 10^{-3}$	6.11
	2.63^1	1.74	1.47	80	$1.39 \cdot 10^{-3}$	6.11
β (80MPa-glass, 273K) (10^{-4} MPa $^{-1}$)	2.70^1	2.65	2.16	0.1	$1.39 \cdot 10^{-3}$	6.11
	2.42^1	2.31	2.30	80	$1.39 \cdot 10^{-3}$	6.11

Table 6.3. Comparison of calculated quantities with experimental data for PS.

property	exper.	calculated,		formation history		
		using $\mu(h)$	$\mu(h,T)$	p MPa	cooling rate q K/s	fig.
T_g (K)		362.9	366.6	0.1	10^{-1}	6.6b
		361.7	365.3	0.1	10^{-2}	6.6b
		360.6	363.3	0.1	10^{-3}	6.6b
		359.5	361.7	0.1	10^{-4}	6.6b
		358.5	360.4	0.1	10^{-5}	6.6b
$dT_g/d(\log q)$ (K)	2.9^9	1.1	1.8	0.1	10^{-5} -0.1	6.6b
T_g (K)	365.8^9	360.9	364.1	0.1	$2.78 \cdot 10^{-3}$	
		372.2	370.5	20	$2.78 \cdot 10^{-3}$	
		383.3	379.2	40	$2.78 \cdot 10^{-3}$	
		392.6	388.2	60	$2.78 \cdot 10^{-3}$	
		402.8	396.3	80	$2.78 \cdot 10^{-3}$	
dT_g/dp (K MPa $^{-1}$)	0.316^{13}	412.0	406.3	100	$2.78 \cdot 10^{-3}$	
		0.51	0.28	0.1-100	$2.78 \cdot 10^{-3}$	
α (0.1MPa-glass, 280K) (10^{-4} K $^{-1}$)	1.97^{13}	1.54	1.47	0.1	$2.78 \cdot 10^{-3}$	
	1.77^{13}	1.32	1.26	100	$2.78 \cdot 10^{-3}$	
β (0.1MPa-glass, 280K) (10^{-4} MPa $^{-1}$)	2.62^{13}	3.21	3.24	0.1	$2.78 \cdot 10^{-3}$	
	2.14^{13}	2.68	2.67	100	$2.78 \cdot 10^{-3}$	

The simulated cooling rate dependence of T_g for PC and PMMA is summarized in tables 6.4 and 6.5, respectively. The deviations between simulations and experimental values of cooling rate dependence appear not to be systematic. For example, for PS too large a value is predicted, for PMMA too low a value.

From the above presented simulations the mobility in the glass during the cooling experiment can be plotted as a function of temperature. This is shown in figure 6.7 for PS and PVAC, together with experimental dynamic mechanical data. It is clear that over a limited temperature range simulations result in reasonable agreement with experimental data for the PVAC and PS glasses with the use of mobility data $\mu(h,T)$. From figure 6.7b it can be anticipated that the mobility in a simulated glass will be

Table 6.4. Comparison of calculated quantities with experimental data for PC.

property	exper.	calculated,		formation history	
		$\mu(h)$	$\mu(h,T)$	p MPa	cooling rate q K/s
T_g (K)		414.3	416.3	0.1	10^{-1}
		411.6	412.8	0.1	10^{-2}
		409.7	409.8	0.1	10^{-3}
		407.8	407.2	0.1	10^{-4}
$dT_g/d(\log q)$ (K)	2.5^9	2.2	3.0	0.1	10^{-4} -0.1
T_g (K)	412.1^9	411	411.5	0.1	$2.78 \cdot 10^{-3}$
		435	426.2	50	$2.78 \cdot 10^{-3}$
		458	439.3	100	$2.78 \cdot 10^{-3}$
dT_g/dp (K MPa $^{-1}$)	0.36^9	0.47	0.278	0.1-100	$2.78 \cdot 10^{-3}$
α (0.1MPa-glass,353K) (10^{-4} K $^{-1}$)	2.55^{14}	1.75	1.56	0.1	$2.78 \cdot 10^{-3}$
		1.91 14	1.13	1.39	100
β (0.1MPa-glass,353K) (10^{-4} MPa $^{-1}$)	2.36^{14}	2.63	2.62	0.1	$2.78 \cdot 10^{-3}$
		1.97 14	2.20	2.22	100

^a After reinterpretation of the pVT data by Zoller 14 . He reports a value 0.52 K/MPa.

Table 6.5. Comparison of calculated quantities with experimental data for PMMA.

property	exper.	formation history			
		calculated, using		p	cooling rate q
		$\mu(h)$	$\mu(h,T)$	MPa	K/s
T_g (K)		377.6	375.8	0.1	10^{-1}
		376.1	374.2	0.1	10^{-2}
		374.5	372.9	0.1	10^{-3}
		372.4	371.6	0.1	10^{-4}
$dT_g/d(\log q)$ (K)	3.3^9	1.7	1.4	0.1	10^{-4} -0.1
T_g (K)	373.4^9	373.5	373.6	0.1	$2.78 \cdot 10^{-3}$
		395.9	385.2	20	$2.78 \cdot 10^{-3}$
		418.5	395.7	100	$2.78 \cdot 10^{-3}$
dT_g/dp (K MPa $^{-1}$)	0.236^{15}	0.45	0.22	0.1-80	$2.78 \cdot 10^{-3}$
α (0.1MPa-glass,303K) (10^{-4} K $^{-1}$)	1.93^{15}	1.65	1.51	0.1	$2.78 \cdot 10^{-3}$
	1.24^{15}	1.19	1.34	100	$2.78 \cdot 10^{-3}$
β (0.1MPa-glass,303K) (10^{-4} MPa $^{-1}$)	2.72^{15}	2.69	2.70	0.1	$2.78 \cdot 10^{-3}$
	2.24^{15}	2.24	2.25	100	$2.78 \cdot 10^{-3}$

too low with the use of $\mu(h,T)$ and too high with the use of $\mu(h)$. In fact this has indeed be found. Using $\mu(h)$, too fast aging is found (figures 6.2a, 6.3a and 6.5a). The use of $\mu(h,T)$, on the other hand, results in a complete freeze in at low temperatures, in contradiction to experimental data¹¹. If one is particularly interested in a quantitative description of aging one might consider to use C in eq. 4.7 as an adjustable parameter. A value for $C \neq 0$ smaller than the value given in table 4.2 improves the description of relaxation processes. Because this approach introduces deviations in other simulations, it will not be pursued here.

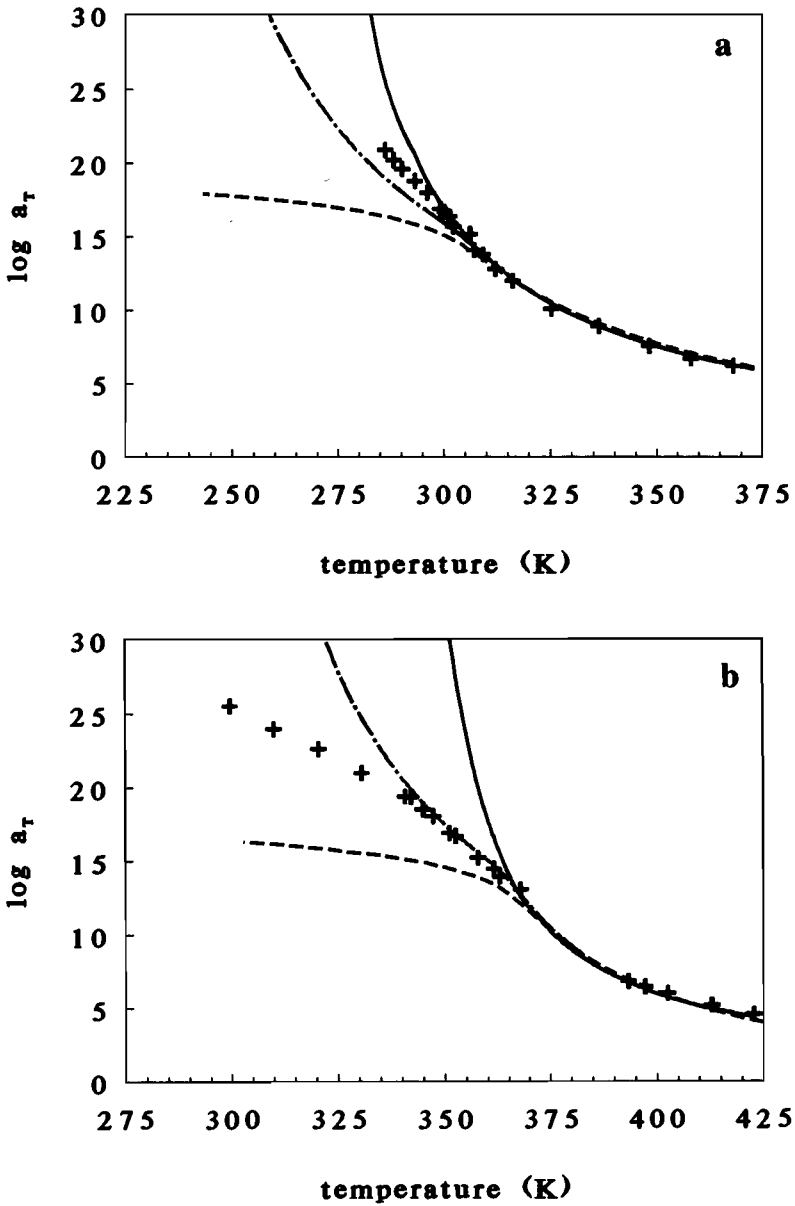


Figure 6.7. Shift factor in the equilibrium and glassy state at atmospheric pressure; (a) PVAC, (b) PS. Calculated from $\mu(h)$ (dashed line); from $\mu(h,T)$ (dash dotted line); equilibrium (solid line); symbols, experimental data (PVAC¹⁶, PS¹⁷).

6.4 The influence of pressure

The influence of pressure on the formation of a glass is shown in figure 6.8 for PVAC. The simulated formation conditions are chosen to mimic the experimental formation history, i.e. cooling rate and pressure of the glass for which data have been reported¹. The dependence of volume on temperature under isobaric cooling is depicted. The agreement for the 0.1MPa curve is excellent in the case $\mu(h)$: maximum deviations ΔV between experimental and theoretical specific volumes do not exceed $2 \cdot 10^{-3} \text{ cm}^3/\text{g}$. If $\mu(h,T)$ is used deviations do not exceed $7 \cdot 10^{-3} \text{ cm}^3/\text{g}$. Although this value is comparable to the experimental accuracy, it is clear that deviations with experimental data are systematic. At a pressure $p=80\text{MPa}$ the maximum deviation ΔV remains less than $8 \cdot 10^{-3} \text{ cm}^3/\text{g}$. If $\mu(h)$ is used the increasing deviations with pressure between theory and experiment in the glassy state can be mainly attributed to too large a predicted value of the pressure dependence of the glass transition temperature (dT_g/dp). If $\mu(h,T)$ is used, the predicted value for the pressure dependence of T_g is excellent, compared to the experimental value (see table 6.2 for PVAC and tables 6.3-6.5 for other polymers). However, still the predicted value for the glass is too high, due to a low thermal expansion coefficient in the glass. This is also the cause of the too high a predicted volume of the 0.1MPa glass. In tables 6.2-6.5 besides the pressure dependence of the glass transition temperature T_g , also values for the thermal expansion coefficient α_g , extracted from the simulations, are summarized and compared with experimental data.

In figure 6.9 the h,T,p results corresponding to the V,T,p data from figure 6.8 are shown. From this it can be concluded that the change in specific volume in the glassy state is mainly due to changes in lattice cell volume and not to changes in free volume, for both $\mu(h)$ and $\mu(h,T)$ simulation.

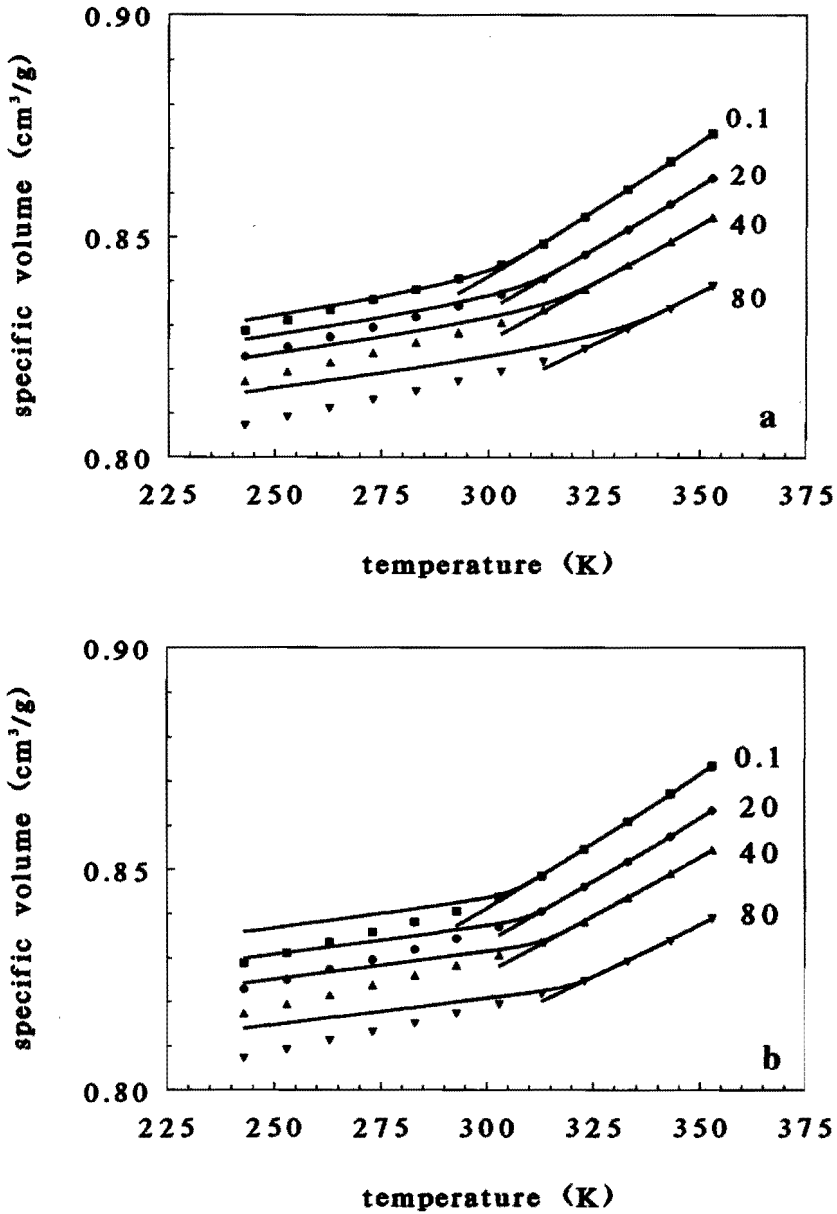


Figure 6.8. Volume versus temperature for indicated formation pressures in MPa for PVAC at a cooling rate 5K/h. Symbols, experimental; solid lines, calculated isobars: (a) $\mu(h)$; (b) $\mu(h, T)$.

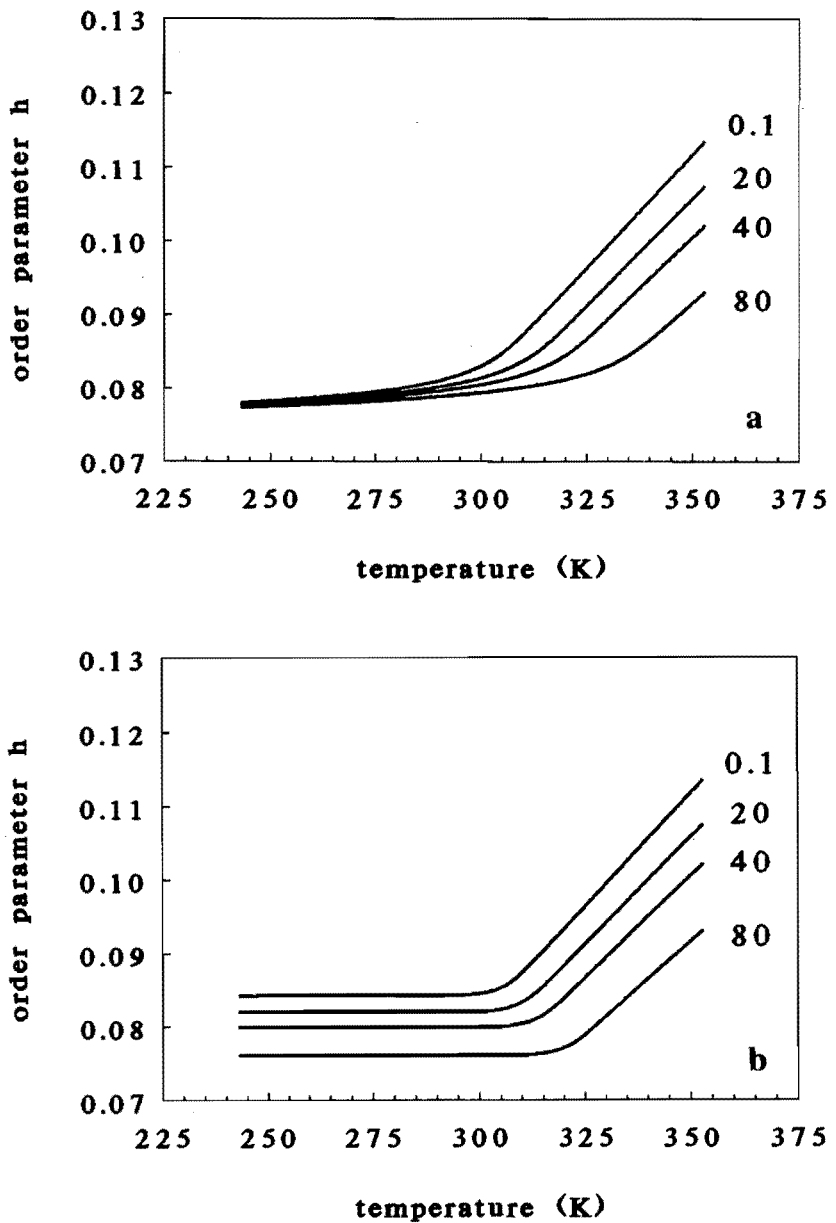


Figure 6.9. Order parameter h versus temperature for indicated pressures in MPa for PVAC at a cooling rate 5K/h. Solid lines, calculated isobars: (a) $\mu(h)$; (b) $\mu(h,T)$.

This is in contrast with results obtained by Simha following a different approach, discussed also in chapter 2. McKinney and Simha¹⁸ extracted the free volume parameter h from the experimental pVT data. The parameter h obtained in this way depends on temperature and pressure. From this analysis it was clear that changes of h had to be assumed to describe the EoS behaviour of the glass. These findings are consistent with the too low a thermal expansion coefficient in the simulated glasses: here changes in h are almost absent in the case $\mu(h)$ (see figure 6.9a) and complete absent in the case $\mu(h,T)$ (see figure 6.9b).

From the simulations it is found that the equilibrium free volume at the glass transition temperature, h_{T_g} , is practically constant if the mobility is described as $\mu(h)$. Thus, in this case, the glass transition can be regarded as a practical iso-free volume transition. For different polymers, different values for h_{T_g} are observed. Because the value of h_{T_g} depends on cooling rate it is certainly not a material constant. The iso-free volume condition seems to be related to the assumption that the mobility depends on the free volume only, eq. 4.6. However, the experimental pressure dependence¹ of T_g yields a linear pressure dependence for h_{T_g} when analyzed with the HH theory

$$h_{T_g} = 0.084 - 8.57 \cdot 10^{-5} p, \quad p \text{ in MPa} \quad (6.1)$$

If mobility is defined as a function $\mu(h,T)$ the T_g can no longer be considered as 'iso free volume' as can be seen from figure 6.9b. Now the experimental pressure dependence of T_g (and therefore also of h_g) is described almost quantitatively (see table 6.2). Also for other polymers comparable results have been found (tables 6.3-6.5).

The simulated pVT behaviour of a PVAC glass formed by cooling at 0.1MPa and by subsequently pressurizing is shown in figure 6.10 together with experimental data¹. Once more the experimental formation history was reproduced accurately. In the case of $\mu(h)$ the maximum deviation between experimental and theoretical volume ΔV is smaller than $3 \cdot 10^{-3} \text{ cm}^3/\text{g}$.

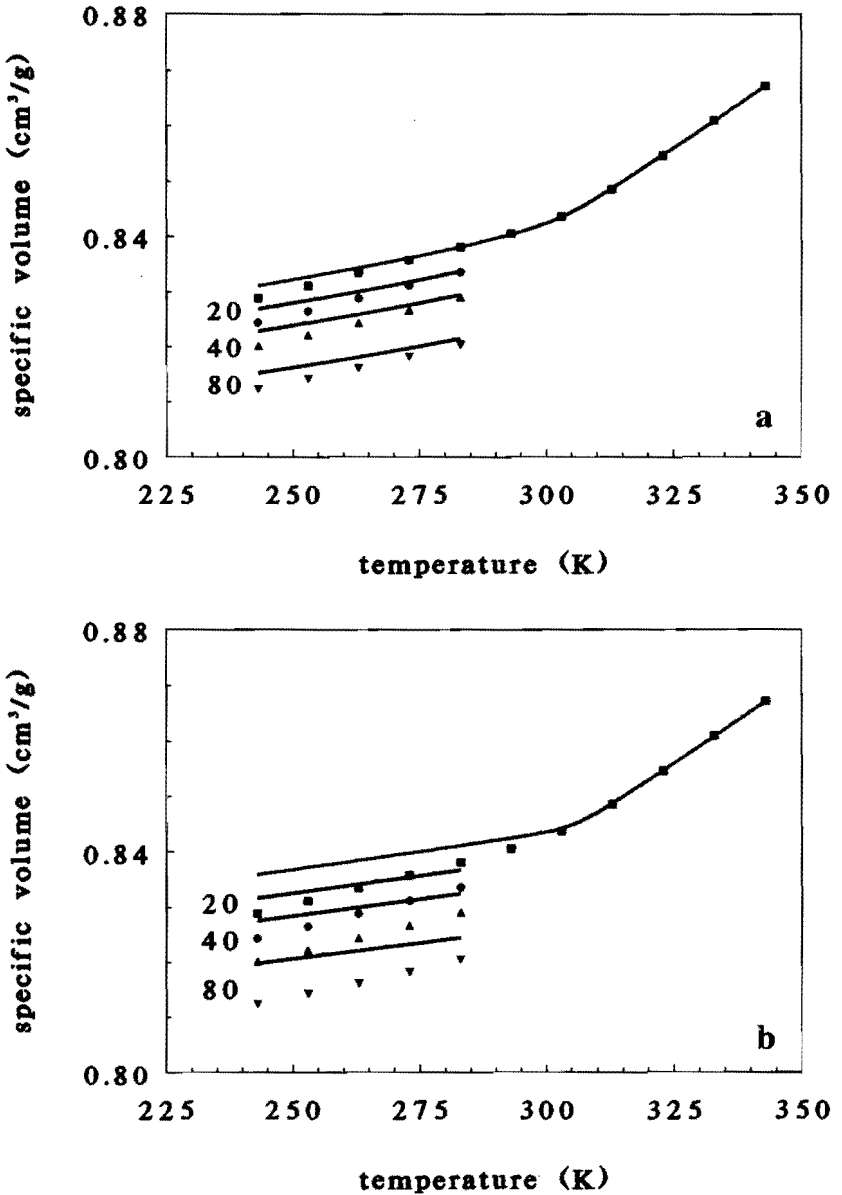


Figure 6.10.

Volume versus temperature for a PVAC glass formed by cooling at 5 K/h at 0.1 MPa and subsequently pressurizing to the indicated pressures in MPa. Symbols, experimental; solid lines, calculated isobars: (a) $\mu(h)$; (b) $\mu(h, T)$.

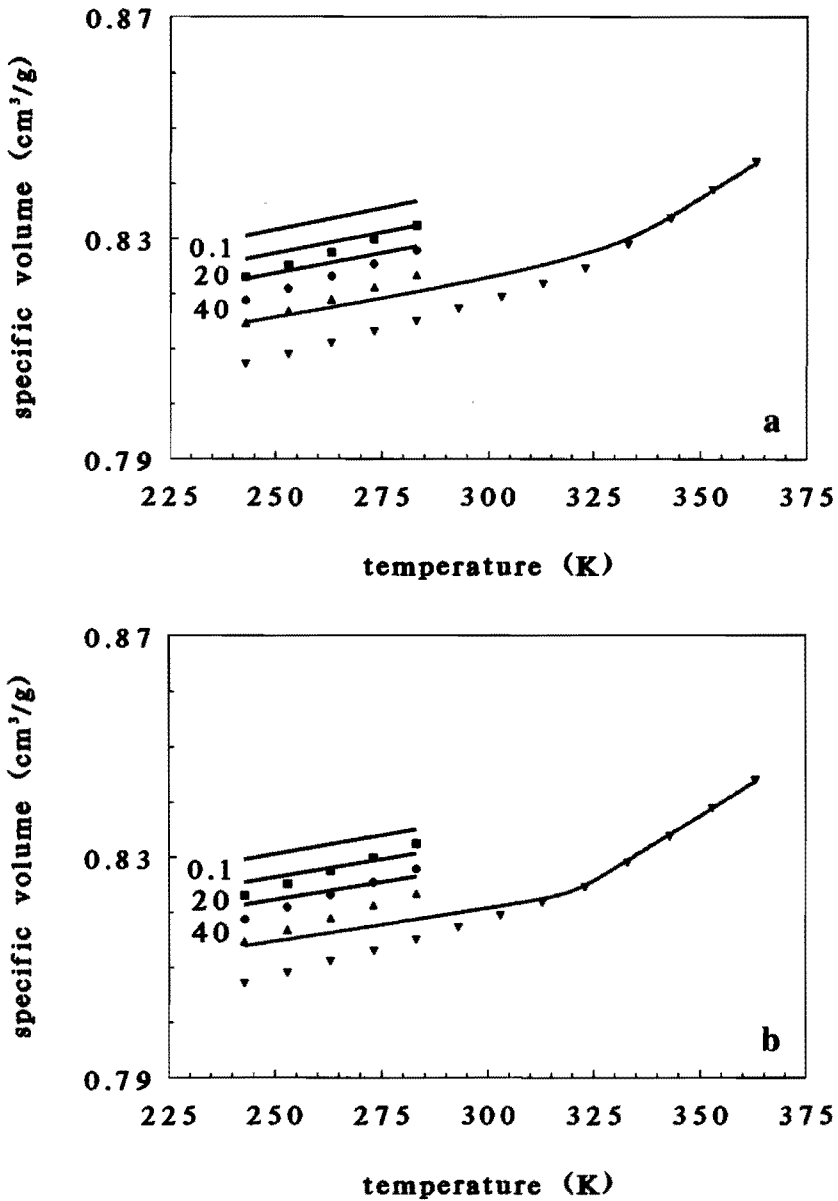


Figure 6.11.

Volume versus temperature for a PVAC glass formed by cooling at 5 K/h at 80 MPa and subsequently depressurizing to the indicated pressures in MPa. Symbols, experimental¹; solid lines, calculated isobars: (a) $\mu(h)$; (b) $\mu(h,T)$.

If $\mu(h,T)$ is used, the simulation results are systematically too high, due to a complete freeze-in of h . For a PVAC glass formed by cooling a melt at elevated pressure ($p=80$ MPa) and by subsequently depressurizing, the results are depicted in figure 6.11, together with experimental data¹. With the use of $\mu(h)$ the deviations ΔV are larger ($\Delta V < 8 \cdot 10^{-3}$ cm³/g) than for the 0.1MPa-glass and can be mainly attributed to the overestimated pressure dependence of the glass transition temperature, as explained earlier. For $\mu(h,T)$ the deviations, which do not exceed $7 \cdot 10^{-3}$ cm³/g, are again due to too low a thermal expansion in the glass. The calculated isothermal compressibilities β_g and thermal expansion coefficient α_g of glasses formed at high and low pressure are summarized and compared with experimental data in table 6.2 for PVAC. For other polymers similar results are obtained, presented in tables 6.3-6.5.

6.5 Dynamic bulk compressibility

So far, the influences of pressure, cooling rate, etc. on the EoS of a polymer glass have been presented. However, also dynamic properties in the melt and glass can be simulated without any new parameters. Decreasing the experimental time scale, c.q. increasing the rate of temperature and/or pressure changes, shifts the α -transition to higher temperatures. This is shown from the simulation of the dynamic compressibility of PVAC. In the simulations a sinusoidal and isothermal pressure change with an amplitude of 0.2MPa (this is well within the linear region) and a cycle frequency of ν Hz is used. After four cycles a steady-state response is observed. From the phase shift between the sinusoidal pressure and the response of the system (the volume) an analysis is made in terms of a storage and loss component B' and B'' , respectively, of the dynamic bulk compressibility B . From B' and B'' also $\tan \delta$ is calculated. In figure 6.12

the isothermal compressibility is plotted versus frequency for several temperatures.

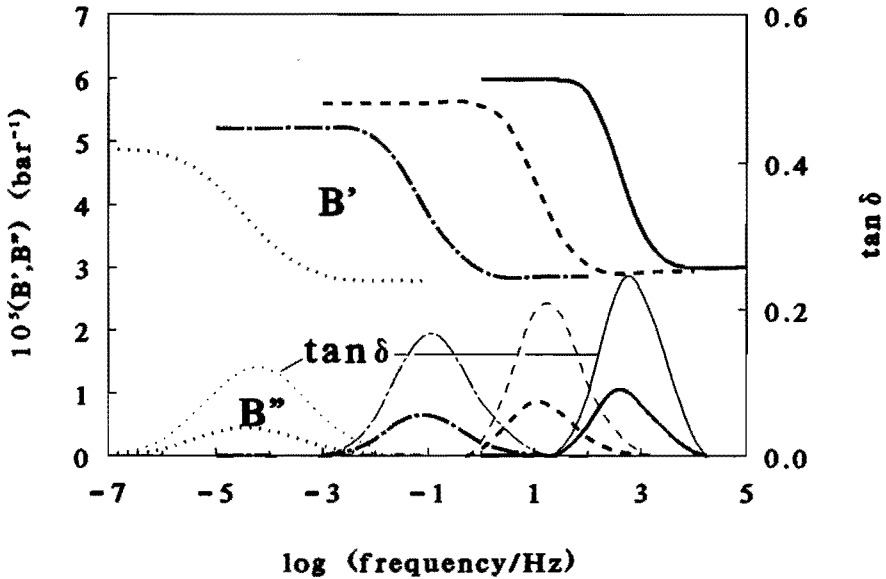


Figure 6.12. *Equilibrium dynamic bulk compressibility versus frequency at 0.1 MPa for PVAC: the storage compressibility B' , the loss compressibility B'' and $\tan \delta$ at 75°C (—), 60°C (---), 45°C (-·-·) and 30°C (···).*

It is clear that for each temperature an increase of the frequency results in a transition from a melt state (high B') to a glassy state (low B'), via a transition region where B'' and $\tan \delta$ reach a maximum. As is also found experimentally¹⁹ the maximum in $\tan \delta$ is always found to be located at higher frequencies, compared to the maximum in B'' . In figure 6.13 the dynamic bulk compressibility is plotted versus the temperature for several frequencies. These results can be compared qualitatively to experimental data by McKinney and Belcher²⁰ on a PVAC sample which has a $T_g = 17^\circ\text{C}$ due to a slight contamination. A satisfying agreement is obtained. From the assumption that underlie the calculations, i.e. a temperature dependent free

volume distribution and a coupling between local free volume and relaxation times, it can be expected that calculated dynamic behaviour will not be rheologically simple: because the shape of the relaxation time distribution depends on temperature, pressure and time, time-temperature superposition is not strictly obeyed. However, the effects on $\tan \delta$ are small, resulting in a practical time-temperature equivalence.

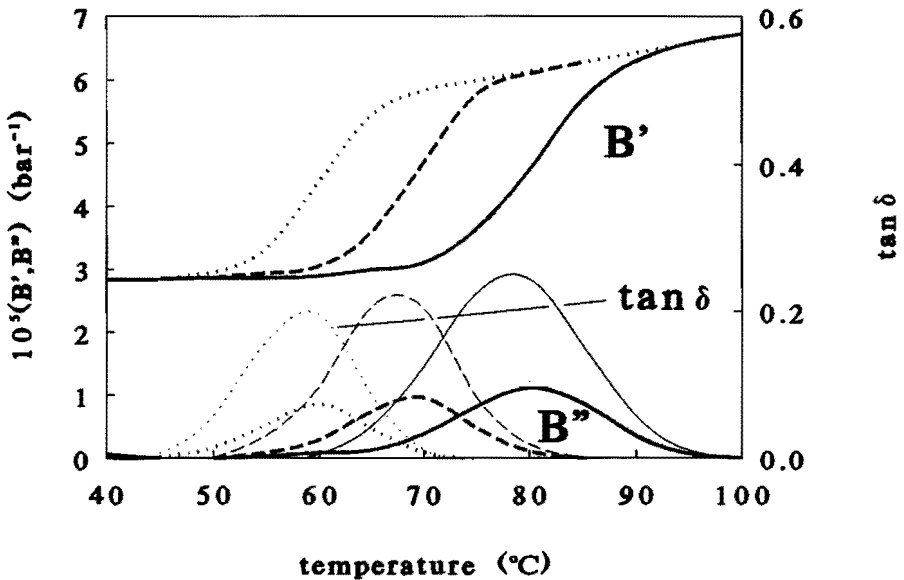


Figure 6.13. Equilibrium dynamic bulk compressibility versus temperature at 0.1 MPa for PVAC: the storage compressibility B' , the loss compressibility B'' and $\tan \delta$ at 1000 Hz (—), 100 Hz (---) and 10 Hz (···).

6.6 Dynamic light scattering

Similarly to the dynamic bulk compressibility, dynamic light scattering (DLS) can be considered related to the compressibility of the system. The time correlation function $C(t)$ is related to the longitudinal bulk compli-

ance²¹ and is by approximation equal to the compressional compliance²². The function $C(t)$ can thus be simulated by the relaxation of volume after an instantaneous pressure jump Δp . In figure 6.14 the predicted $C(t)$ for PS at 105.1°C is compared to experimental data²³, which are published in the form of a stretched exponential (eq. 3.15). It is clear that the predicted position in time is shifted 2-3 decades towards shorter times. Also discrepancies in shape are found, the experimental correlation function spanning a considerably wider time span than the simulated one.

Because DLS experiments can be performed in the polymer melt, that is in the equilibrium state, the use of DLS to obtain the value for R (eq. 5.21) enables prediction of the glass transition with *only* parameters

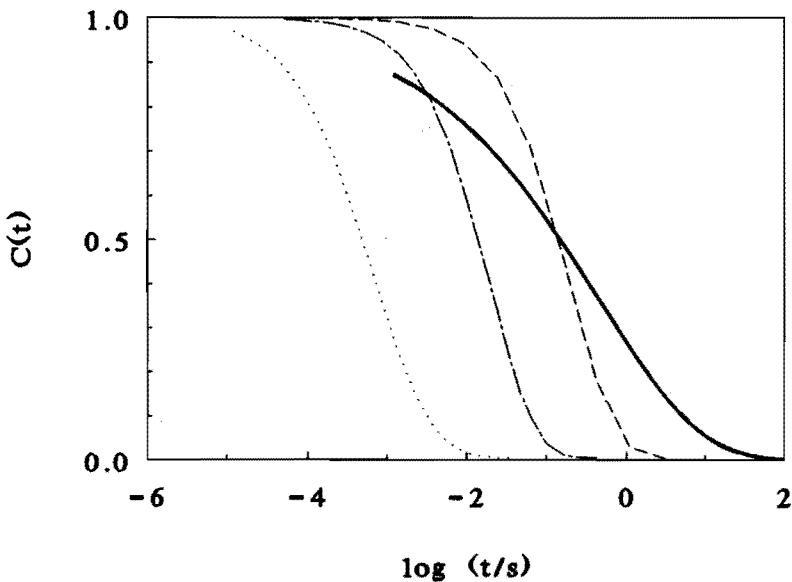


Figure 6.14. Dynamic light scattering time correlation function for PS at 105.1°C, 0.1MPa; experimental²³ (bold line); calculated with the use of $\mu(h)$ (dotted line); calculated with $\mu(h,T)$ (dash dotted line); calculated with an optimal value for R (dashed line).

obtained in the polymer melt (pVT data, dynamic mechanical shift factors, DLS data). As an example, the location of the correlation function in the DLS experiment for PS at 105.1°C has been used to fix the value for R: a value $R=10^7$ is obtained with $\mu(h,T)$. The use of this value for R results in a predicted value for PS of $T_g=359.5\text{K}$ at atmospheric pressure, only 6K lower than the experimental value⁹.

From DLS data²³ (see e.g. figure 6.14) and from volume relaxation data after a pressure jump³ (see e.g. figure 6.4) it can be estimated that the complete relaxation after a pressure jump takes place in a time range of about 5-6 decades, whereas in the simulations this time range is only 3-4 decades. The origin of this discrepancy is not clear.

6.7 Enthalpy, entropy and density fluctuations

In previous paragraphs of this chapter the behaviour of volume has been presented. As explained in chapter 5 the central quantities in the glass formation theory are the order parameter h and its distribution. From h the volume can be evaluated (eq. 2.13), as is done in the first part of this chapter. Using the appropriate equations, also the values for e.g. enthalpy, entropy and density fluctuations can be obtained from h .

The configurational part of the enthalpy H can be obtained using eq. 2.18. In figure 6.15 the calculated enthalpy is plotted for PVAC glasses formed at different pressures using $\mu(h)$. The volume of these glasses has already been presented in figure 6.8a. As an example, at 30°C and 0.1MPa simulations yield $\Delta H=H_{\text{act}}-H_{\text{eq}}=0.25\text{ J/g}$ for a cooling rate 5K/h and $\Delta H=3.9\text{ J/g}$ for a cooling rate of 1 K/s. Experimental data by Cowie et al.²⁴ show an initial ΔH at 30°C of 1.9 J/g for a quenched PVAC glass. Experimental data on a PVAC glass cooled at 0.31 K/min by Sasabe and Moynihan¹² yield $\Delta c_p=c_{p,l}-c_{p,g}=0.5\text{ J/gK}$ at 30°C. For the same cooling rate calculations yield $\Delta c_p=0.32\text{ J/gK}$.

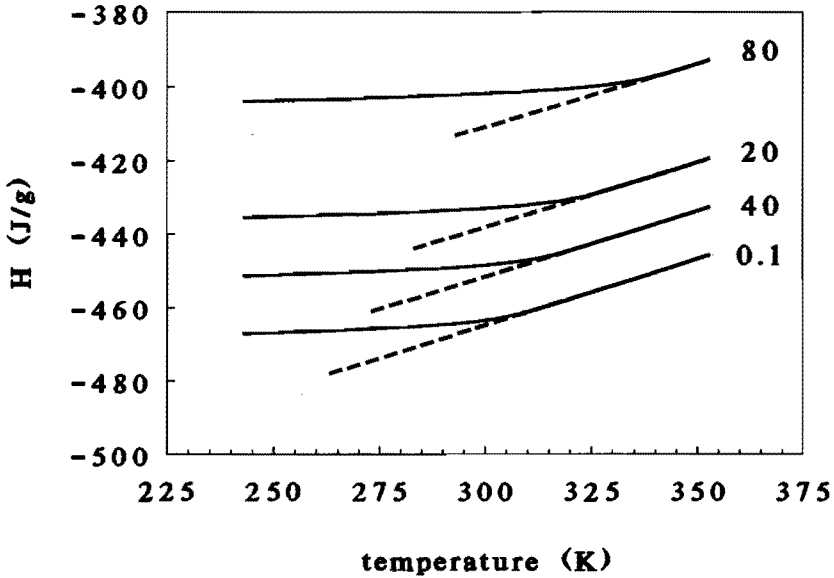


Figure 6.15. *Enthalpy versus temperature for PVAC glasses formed by cooling at 5 K/h at the indicated pressures in MPa; actual value H_{act} (solid lines), extrapolated equilibrium value H_{eq} (dashed lines).*

The simulations of differential scanning calorimetry (DSC) experiments (cooling at 40 K/min to the aging temperature, aging, further cooling at 40 K/min to 300K and subsequent heating at 10 K/min) on PS are compared to experimental data²⁵ in figure 6.16. The height of the normalized c_p peaks shows excellent agreement with experiments, the location is shifted to lower temperatures over about 8K.

The entropy S can be evaluated from h , using eq. 2.16. Results for PVAC glasses formed at different pressures (for which the volume was shown in figure 6.8a and the enthalpy in figure 6.15) are presented in figure 6.17.

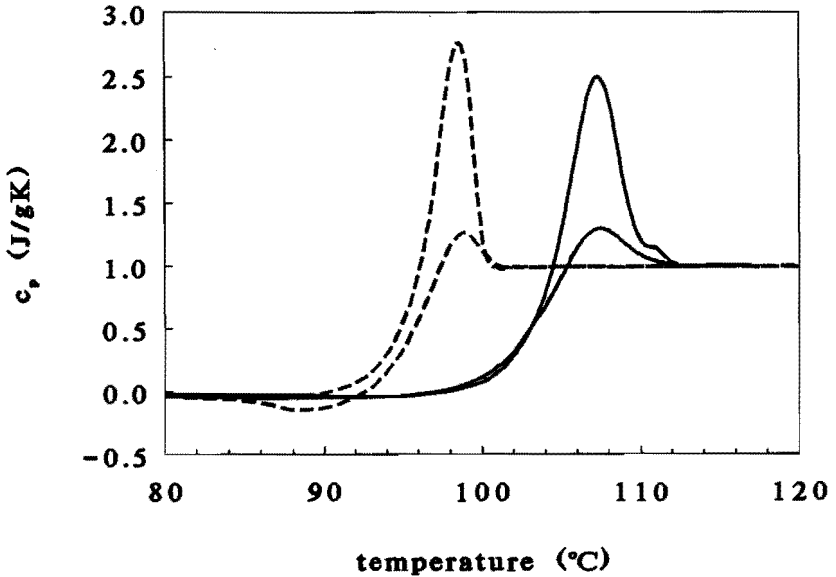


Figure 6.16. The specific heat c_p versus temperature for PS during heating at 40 K/min from 300K after the following thermal history: cooling at 10 K/min from 420K to T_a , aging at T_a during a time t_a , cooling at 10 K/min from T_a to 300K. Lower curves: $t_a=0s$ (simulations, dashed line; experimental²⁵, solid line); upper curve $t_a=3600s$ (simulations, dashed line; experimental²⁵, solid line).

The distribution of free volume used in the theory presented is based on calculations of fluctuations of free volume at a fixed temperature, volume and number of particles N , see eq. 2.23. Therefore these fluctuations are not directly related to e.g. density fluctuations, expressed at T and N constant²⁶, eq. 2.22. By evaluating the term $(\partial\mu/\partial N)_{T,v}$ in the non-equilibrium case Lee et. al.²⁷ have presented a method to calculate the density fluctuations based on the hole theory. Results of calculations of density fluctuations in a simulated glass are presented in figure 6.18 for PS.

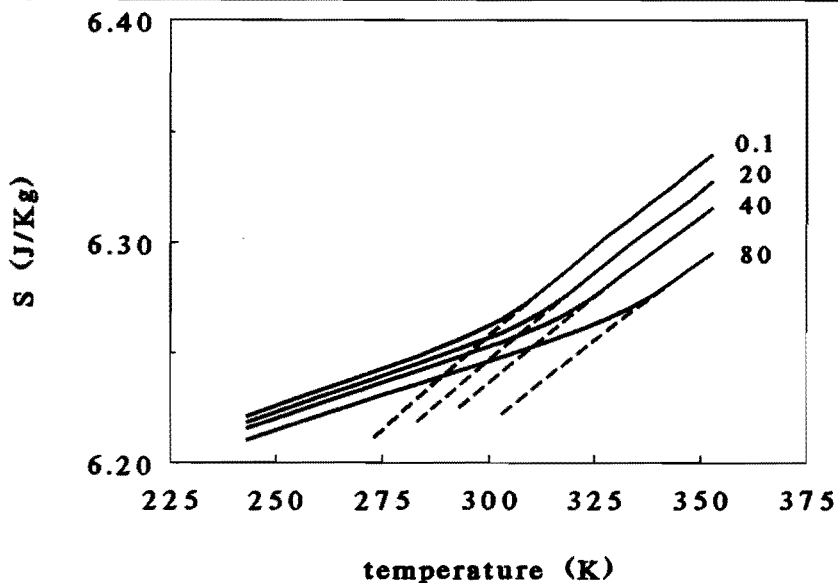


Figure 6.17. Entropy versus temperature for PVAC glasses formed by cooling at 5 K/s at the indicated pressures in MPa; actual value S_{act} (solid lines), extrapolated equilibrium value S_{eq} (dashed lines).

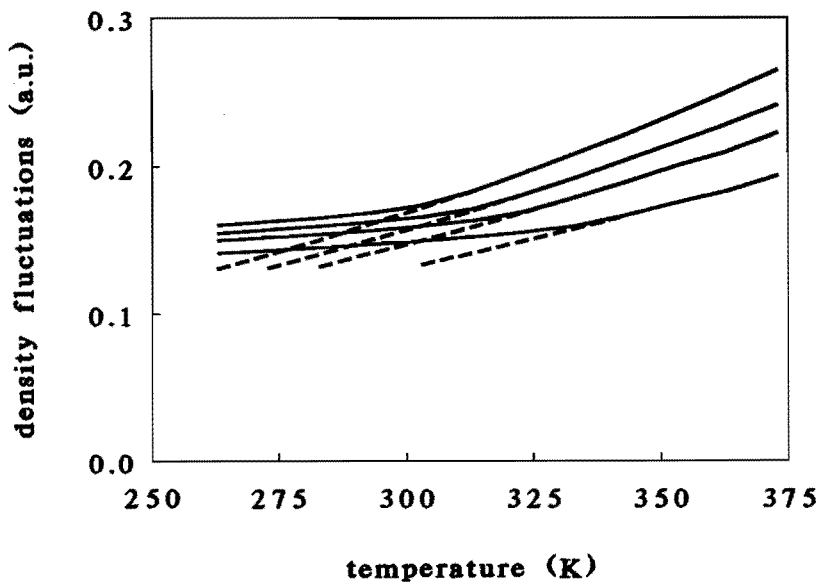


Figure 6.18. Calculated density fluctuations (arbitrary units) versus temperature for PVAC at the indicated pressures in MPa; actual (solid lines), equilibrium (dashed lines).

Once the volume, enthalpy and T_g of simulated glasses are evaluated, the Ehrenfest relations (see chapter 3) can be investigated. PVAC glasses, formed by cooling isobarically at different pressures, have been analyzed. Analogous to the experimental method used by Oels and Rehage²⁸ the compressibility of the polymer during cooling is obtained by applying a small pressure jump and monitoring the instantaneous effect on volume. By extrapolating the liquid and glass towards T_g , the value for $\Delta\kappa^* = \kappa_{l}^* - \kappa_{g}^*$ can be determined, with $\kappa^* = (dp/dV)_T$ and the subscripts l and g referring to the melt and glass, respectively. This is illustrated in figure 6.19 for $\mu(h)$. Values for $\Delta\alpha^* = \alpha_{l}^* - \alpha_{g}^*$, and $\Delta c_p = c_{p,l} - c_{p,g}$ with $\alpha^* = (dV/dT)_p$ and $c_p = (dH/dT)_p$, are obtained from the appropriate slopes in the V-T-plot and H-T-plot, respectively. Results are summarized in table 6.6 for $\mu(h)$ and $\mu(h,T)$. As can be expected the first Ehrenfest relation does not hold if $\mu(h,T)$ is used.

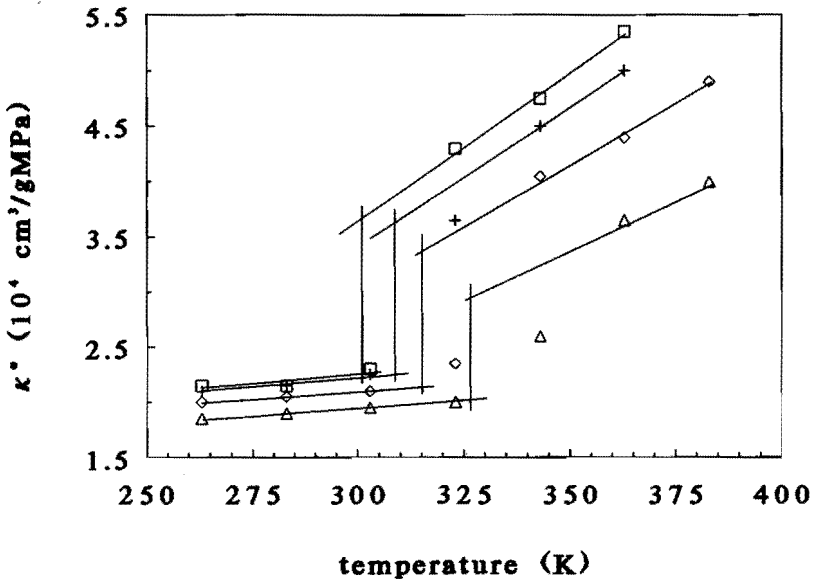


Figure 6.19.

The calculated compressibility $\kappa^* = (dV/dp)_T$ versus temperature for PVAC during isobaric cooling (\square , 0.1MPa; $+$, 20MPa; \diamond , 40MPa; \triangle , 80MPa). The mobility is described by $\mu(h)$. The lines illustrate the method used to determine $\Delta\kappa^*$ at T_g .

In this case mobility is not only governed by the order parameter h but also by the temperature, which will cause a dependence of h_r on pressure or temperature. But also in case $\mu(h)$ is used the simulated T_g cannot be regarded a single order parameter transition due to the use of a free volume distribution. However, h is in approximation constant along the transition line, which is reflected in reasonable agreement between $\Delta\kappa^*/\Delta\alpha^*$ and the simulated dT_g/dp (see table 6.6). The second Ehrenfest relation does not hold in either case $\mu(h)$ or $\mu(h,T)$. As explained in chapter 2 only the configurational part is counted for in the hole theory, resulting in too low values for c_p and Δc_p . In the melt values are calculated considerably lower than the experimental value (e.g. $c_{p,l}=0.35$ compared to an experimental $c_{p,l}=1.77$ J/gK). The values for Δc_p merely reflect a freeze-in of the glass: $c_{p,g}=0.02$ J/gK in case of $\mu(h,T)$. Based on the evaluation of an experimental PVAC glass data McKinney and Simha¹⁸ presented a calculated value of $c_{p,g}=0.103$ J/gK at 0.1MPa using the P.F. method.

Table 6.6. Evaluation of the Ehrenfest relations for PVAC glasses.

p MPa	$10^4\Delta\kappa^*$ cm ³ /gK	$10^4\Delta\alpha^*$ cm ³ /gMPa	Δc_p J/gK	T_g K	$\Delta\kappa^*/\Delta\alpha^*$ K/MPa	dT_g/dp K/MPa	$T_g\Delta\alpha^*/\Delta c_p$ K/MPa
$\mu(h,T)$							
0.1	1.51	5.18	0.35	304.4	0.29	0.19	0.45
20	1.44	4.69	0.34	309.0	0.31		0.42
40	1.25	4.16	0.34	312.4	0.29		0.40
80	1.08	3.65	0.32	319.1	0.30		0.36
$\mu(h)$							
0.1	1.44	4.81	0.32	301.0	0.30	0.33	0.45
20	1.37	4.39	0.32	307.3	0.31		0.42
40	1.31	4.03	0.32	314.0	0.33		0.40
80	0.99	3.48	0.31	327.1	0.28		0.37

6.8 The molar mass dependence of T_g

In figure 6.20 the simulated influence of the molar mass M on the T_g of PS is given. In the simulations the polymer is assumed to be monodisperse. A reciprocal relation between T_g and M is found. The molar mass dependence finds its origin in the increased free volume content near chain ends, caused by the extended degrees of freedom near chain ends. Therefore in polydisperse polymers the T_g is governed by the number average molar mass \bar{M}_n . The experimental dependence of T_g on the molar mass can be described by the empirical Fox and Flory equation²⁹

$$T_g = T_g^\infty - \frac{K_g}{\bar{M}_n} \quad (6.2)$$

with T_g^∞ and K_g constants. The experimental value for $K_g = 10^5$ gK/mol²⁹. The simulations yield $K_g = 3.3 \cdot 10^3$ gK/mol. It should be noted that the effect of chemically different end groups is not taken into account and it is expected that including this effect will decrease the discrepancies.

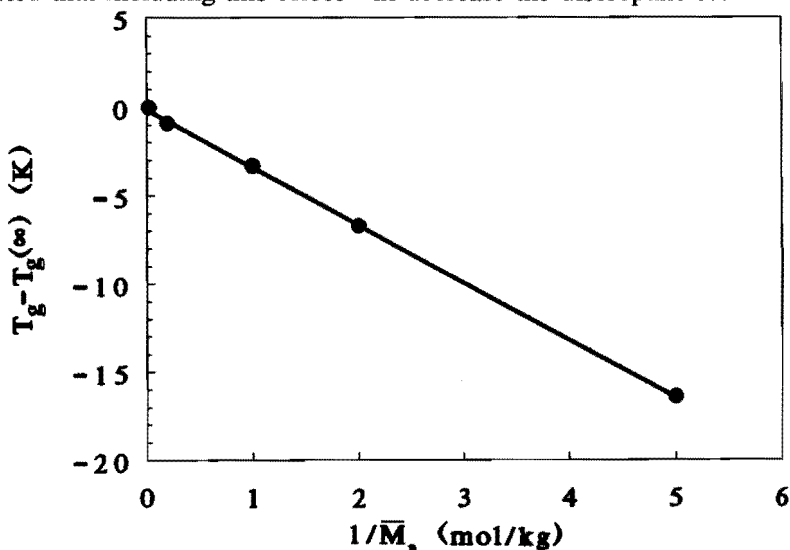


Figure 6.20. The calculated glass transition temperature T_g versus the reciprocal molar mass \bar{M}_n^{-1} for PS. Symbols, calculated; line, eq. 6.2 with $K_g = 3.3 \cdot 10^3$ gK/mol.

6.9 The influence of the model parameters

In the previous paragraphs of this chapter results have been presented for several polymers. For each polymer the constants, determined from pVT and dynamic mechanical data, were kept constant. It is now in place to give attention to the influence of the parameters on the calculated results. As an example, the simulations of PS will be analyzed using $\mu(h)$. A first group of parameters is formed by those that have been fixed to more or less arbitrary values. In an optimal case, a change in these parameters should have no influence on the simulated results. These parameters are:

z_n , the coordination number in the fcc lattice, $z_n = 12$ (eq. 5.18), and N_s , the number of segments in the volume unit in which configurational changes can take place without necessary changes in the surroundings ($N_s = N_s$ in eq. 2.23). In practice N_s can be treated as an adjustable parameter². Both parameters z_n and N_s have an influence on the width of the free volume distribution. Increasing z_n can be compared to decreasing N_s . Here only the influence of N_s will be investigated. Figure 6.21 illustrates the influence of N_s on the distribution.

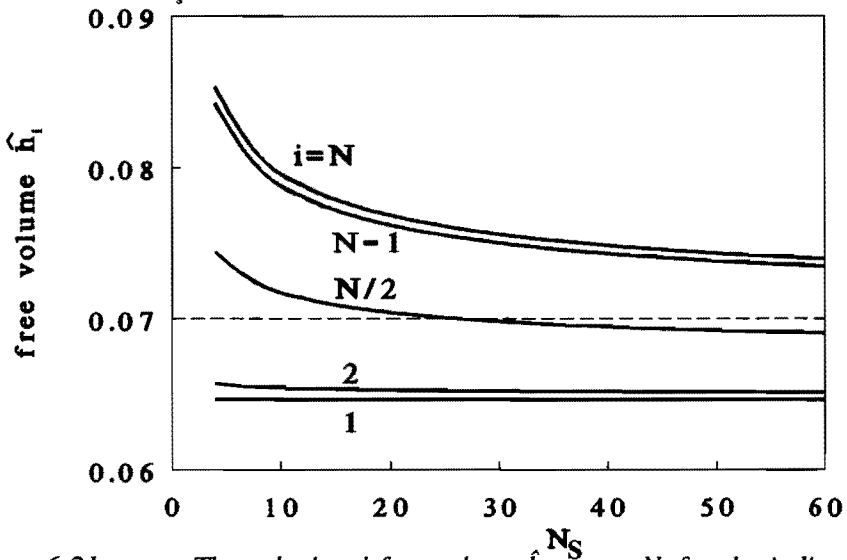


Figure 6.21. The calculated free volume \hat{h}_i versus N_s for the indicated values of i with the average free volume $\langle h \rangle = .07$ (dashed line) and the distribution width $\langle \delta h^2 \rangle = 0.01$.

The free volume levels of a few representative states of the distribution ($i=1,2,1/2n,n-1,n$) are shown. It can be seen that especially the free volume content of states with high levels of free volume are influenced. The influence on the simulated T_g and on the properties of the glasses are very minor. The shape of relaxation curves broadens if N_s is decreased, due to a wider relaxation time distribution.

n , a computational parameter (eq. 5.16), equal to the number of states in which the distribution is divided. In all simulations presented $n=20$ has been used. The value for n has been chosen in the range where no effect on results is observed. Using $n=15$ gave identical results. A decrease to $n=10$ resulted in non-smooth changes during e.g. heating and cooling.

M_0 , the mass of the repeat unit in the hole theory (eq. 2.15). M_0 has been put equal to the mass of the monomer unit. To test its influence the value for M_0 for PS has been varied in the range $0.025 \leq M_0 \leq 0.25$ kg/mol. Subsequently the same equilibrium pVT data have been used to determine ϵ^* , v^* and c_s . Results for these parameters are given in table 6.7.

Table 6.7. Influence of M_0 on the calculated EoS parameters and on the simulated glass transition temperature T_g (at 0.1MPa and a cooling rate 10K/h and with $\mu(h)$).

M_0 kg/mol	ϵ^* J/mol	$10^5 v^*$ m ³ /mol	c_s	χ^2 ^a	$h(0.1\text{MPa},$ 363K)	T_g K	\bar{T}_g	$10^4 \alpha_g(303\text{K})$ K ⁻¹
.025	1671.1	2.4194	.12956	27	.06133	363	.0233	1.01
.050	3258.3	4.7689	.35836	28	.06237	361	.0330	1.38
.104	6689.6	9.8466	.85284	30	.06214	361	.0379	1.59
.175	11199.	16.524	1.5026	31	.06187	361	.0402	1.66
.250	15960.	23.578	2.1886	31	.06170	361	.0411	1.70

^a χ^2 is a relative measure for the total deviations between experimental pVT data¹³ and the description by theory.

The value of M_0 is found to have a negligible influence on the quality of the EoS description and on the values for $h(p,T)$. In table 6.7 as an example the order parameter h at 0.1MPa and 363K is listed. Simulation results of T_g at 0.1MPa with the use of $\mu(h)$ are also shown in table 6.7. The influence of M_0 on the simulated T_g is only very minor. This change could easily be absorbed by a different value for R (eq. 5.21), thus completely compensating changes in M_0 . Surprisingly, the calculated thermal expansion coefficient of the glass is significantly lower for the lower M_0 values. Finally, table 6.7 shows that if T_g is analyzed in terms of reduced variables, a significant dependence of \tilde{T}_g on M_0 is found.

Besides the above mentioned parameters (M_0 , z_n , N_s and n), the parameters essential for the description of a particular polymer are: ϵ^* , v^* , c_s , M_0 , R and the kinetic parameters A and B . Changes in one or more of these parameters will change the character of the polymer. Generally, these parameters have different values for different polymers. To illustrate the influence of changes in these parameters, again PS will be used as a reference state and $\mu(h)$ to describe mobility. It must be emphasized that after changing one (or more) parameters, not PS is described but another fictive polymer. In table 6.8 and in figure 6.22 results are presented. From this figure it can be seen that by changing ϵ^* or c_s , especially T_g is changed, whereas \tilde{T}_g does not change significantly. A 'practical' principle of corresponding states is obeyed. The value for v^* has no influence on T_g or \tilde{T}_g . Finally M_0 , R and the kinetic parameters A and B change both T_g and \tilde{T}_g , while their ratio T^* is constant. Because in all cases $\mu(h)$ (eq. 4.6) is used to describe the mobility-free volume relation, the (iso-mobility) T_g will always be located at the same free volume level, which appears to be $h_g=0.061 \pm 0.001$ for a cooling rate of 10 K/h.

Table 6.8. Influence of changes of molecular parameters on the simulated T_g (at 0.1MPa and a cooling rate 10 K/h)

parameter varied ^a	T_g K	T_g	$V_{eq}(T_g)$ cm ³ /g
-	361	0.0379	0.9726
$M_0=0.025$ kg/mol ^b	264	0.0280	0.9583
$M_0=0.25$ kg/mol ^b	385	0.0408	0.9753
$\epsilon^*=5000$ J/mol	270	not changed	not changed
$\epsilon^*=8000$ J/mol	431	not changed	not changed
$v^*=8 \cdot 10^{-5}$ m ³ /mol	not changed	not changed	0.7902
$v^*=12 \cdot 10^{-5}$ m ³ /mol	not changed	not changed	1.1851
$c_s=0.75$	399	0.0372	0.9697
$c_s=1.15$	275	0.0393	0.9735
$R=3 \cdot 10^6$	364	0.0382	0.9740 ^c
$R=3 \cdot 10^{10}$	358	0.0376	0.9712 ^c

^a Of all parameters (namely M_0 , ϵ^* , v^* , c_s and R) only one is varied at a time. The others are equal to the parameters of PS ($M_0=0.104$, $\epsilon^*=6689.6$, $v^*=9.8466 \cdot 10^{-5}$, $c_s=0.85284$ and $R=3 \cdot 10^8$).

^b The parameters ϵ^* , v^* and c_s expressed per gram have been kept constant.

^c In this case $h_g=h_{eq}(T_g)$ differs from 0.061 ± 0.001 .

The universality of the iso-mobility principle of T_g can be investigated by comparing different polymers. If different polymers are compared, $(\mu + \log R)$ is a relevant measure for the absolute mobility. In figure 6.23 $(\mu + \log R)$ is plotted versus free volume for PS, PVAC, PC and PMMA with $\mu(h)$. The locations of T_g are indicated. The absolute mobility at T_g appears to be constant for all polymers: $(\mu + \log R) = -8.3 \pm 0.3$, for the same cooling rate. Similar results are found if $\mu(h, T)$ is used. Also the slope of $(\mu + \log R)$ versus h at T_g influences the glass transition. Both the width and the dependence on cooling rate are influenced. The higher the slope, the narrower the glass transition region is and the lower the cooling rate dependence. The use of the equilibrium average free volume content at T_g to characterize the T_g is at best only an approximation. At T_g the actual free volume is slightly higher than the equilibrium value.

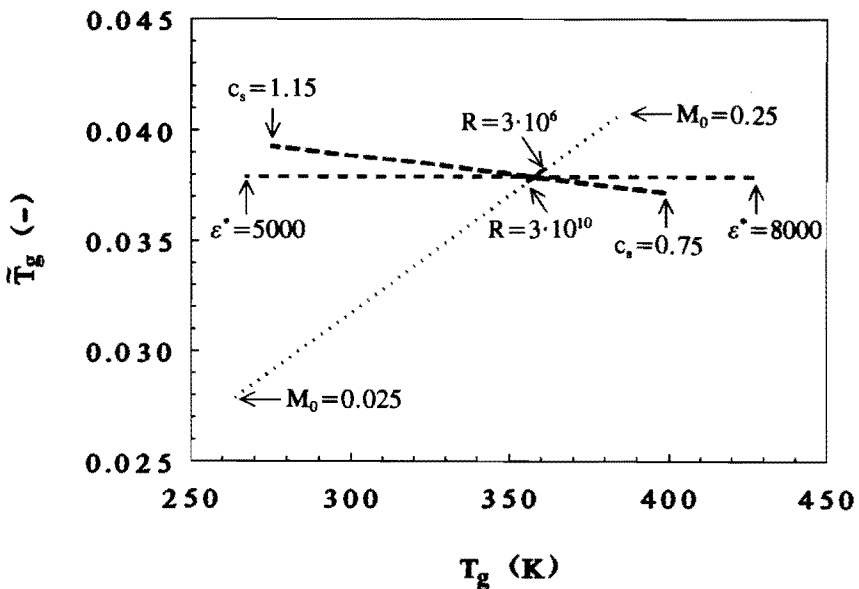


Figure 6.22. The influence of the molecular parameters on \bar{T}_g and T_g with PS as reference. Changes of parameters as indicated.

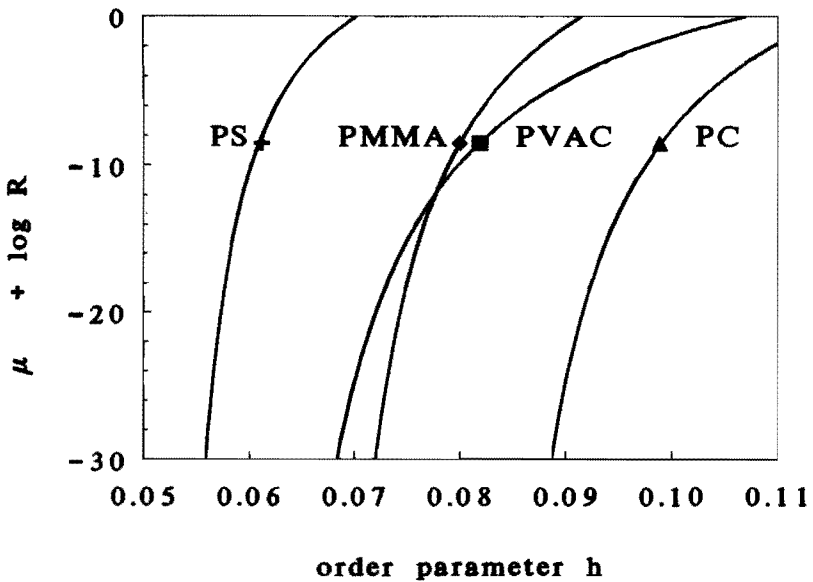


Figure 6.23. The equilibrium mobility ($\mu + \log R$) versus the order parameter h for indicated polymers. The symbols indicate the location of T_g .

6.10 Conclusions

From equilibrium pVT-data, equilibrium dynamic mechanical shift factors and only one non-equilibrium volume relaxation experiment, it is possible to predict the equation of state behaviour of glasses, the glass transition temperature and its dependence on formation history (important conditions are cooling rate, pressure, pressurizing rate, temperature and annealing time). Simulations at ambient pressure generally show good agreement with experimental data (see e.g. table 6.2).

Discrepancies between theory and experiment at elevated pressures are almost entirely related to the dependence of T_g on the glass formation

pressure. The use of shift factor data, obtained at ambient pressure, to obtain a relation between mobility and free volume, is probably limited to low pressures. Discrepancies at elevated pressures, as shown in this work, suggest that mobility at elevated pressure is not only described by the order parameter h , which is here used as a measure for free volume. An empirical relation with $\mu(h,T)$ (eq. 4.7) improves the pressure dependence of T_g considerably, see figure 6.8. The choice of the relation between free volume and mobility especially influences simulation results of pressure experiments. Generally good results are obtained by using the extended mobility relation. The explicit temperature dependence of mobility also influences relaxation phenomena in the glass. Relaxation times increase, i.e. mobility decreases, which is reflected in the simulation of several experiments. Relaxation after a temperature jump close to T_g (figure 6.1), but also relaxation in glasses cooled to temperatures far below T_g (figures 6.7 and 6.8) is impeded by the explicit use of temperature to describe mobility.

The only non-equilibrium data used for the predictions are data of a single relaxation experiment, to estimate a value for R . In the relaxation curves shown in paragraph 6.2, a change in R of one order of magnitude brings about a shift of one decade to longer times. This has been shown to change the location of the predicted T_g by about 1.5K. The relative insensitivity of the location of T_g on the value for R makes the determination of R from jump experiments not very critical. As a first approximation one might even consider using an average value for R determined from table 6.1 (e.g. $R=10^{10}$). For the polymers analyzed this would result in predicted T_g 's very close to the experimental values, with the use of only parameters obtained from equilibrium pVT data and equilibrium mobility data.

6.11 References

1. J. E. McKinney and M. Goldstein, *J. Res. Nat. Bur. Stand.-A. Phys. Chem.*, **78A**, 331 (1974).
2. R. E. Robertson, R. Simha and J. G. Curro, *Macromolecules*, **17**, 911 (1984).
3. G. Rehage and G. Goldbach, *Ber. Bunsenges.*, **70**, 1144 (1966).
4. A. J. Kovacs, *Fortschr. Hochpolym.-Forsch.*, **3**, 394 (1963).
5. R. E. Robertson, R. Simha and J. G. Curro, *Macromolecules*, **18**, 2239 (1985).
6. R. E. Robertson, R. Simha and J. G. Curro, *Macromolecules*, **21**, 3216 (1988).
7. R. E. Robertson, *Macromolecules*, **18**, 953 (1985).
8. A. J. Kovacs, *J. Polym. Sci.*, **30**, 131 (1958).
9. R. Greiner and F. R. Schwarzl, *Rheol. Acta*, **23**, 378 (1984).
10. R. Greiner and F. R. Schwarzl, *Colloid Polym. Sci.*, **267**, 39 (1989)
11. H. H. D. Lee and F. J. Mc Garry, *J. Mac. Sci.-Phys.*, **B29**, 185 (1991).
12. H. Sasabe and C. T. Moynihan, *J. Polym. Sci., Polym. Phys. Ed.*, **16**, 1447 (1978).
13. A. Quach and R. Simha, *J. Appl. Phys.*, **42**, 4592 (1971).
14. P. Zoller, *J. Polym. Sci., Polym. Phys. Ed.*, **20**, 1453 (1982).
15. O. Olabisi and R. Simha, *Macromolecules*, **8**, 206 (1975).
16. K. Ninomiya and H. Fujita, *J. Colloid Sci.*, **12**, 204 (1957).
17. W. F. Zoetelief, *unpublished* (1990).
18. J. E. McKinney and R. Simha, *Macromolecules*, **9**, 430 (1976).
19. J. D. Ferry, *Viscoelastic Properties of Polymers*, Wiley & Sons, New York, 1980.
20. J. E. McKinney and H. V. Belcher, *J. Res. Nat. Bur. Stand.-A. Phys. Chem.*, **67A**, 43 (1963).
21. C. H. Wang and E. W. Fischer, *J. Chem. Phys.*, **82**, 632 (1985).

22. G. Meier, J.-U. Hagenah, C. H. Wang, G. Fytas and E. W. Fischer, *Polymer*, **28**, 1640 (1987).
23. C. P. Lindsey, G. D. Patterson and J. R. Stevens, *J. Polym. Sci., Polym. Phys. Ed.*, **17**, 1547 (1979).
24. J. M. G. Cowie, S. Elliott, R. Ferguson and R. Simha, *Polym. Comm.*, **28**, 298 (1987).
25. I. M. Hodge and G. S. Huvar, *Macromolecules*, **16**, 371 (1983).
26. J. H. Wendorff and E. W. Fischer, *Kolloid-Z. u. Z. Polym.*, **251**, 876 (1973).
27. H. Lee, A. M. Jamieson and R. Simha, *Colloid Polym. Sci.*, **258**, 545 (1980).
28. H.-J. Oels and G. Rehage, *Macromolecules*, **10**, 1036 (1977).
29. T. G. Fox and P. J. Flory, *J. Polym. Sci.*, **14**, 315 (1954).

Chapter 7*

Positron annihilation spectroscopy

7.1 Introduction

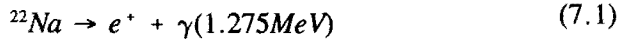
The technique of Positron Annihilation Lifetime Spectroscopy (PAS) has proven to be a powerful tool to study defects like dislocations and vacancies in metals^{1,2}. The occurrence of relatively well defined lattices in these solids has been helpful to obtain understanding of processes underlying phenomena observed in PAS. Since the 70's the use of PAS to study polymers has increased¹. Providing a way to study cavities on molecular scale in an amorphous polymer matrix PAS gives in principle unique insight in the free volume concept. However, the mechanism of positron annihilation in molecular solids in general and in polymers in particular is different from that in metals³ and is not as well understood^{1,4}. A complicating factor is the presence of a distinct hole size distribution in the polymer, which obscures the relation between hole sizes and PAS results.

In this chapter a hole size distribution model, based on a disordered lattice model with the free volume fraction h as a central quantity (see chapter 2), is developed to explain PAS data. It is shown that the calculated distribution and its temperature dependence can be successful correlated to PAS results. The consequences of different assumptions for mechanisms of glass formation will be compared to experimental PAS results.

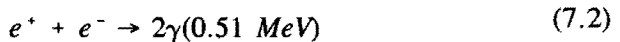
*Reprinted in part from: S. Vleeshouwers, J.-E. Kluin, J. D. McGervey, A. M. Jamieson and R. Simha, *J. Polym. Sci., Polym. Phys. Ed*, **30**, 1429 (1992).

7.2 Positron annihilation spectroscopy

In a typical PAS experiment the positrons e^+ are formed by the radioactive decay of ^{22}Na



The γ photon emitted is called the birth gamma. Usually the ^{22}Na -source is sandwiched between two pieces of the material to be examined, allowing most positrons to thermalize by inelastic collisions with electrons in the sample within 2 mm from the surface of the polymer⁵. The thermalization process takes typically 10^{-12} - 10^{-11} s⁶. Once thermalized, a fraction I_2 of the positrons annihilate directly with an electron from the surrounding medium and emitting two annihilation gammas



The time between thermalization and annihilation of a free positron in a molecular solid, τ_2 , is about 400 - 500 ps⁷.

However, in a PAS experiment not the annihilation of free positrons is most interesting, but the annihilation of the positronium, the product of



It is still subject to discussion if the reacting e^- is a secondary electron, removed from an atom during the last stage of the thermalization process of e^+ (the spur model⁸) or if it is captured by the positron from a neighbouring atom (the Ore model⁹). However, both models do not automatically exclude each other¹⁰.

Two different Ps particles are formed: a fraction I_1 of all positrons form para-positronium (p-Ps) in which the e^+ and e^- have opposite spin, and a fraction I_3 form ortho-positronium (o-Ps), in which they have parallel spin. According to quantum mechanics the ratio I_1/I_3 is equal to 1/3. Due to the parallel spin in o-Ps the e^- and e^+ which form the particle can not annihilate.

The o-Ps annihilates by 'pick-off' of an electron from the surrounding medium. Repulsion between the electron of the o-Ps and electrons of surrounding atoms further stabilizes the o-Ps. The annihilation rate of o-Ps is about an order of magnitude lower than that of p-Ps: the lifetime of p-Ps, τ_1 , is 125 ps, compared to a typical lifetime for o-Ps of 1.5-3 ns. So the positrons in both p-Ps and o-Ps annihilate according to eq. 7.2, but the source of the electrons is different.

The fraction of positrons that form o-Ps, I_3 , depends on the medium. While in metals no o-Ps is formed due to the high density of conducting electrons¹, up to 70% of the positrons can form o-Ps in molecular media.

7.3 Positron annihilation in polymers

In molecular media it has been found that both the lifetime of o-Ps, τ_3 , and the fraction of positrons that form o-Ps, intensity I_3 , are temperature dependent. Focusing on amorphous polymers, τ_3 has been found to increase almost linearly with temperature, both below and above T_g , with a change in slope at T_g (see paragraph 7.6 and e.g. refs. 12-14). For polystyrene (PS) the slope with temperature of τ_3 in the glass is $1.9 \cdot 10^{-3}$ ns/K and in the melt $8.4 \cdot 10^{-3}$ ns/K (paragraph 7.6). The behaviour of I_3 for different polymers shows more variation. For example in the melt, with increasing temperature, I_3 increases for chlorinated PS¹¹, increases and then levels off for epoxies¹², exhibits a maximum for PS (paragraph 7.6), and decreases for poly(vinyl acetate) (PVAC)¹³. In the glass, with decreasing temperature, I_3 can increase (chlorinated PS¹¹), be constant (PS, paragraph 7.6), or first decrease and then become constant (epoxy¹², PC¹⁴). It must be noted that especially the behaviour of I_3 in a polymer glass can depend strongly on the formation history of the glass. In PS I_3 is essentially independent of temperature when measured immediately after quenching from the melt (paragraph 7.6). However, in an 'old' PS-sample, I_3 decreases rapidly with decreasing

temperature¹⁵. These results are consistent with aging experiments on PS. The apparently totally different features of I_3 in different glasses can therefore at least partly be attributed to the formation histories of the glasses.

Brandt¹⁶ has explained the τ_3 temperature dependence in molecular solids by assuming the o-Ps to be localized in regions of minimal electron density. These regions can be visualized as cavities, or as free volume pockets. The Ps annihilation rate, from eq. 7.2, is proportional to the overlap between the wave function of the positron and that of the pick-off electron¹⁷, so within the scope of free volume theories the lifetime τ_3 increases with increasing hole size.

The o-Ps intensity I_3 is related to the concentration of regions with low electron density, in which o-Ps can be found. Besides depending on the concentration of cavities, I_3 can be influenced by inhibition processes. Inhibition of o-Ps formation can occur¹⁰ by strong electronegative atoms such as halogens or by positive metal ions. The occurrence of a saturation level of the inhibition has given rise to the 'hot positronium reaction model'¹⁰, according to which a Ps needs a certain energy to react with the inhibitor. By this reaction the annihilation of unreacted Ps particles decreases. This model is closely related to the Ore model⁹. In the spur model⁸ inhibition is explained by the scavenging of electrons by the inhibitor, preventing the formation of Ps. In low molar mass liquids the quench is stronger than in solids, due to a larger mobility of quenching groups. According to Wang et al.³, quenching of o-Ps formation also influences τ_3 because in the formed Ps-molecule-complex Ps has a lifetime around 0.4ns, indistinguishable from the lifetime τ_2 of free positrons. On the other hand, experimental results on chlorinated PS¹¹ suggest that partial quenching does not influence the lifetime τ_3 of the remaining o-Ps.

For a given polymer the study of o-Ps lifetimes τ_3 and intensities I_3 seems to be an appropriate way to study free volume in the polymer matrix: τ_3 is related to the size of cavities, I_3 to the concentration of cavities. Kobayashi et al.¹³ have investigated this approach with respect to PVAC.

Assuming a proportionality between I_3 and hole concentration, and using a relation between τ_3 and a mean hole size $\langle v \rangle$, they calculated a free volume fraction $f_{PAS} = C \cdot I_3 \cdot v(\tau_3)$, where the constant C was chosen to give a good fit at one particular temperature in the melt. Reasonable good agreement between f_{PAS} and the fractional free volume h_{th} , calculated using the SS-theory, was found. At high temperatures and at temperatures below T_g , however, discrepancies were found.

A question arises if the behaviour of the matrix is influenced by the presence of o-Ps. It is shown that in liquids positrons form bubbles¹⁸. Observed lifetimes in liquids are substantially longer than to be expected from free volumes calculated from molar volumes¹⁹. By minimizing the free energy of the Ps-bubble system an increase of the hole size of 30 times has been calculated. For hexane, e.g., Ujihira et al.¹⁹ yield an average free volume radius $r = 0.0592 \text{ nm}$ at 20°C , and $r_{\text{bubble}} = 0.46 \text{ nm}$. The calculated hole size is comparable to that for polymers. For zeolites²⁰ and resins²¹ a correlation has been shown between matrix structure and τ_3 ²² and I_3 ²³. Tao²² has presented a correlation between the radius of a hole and the corresponding τ_3 . Using a square well potential of radius r_o with an electron layer of thickness δr in which the lifetime of o-Ps equals 0.5 ns (the spin averaged lifetime of o-Ps and p-Ps) the lifetime τ_3 can be described by

$$\tau_3 = \frac{1}{2} \left[1 - \frac{r}{r_o} + \frac{\sin(2\pi r/r_o)}{2\pi} \right]^{-1} \quad (7.4)$$

With a value $\delta r = r_o - r = 0.1656 \text{ nm}$ good agreement between eq. 7.4 and experiment is obtained in at least the range $0.2 \text{ nm} \leq r \leq 0.6 \text{ nm}$, for molecular solids²¹, zeolites²⁰ and liquids (with $r = r_{\text{bubble}}$)¹⁹. Unfortunately the calculations of radii are based on different methods (sound velocity¹⁹, molar volumes²¹, silicate structure²⁰). Moreover the relation between τ_3 and the hole radius can also be described reasonably well by a proportionality between τ_3 and the volume v of the hole. Combining this with results from percolation theory (see

figure 7.1) that in irregular holes the surface area is proportional to the volume v of a hole, rather than to $v^{2/3}$, this would also lead to a proportionality between τ_3 and the surface of a hole.

I_3 is found to be correlated to the total internal surface area²³. For porous resins (with pore diameters between 5 and 130 nm) I_3 was found to be proportional to the void concentration, calculated assuming spherical voids²³. However, I_3 was not assigned to the total fraction of o-Ps formed, but only to o-Ps formation in pores and interfacial spaces, with corresponding apparently hole size independent lifetimes of 80-100ns. Application of the proportionality between I_3 and void concentration to o-Ps in molecular voids, with $\tau_3 \approx 2$ ns, is therefore possibly not correct. It might be better to compare the second component in ref. 23 (with lifetime ≈ 4 ns) to o-Ps in molecular voids. However, the lifetime of this component, τ_2 , shows no correlation with the radius and the corresponding I_2 is influenced by the presence of the third species by the constraint $\Sigma I_i = 1$, because the intensities of all positron species are coupled by this constraint. Conclusions concerning o-Ps lifetimes for amorphous non-porous polymers seem therefore difficult to make. For polymers the o-Ps lifetime τ_3 is found to have values between 1.5 and 3 ns, corresponding to radii $0.23 < R < 0.36$ nm (eq. 7.4).

7.4 Calculation of Cluster Size Distributions

As pointed out in paragraph 7.3 the value of τ_3 depends on the electron density in the immediate vicinity of the o-Ps particle¹⁷ which preferentially locates in regions of low electron density, and τ_3 increases with decreasing electron density. Within the scope of free volume theories the o-Ps particle is bound inside a free volume region or hole¹⁶, and the lifetime τ_3 increases with increasing hole size. The total fraction of positrons that form o-Ps, I_3 , is assumed to depend on the preponderance of regions with low electron density in which o-Ps can exist¹⁶. Thus, in terms of free volume theories, I_3 is

assumed to be related to the concentration of holes and increases with increasing hole concentration. The PAS technique can therefore be used, in principle, to obtain direct information about both hole size and hole concentration in the polymer matrix.

It is known that the distribution of free volume in a polymer, which is a measure for the degree of disorder in the structure factor observed by x-ray scattering methods, and the associated distribution of viscoelastic relaxation times, may play an important role in understanding the mechanical properties of polymers²⁴, the formation of polymer glasses and relaxation processes in glasses (see chapter 5 and 6). However, only very recently has the concept of free volume distribution been introduced quantitatively into the analysis of PAS experiments²⁵. Specifically, Deng et al.²⁵ assume that the lifetimes measured by PAS are not single exponential decays but are the result of Gaussian distributions. In this chapter we wish to quantify the free volume distribution concept in a different way by taking as a basis for our investigation the Holey-Huggins²⁶ (HH) model (chapter 2). We assume a random distribution of empty lattice sites which form clusters of different sizes. Lattice simulations are used to analyze the cluster size distribution as a function of the occupied fraction $1-h$ of the lattice. The effect of the resulting site cluster distribution on hole concentration and hole size are examined, taking into account certain properties of the PAS analysis process.

The lattice used in the HH-theory to describe the polymer is a partly filled fcc lattice with coordination number $z=12$. Assuming randomness in the placement of holes, only the degree of occupancy $y=1-h$ determines the clustering of empty lattice sites. It may be recognised that the problem of determining the distribution of clusters is closely related to a percolation problem²⁷. However no analytical solution is available for a three dimensional lattice with $z=12$ ^{27,28}. Furthermore the application of published percolation results to our problem is restricted because most of the literature is focused on processes close to the percolation threshold h_{th} which in this instance

equals $0.198^{27,28}$. The region of interest to our problem turns out to be $0.05 < h < 0.15$, with particular interest in the smaller clusters.

We define i as the number of sites forming a single cluster, $i=1,2,3,\dots$, and p_i as the probability that any empty site is part of a cluster of size i . The quantity p_i is by definition equal to the fraction of free volume present in clusters of size i . For $i=1$, p_1 can easily be calculated

$$p_1 = y^{12} \quad (7.5)$$

with y the fraction of occupied lattice sites. The exponent in eq. 7.5 represents the perimeter t (the number of surrounding sites that are occupied), and equals $t=12$ for an isolated empty lattice site. Similarly, we find for p_2 , taking into account all possible configurations

$$p_2 = 2(1-y)6y^{18} \quad (7.6)$$

For $i=2$, six different configurations of the cluster are possible, each having a perimeter $t=18$. The prefactor 2 arises from the size of the cluster. For $i=3$ not all possible configurations have the same perimeter t . For example, for three empty sites in a straight line, $t=24$, and for an equilateral triangle, $t=22$. We find

$$p_3 = 3(1-y)(28y^{24}+12y^{23}+8y^{22}) \quad (7.7)$$

Analytical calculations for p_i when $i > 3$, involve a large number of possible configurations. Using lattice simulations it is possible to obtain p_i for values $i > 3$.

In the simulations, we selected a lattice of size $20 \times 20 \times 20$. It was filled 400 times randomly, with a prescribed value for y . This was sufficient to render the results independent of further trials. The procedure was carried out for 10 different values of y , $0.8 \leq y \leq 0.99$. After the filling procedure, the lattice was analyzed by counting the number of clusters of different sizes. For all clusters present, the size i and the perimeter t were determined. To minimize the effect of boundaries, periodic boundary conditions were used.

In agreement with percolation theory, the perimeter t is found to be proportional to the cluster size i , except for small values of i , as is shown in figure 7.1. To obey the coordination number $z=12$ on the three dimensional array used in the simulations, 12 sites near a particular sites were defined as nearest neighbours of that site.

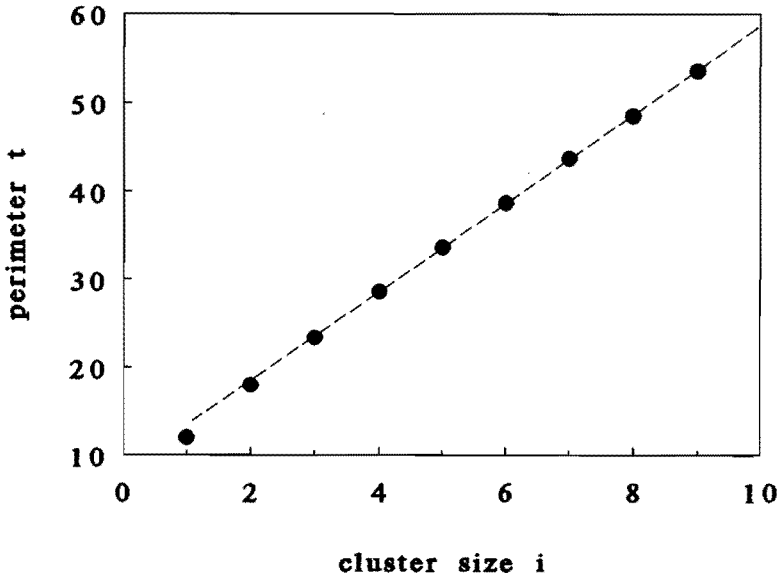


Figure 7.1. The perimeter t versus the cluster size i . Symbols, calculated; dashed line, linear fit.

In figure 7.2 the volume fraction of clusters of size i , p_i , is plotted versus the size of the cluster i for different values of y , $0.80 < y \leq 0.99$. For this range $0.84 < y \leq 0.99$ the simulation results are supported quantitatively by the analytical calculations. However, for $0.8 \leq y \leq 0.84$ we find some deviations between the two methods. This is due to the fact that for values of $y \leq 0.84$ the occurrence of holes connecting two opposite sides of the $20 \times 20 \times 20$ lattice begins to play a role in the counting process in the simulations. Therefore for $0.8 < y < 0.85$ some deviations between simulations and analytical calculations may be expected. Considering $y=0.85$ as the

lowest pertinent value for our application, the lattice used in the simulations has to be chosen large enough to accurately describe cluster sizes for $\gamma=0.85$. The size $20 \times 20 \times 20$ fulfils this requirement. Also plotted in figure 7.2 are the results of analytical calculations using eqs. 7.5-7.7 for values $i=1,2,3$.

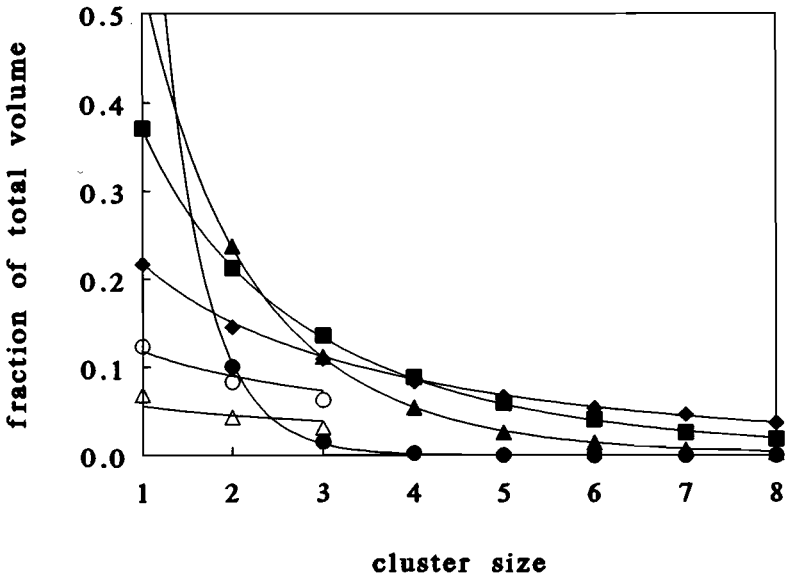


Figure 7.2. Volume fraction distribution of cluster sizes versus cluster size for different values of γ . Simulations (solid symbols) and analytical calculations (open symbols). ●, 0.99; ▲, 0.95; ■, 0.92; ◆, 0.88; ○, 0.84; △, 0.80. Solid lines represent the stretched exponential eq. 7.8.

To use the simulation results for further calculations, distributions for intermediate values of γ must be available. These are found to be represented by the empirical function

$$p_i = p_n \exp \left[- \left[\frac{i}{l(\gamma)} \right]^{\beta(\gamma)} \right] \quad (7.8)$$

where $l(y)$ and $\beta(y)$ are polynomial functions of y , and p_n is a normalization factor, so that $\sum p_i = 1$. Of course eq. 7.8 is only meaningful for integer values of i . To determine p_n and the coefficients in the polynomials $l(y)$ and $\beta(y)$, eq. 7.8 was fitted to the simulation results for $0.84 < y \leq 0.99$ and to the analytical results for $0.8 \leq y \leq 0.84$. The analytical results were included to enable extension of eq. 7.8 to values of y for which the simulations showed deviations, although these values of y and also values of $y \approx 1$ are not necessary for applications in this work. Strictly $l(y)$ has to obey the following boundary condition

$$l(y) \rightarrow 0 \quad \text{if} \quad y \rightarrow 1 \quad (7.9)$$

to force the distribution to become a delta function. Probably due to the choice of polynomial expressions for $l(y)$ and $\beta(y)$ this boundary condition could not be satisfied without drastically decreasing the quality of the fit of eq. 7.8. Because the region of interest of y does not include values y close to 1, the boundary condition was not used in the fitting procedure. The final result is

$$l(y) = 12.44 - 12.051y \quad (7.10)$$

$$\beta(y) = 2.7504 - 8.0327y + 6.3595y^2 \quad (7.11)$$

Together with eq. 7.8, eqs. 7.10 and 7.11 represent the results of both simulations and analytical calculations with a maximum deviation for p_i of 0.006 in the range $0.84 < y \leq 0.99$ and 0.013 in the range $0.8 \leq y \leq 0.84$. These deviations are comparable with deviations between analytical calculations and simulations. Some results are depicted in figure 7.2. A summary of the simulation results, the analytical calculations and the fit of the stretched exponential, for the values of y shown in figure 7.2, is given in table 7.1.

Table 7.1. Calculated cluster size distribution in a partly filled lattice with coordination number $z=12$, and the fit to a stretched exponential (eq. 7.8), for different values of occupied fraction y .

	cluster size i	analytical eqs. 7.5-7.7	simulation	stretched exp. eq. 7.8	deviations of stretched exp. ^a
y=0.80	1	0.0687	0.1387	0.0560	-0.013
	2	0.0432	0.0891	0.0455	+0.002
	3	0.0315	0.0664	0.0392	+0.008
	5		0.0436	0.0313	
	7		0.0328	0.0263	
y=0.84	9		0.0241	0.0227	
	1	0.1234	0.1290	0.1184	-0.005
	2	0.0832	0.0876	0.0902	+0.007
	3	0.0627	0.0682	0.0734	+0.011
	5		0.0468	0.0530	
y=0.88	7		0.0355	0.0407	
	9		0.0300	0.0325	
	1	0.2157	0.2172	0.2185	+0.001
	2	0.1442	0.1455	0.1512	+0.006
	3	0.1044	0.1094	0.1123	+0.003
y=0.92	5		0.0663	0.0684	+0.002
	7		0.0464	0.0450	-0.001
	9		0.0319	0.0310	-0.001
	1	0.3677	0.3709	0.3699	+0.001
	2	0.2140	0.2133	0.2142	+0.001
y=0.95	3	0.1311	0.1363	0.1336	-0.003
	5		0.0593	0.0582	-0.001
	7		0.0261	0.0277	+0.002
	9		0.0139	0.0140	0.000
	1	0.5404	0.5418	0.5409	-0.001
y=0.99	2	0.2383	0.2382	0.2364	-0.002
	3	0.1084	0.1120	0.1112	-0.001
	5		0.0258	0.0277	+0.002
	7		0.0065	0.0076	+0.001
	9		0.0017	0.0022	+0.001
y=0.99	1	0.8864	0.8812	0.8813	0.000
	2	0.1001	0.1007	0.1051	+0.004
	3	0.0114	0.0154	0.0131	-0.002
	5		0.0002	0.0002	0.000
	7		0.0000	0.0000	0.000

^a Deviations with analytical results for $y \leq 0.84$ and with simulations for $y > 0.84$.

Having an expression for the volume fraction p_i we can calculate the volume averaged cluster size

$$\langle n \rangle_v = \frac{\sum ip_i}{\sum p_i} \tag{7.12}$$

It was also possible to calculate the number distribution of clusters n_i and the number average cluster size $\langle n \rangle_n$. Let n_i be the number fraction of holes of size i , then

$$n_i = \frac{(p_i/i)}{\sum (p_i/i)} \tag{7.13}$$

and

$$\langle n \rangle_n = \frac{\sum p_i}{\sum (p_i/i)} \tag{7.14}$$

In figure 7.3 $\langle n \rangle_n$ and $\langle n \rangle_v$ are plotted versus y .

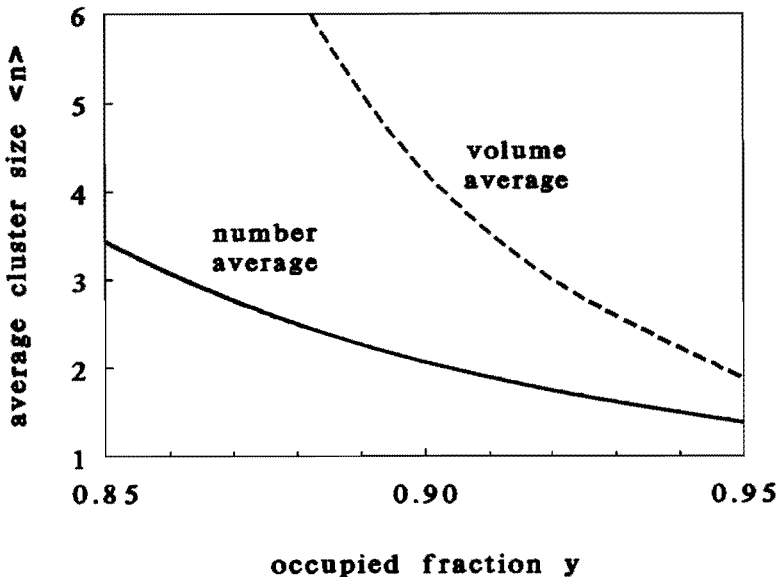


Figure 7.3. The simulated number average cluster size (solid line) and volume average cluster size (dotted line) versus y .

7.5 Analysis of experimental data

To analyze experimental τ_3 and I_3 data, expressions for the cluster concentration and the average cluster size must be developed. Adopting the assumption that the probability for a positron to become trapped in a hole and to form o-Ps is independent of the size of the hole, the total amount of o-Ps formed is proportional to the number of holes. For this case the intensity I_3 is proportional to the cluster concentration in the lattice model. Eq. 7.4 relates the lifetime τ_3 of o-Ps to the radius of a spherical hole. To calculate τ_3 for a non-spherical hole we employed an equivalent spherical cavity. That holes formed by clustering of lattice sites are generally not spherical is shown clearly by the perimeter t which is proportional to i for large holes, rather than proportional to $i^{2/3}$ as would be the case for spheres (see figure 7.1). For a particular polymer at a specified temperature and hence for a known value of y , eq. 7.8 provides the distribution p_i . The number-averaged cluster size $\langle n \rangle_n$ could be calculated by eq. 7.14, and the total cluster concentration N_{cl} (nm^{-3}) by

$$N_{cl} = \frac{h}{\langle v \rangle_n} = \frac{h}{\langle n \rangle_n v_1} \quad (7.15)$$

with $h=1-y$ and v_1 (nm^3) the size of one lattice site

$$v_1 = 10^{24} y V M_0 / N_A \quad (7.16)$$

and V the specific volume of the polymer in cm^3/g , M_0 the mass of the repeat unit used in the lattice theory in kg/mol , and N_A Avogadro's number. For the number average cluster volume $\langle v \rangle_n = \langle n \rangle_n \cdot v_1$, the o-Ps lifetime could be calculated using eq. 7.4 with r the radius of a spherical hole with volume $\langle v \rangle_n$. Focusing now on a particular polymer at a temperature T , the only adjustable parameter in the description of cluster size and cluster concentration was M_0 , which scales the size of the lattice. A value for M_0 was chosen to give best agreement between predicted and experimental τ_3 values. Because

h is only a very weak function of M_0 (see e.g. chapter 6, table 6.7), recalculation of the lattice free volume fraction h did not have to be considered as long as M_0 was close to the value used to describe the equation of state behaviour. Such value could therefore directly be used in eq. 7.16.

Finally the analysis must deal with the fact that experiment provides a single lifetime $\tau_{3,\text{exp}}$, whereas the theory leads to a spectrum $\tau_{3,i}$, $i=1,2,\dots$. Thus an appropriate averaging operation must be performed. In the simplest approximation $\tau_{3,\text{exp}}$ can be compared to the lifetime τ_3 computed from the average cavity volume $\langle v \rangle_n$. In the glass an equilibrium cluster distribution is assumed, depending only on h . I_3 is to be compared to the cluster concentration N_{cl} , with a proportionality between $I_{3,\text{exp}}$ and N_{cl} . Generally, a maximum in cluster concentration is calculated at a temperature corresponding with $h=0.11$. This arises from the fact that at high temperatures the average cluster size $\langle n \rangle_n$ increases faster with increasing temperature than the total amount of free volume h , and hence, according to eq. 7.15, N_{cl} decreases. In addition, below T_g , N_{cl} remains almost constant because h is almost constant.

Instead of relating $\tau_{3,\text{exp}}$ directly to the volume $\langle v \rangle_n$ or $\langle v \rangle_v$ alternative possibilities could be considered. If o-Ps spends its whole lifetime in the same hole, a distribution of hole sizes gives rise to a spectrum of lifetimes $\tau_{3,1}$, $\tau_{3,2}$, $\tau_{3,3}, \dots$, each with a corresponding intensity. Generally in the analysis of a PAS experiment however, only three lifetimes τ_1 , τ_2 and τ_3 are resolved, where τ_1 and τ_2 represent annihilation of para-positronium (p-Ps) and free positrons, respectively. Thus in the mathematical analysis of the spectrum an averaging of $\tau_{3,1}$, $\tau_{3,2}$, $\tau_{3,3}, \dots$ to a single τ_3 takes place. To establish a connection between experiment and theory we had to mimic the fitting procedure used in the PAS experiment. In this procedure the statistical weight of the content of a channel is proportional to the square root of the number of counts in that channel²⁹. Hence in the fitting of a single exponential decay to a spectrum of such decays the same weighting factor must be used. Taking this constraint into account, we can now obtain a mean value for τ_3 based on the distribution of hole sizes for a specified y and thus temperature.

The values of both $\tau_{3,\text{calc}}$ and $I_{3,\text{calc}}$ depend strongly on the width of the distribution. This can be seen from figure 7.4. The intercept of the curve formed by the sum of exponential decays and the ordinate is proportional to the number of positrons that have formed o-Ps, which is proportional to I_3 . It is evident that the fitted single exponential decay has a lower intercept, so the apparent value of I_3 will be lower than the true $I_3 = \sum I_{3i}$, which is proportional to the hole concentration. The difference increases with increasing width of the distribution.

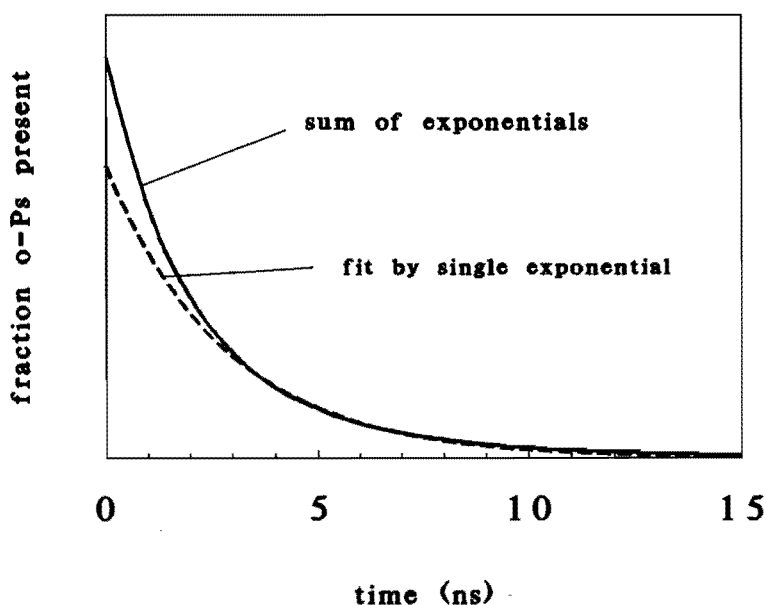


Figure 7.4. Schematic representation of the decay spectrum of o-positronium (o-Ps); the fraction of initial positrons still present as o-Ps versus time. The solid curve is the result of the o-Ps decay assuming a hole size distribution. The dotted curve represents a single exponential decay fitted to the solid curve.

7.6 Results of calculations

To calculate the free volume fraction h for bisphenol-a polycarbonate (PC), experimental pVT-data by Zoller³⁰ were employed. In the HH-theory, the mass of a repeat unit M_0 has to be chosen²⁶. Usually the monomeric unit ($M_0 = 0.254$ kg/mol in the case of PC) is taken, but here we used $M_0 = 0.05$ kg/mol (see paragraph 7.5). In the case of PC changing M_0 from 0.254 kg/mol to 0.05 kg/mol alters the value of h at 420K from 0.1024 to 0.1005, a difference of 2%. Using Zoller's pVT-data for the melt, the characteristic parameters e^* , v^* and c/s were obtained, employing the fitting procedure described in chapter 2. The values for the characteristic parameters are listed in table 7.2. To determine h below the glass transition temperature T_g the glass was treated by the A.P. method (see chapter 2). The temperature dependence of h is almost linear both above and below the T_g ($T_g = 416.5$ K) and can be represented well by linear functions in the melt and in the glass by the parameters given in table 7.2. Maximum deviations from the exact solution in the given validity ranges are also listed.

In figure 7.5a experimental τ_3 values for PC¹⁴ are compared to values for τ_3 calculated from $\langle v \rangle_n$ with $M_0 = 0.051$ kg/mol, a value selected to give a good fit at T_g . In the glass an equilibrium cluster distribution was assumed, depending only on h . In figure 7.5b experimental data of I_3 for PC¹⁴ are compared to the cluster concentration N_{cl} . The numbers on the ordinate correspond to a proportionality between $I_{3,exp}$ and N_{cl} .

Whereas $\tau_{3,exp}$ and $\tau_{3,calc}$ are in good agreement as seen in figure 7.5a, significant discrepancies between $I_{3,exp}$ and $N_{cl} \propto I_{3,calc}$ are clear from figure 7.5b. In particular, the calculated maximum in I_3 in the melt has not been found experimentally. In addition, below T_g , $I_{3,exp}$ decreases rapidly with decreasing temperature, whereas N_{cl} remains almost constant. If instead of the number average $\langle v \rangle_n$ the volume average $\langle v \rangle_v$ is used to calculate τ_3 and N_{cl} (with eqs. 7.4 and 7.15) similar agreement between calculations and experiment is found as shown in figure 7.6. The choice for $\langle v \rangle_v$ instead of

$\langle v \rangle_n$ in calculations does not seem to be justified by comparison of figures 7.5 and 7.6. Therefore $\langle v \rangle_n$ will be used in further calculations.

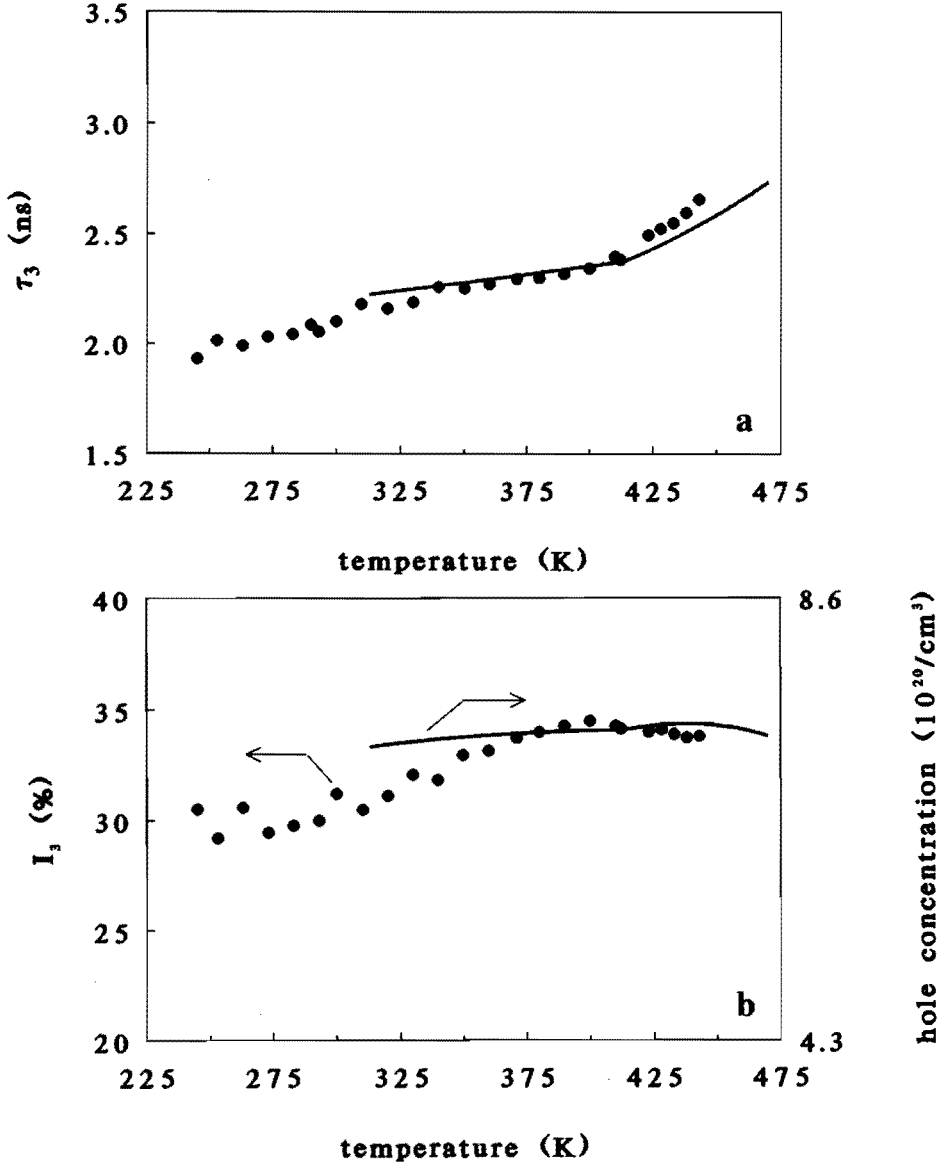


Figure 7.5. *o*-Positronium lifetime (a) and intensity (b) for polycarbonate¹⁴ (●) versus temperature, compared with *o*-PS lifetime and hole concentration calculated using the number average hole size $\langle v \rangle_n$ (solid line).

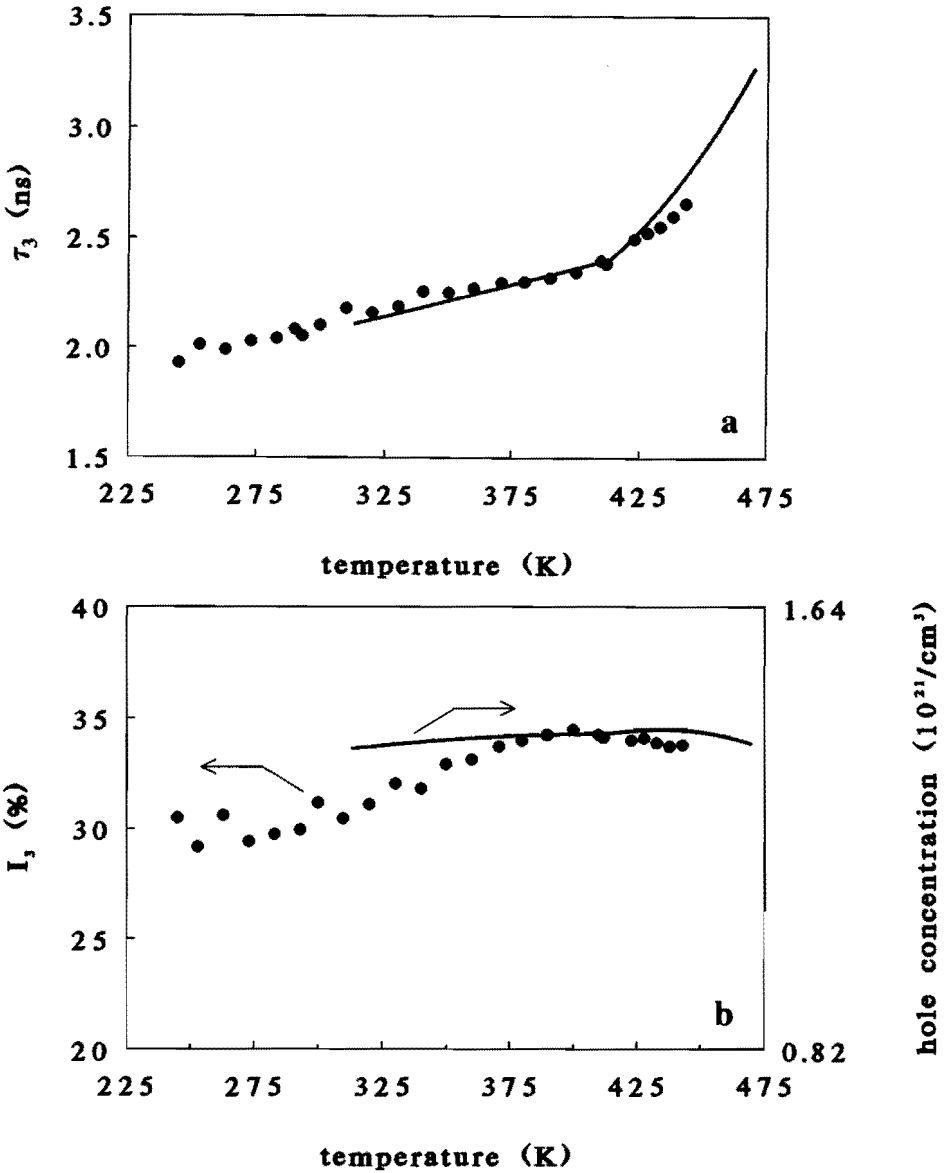


Figure 7.6. *o*-Positronium lifetime (a) and intensity (b) for polycarbonate¹⁴ (●) versus temperature, compared with *o*-Ps lifetime and hole concentration calculated using the volume average hole size $\langle v \rangle_v$ (solid line).

Let us now use the method pointed out in paragraph 7.5, which takes into account the properties of the experimental fitting procedure. In figure 7.7a the experimental and calculated τ_3 are compared for PC, using $M_0=0.0425$ kg/mol to scale the calculation to experimental values at T_g .

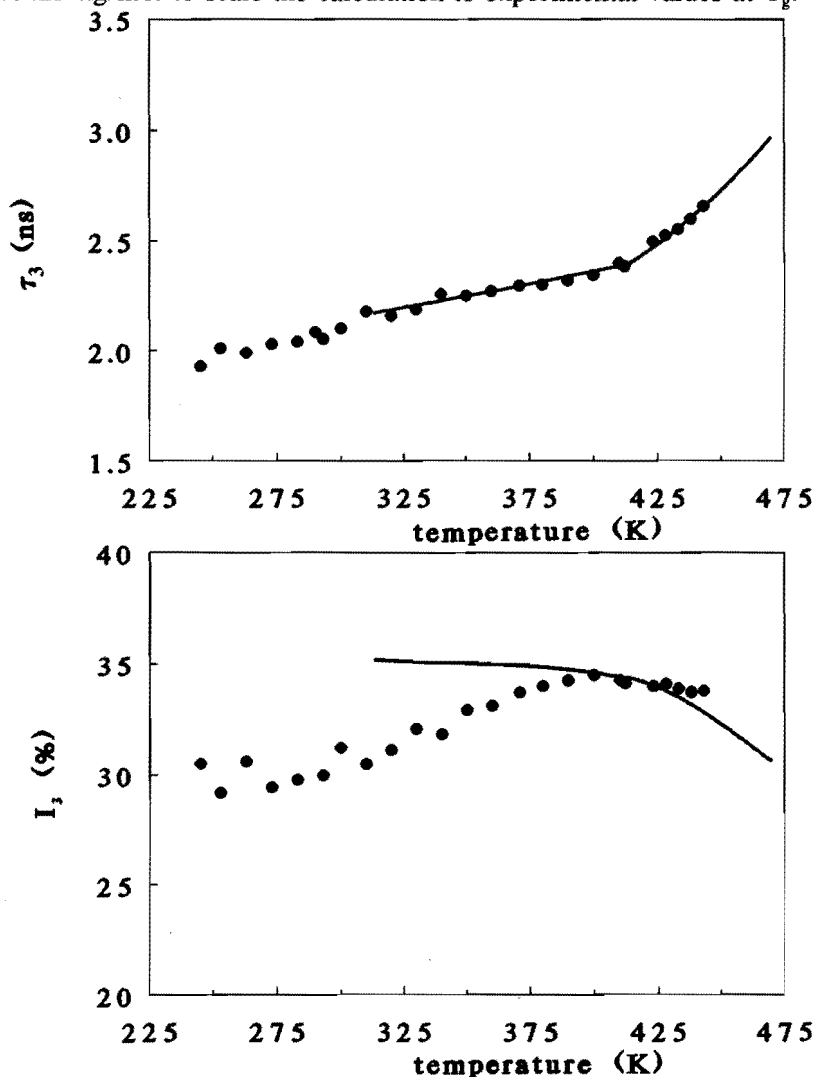


Figure 7.7. *o*-Positronium lifetime (a) and intensity (b) for polycarbonate¹⁴ (●) versus temperature, compared with *o*-Ps lifetime and intensity calculated following the procedure illustrated in figure 7.4 (solid line).

Improved agreement between theory and experiment is observed. In figure 7.7b the experimental and calculated I_3 are compared. A proportionality factor is involved between the calculated and experimental I_3 values, which is determined by scaling $I_{3,\text{calc}}$ to $I_{3,\text{exp}}$ at T_g . In the melt both experiment and calculation indicate a decrease of I_3 with increasing temperature. Below T_g however, $I_{3,\text{calc}}$ is almost temperature independent whereas $I_{3,\text{exp}}$ decreases by about 10% over a temperature range of 100K.

Similar computations to those presented for PC have been applied to polystyrene and poly(vinyl acetate), with comparable results. Moreover, the access to a wider temperature range in the melt for these polymers further supports the kind of agreement between theory and experiment as shown in figures 7.8 and 7.9. The characteristic parameters used in the calculation of h are listed in table 7.2.

Table 7.2. Characteristic values used to describe equation of state behaviour with the HH-theory in connection with PAS data, and parameters to approximate h as a linear function of temperature.

	PC	PS	PVAC
Temperature range pVT data for melt and glass (K)	303-610	281-469	243-373
Reference pVT data	30	31	32
HH theory			
M_0 (kg/mol)	0.050	0.050	0.03418
ϵ^* (J/mol)	4027.9	3258.3	2467.75
v^* (m ³ /mol)	$4.0339 \cdot 10^{-5}$	$4.7689 \cdot 10^{-5}$	$2.7559 \cdot 10^{-5}$
c_s (-)	0.51226	0.35836	0.37158
Linear approximation of h			
$(dh/dT)_{\text{melt}}$ (K ⁻¹)	$4.88 \cdot 10^{-4}$	$4.50 \cdot 10^{-4}$	$6.12 \cdot 10^{-4}$
$(dh/dT)_{\text{glass}}$ (K ⁻¹)	$1.30 \cdot 10^{-4}$	$1.40 \cdot 10^{-4}$	$1.29 \cdot 10^{-4}$
T_g (K)	416.5	365.7	304.7
$h(T_g)$ (-)	0.0985	0.0625	0.0839
validity range (K)	303-500	281-469	243-373
maximum deviation linear approximation	0.0003	0.0003	0.0003

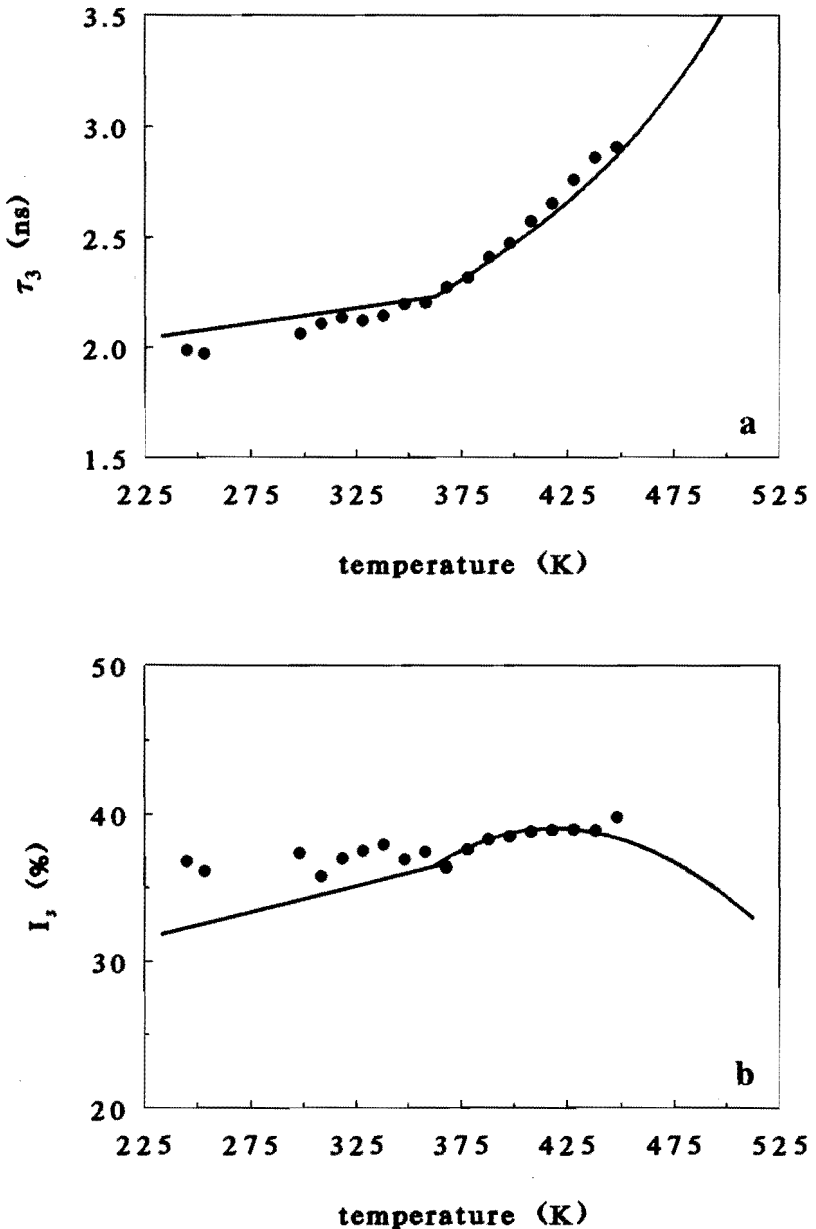


Figure 7.8. *o*-Positronium lifetime (a) and intensity (b) for polystyrene³³ (●) versus temperature, compared with *o*-Ps lifetime and intensity calculated following the procedure illustrated in figure 7.4 (solid line).

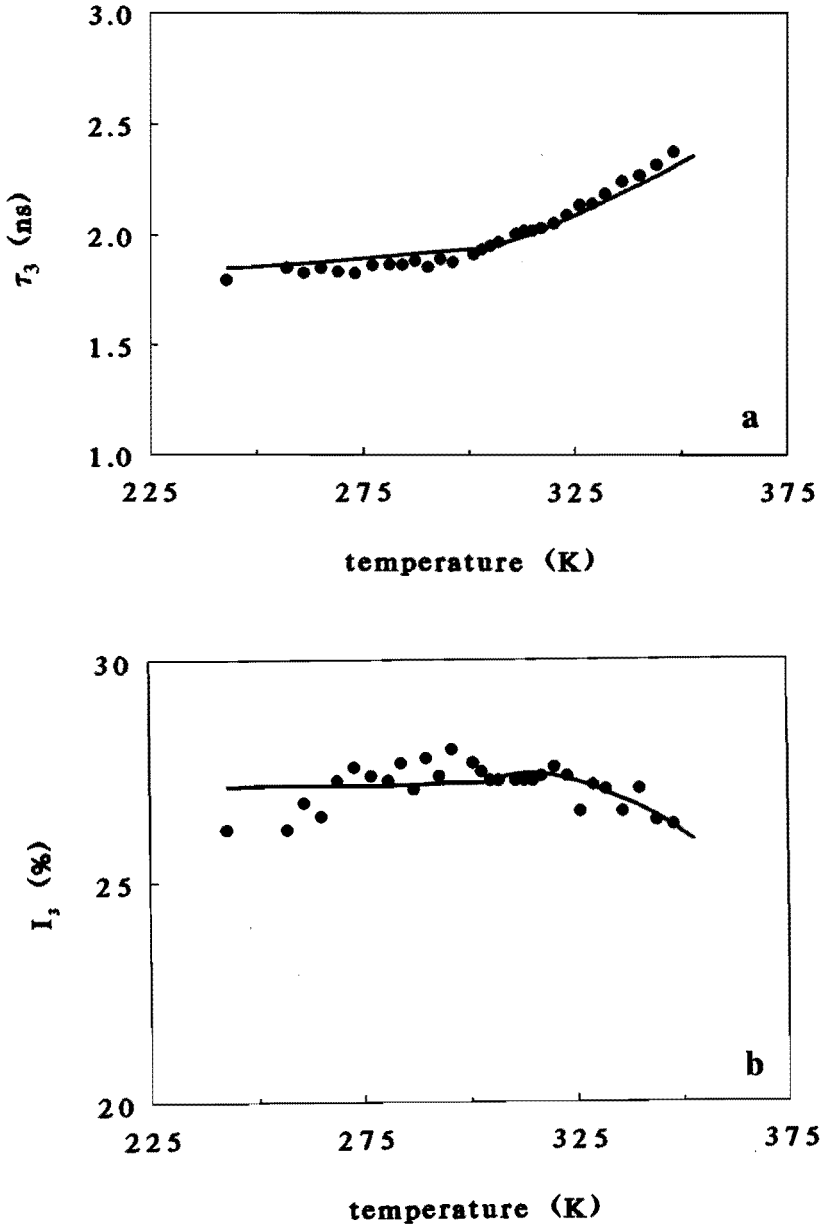


Figure 7.9. *o*-Positronium lifetime (a) and intensity (b) for poly(vinyl acetate)¹³ (●) versus temperature, compared with *o*-Ps lifetime and intensity calculated following the procedure illustrated in figure 7.4 (solid line).

7.7 Conclusions

In this chapter it has been shown that the relationship between $I_{3,\text{exp}}$ and $\tau_{3,\text{exp}}$ on one hand, and cluster concentration and hole size on the other is not straightforward. Taking into account a lifetime distribution and the peculiarities of the numerical procedures used in PAS analysis, it was possible to explore this complex relationship. It was shown that, with the assumption of a hole distribution, PAS results above T_g could be described satisfactorily for several polymers. The distribution was derived by analyzing a randomly filled lattice, with a fraction empty sites equal to the free volume fraction calculated with the HH theory. Below T_g there could be discrepancies: $I_{3,\text{calc}}$ remained essentially constant with temperature, whereas $I_{3,\text{exp}}$ could show a pronounced temperature dependence. Preliminary calculations¹¹ based on formation of non-equilibrium distributions in the glass show that $I_{3,\text{calc}}$ decreases substantially, while τ_3 decreases to a lesser extent, which is consistent with the experimental observations of decreasing $I_{3,\text{exp}}$ with decreasing temperature. For example, if the cluster distribution at a temperature T_1 in the glass is not determined by $y(T_1)$, but by $y(T_2)$ with $T_1 < T_2 < T_g$, then for both τ_3 and I_3 values are calculated which are lower than the values at T_g . This procedure results in a distribution wider than the distribution used for the calculations presented in this chapter.

The calculated deviation in I_3 indicates too large a calculated hole concentration. This might be caused by the use of an equilibrium cluster distribution in the non-equilibrium glass. A distortion of the distribution, which also results from the approach presented in chapters 5 and 6, can improve the similarity between calculations and experiments in the glass.

A comment is in order with regard to the deviation in figure 7.4 between the sum of exponential decays and the fitted single exponential decay at times shorter than 2 ns. This discrepancy corresponds to the part of the o-Ps decay that in the PAS fitting procedure is assigned to species other than o-Ps, i.e. free positrons and p-Ps. The fitted values of $I_{1,\text{exp}}$ and $I_{2,\text{exp}}$ are

therefore larger than the true fraction of positrons that annihilate as p-Ps and as free positrons, respectively. In addition, $\tau_{1,\text{exp}}$ and $\tau_{2,\text{exp}}$ are larger than the true values because part of the relatively long o-Ps lifetimes are interpreted as contributing to τ_1 and τ_2 . In PAS experiments on polymers it is found^{11-14,25,34} that the ratio $I_{1,\text{exp}}/I_{3,\text{exp}}$ is indeed larger than the value 1/3, which is expected on a quantum mechanical basis. Values for $\tau_{1,\text{exp}}$ and $\tau_{2,\text{exp}}$, larger than the expected 125ps and 0.4-0.5ns respectively, have been reported (see ref. 11,13-15,25). All these observations support the relevance and validity of the fitting procedure presented in this chapter and the presence of a o-Ps lifetime distribution.

Clearly the procedure presented in this chapter, which fits a distribution of τ_3 to a single value for τ_3 separately from the fitting of τ_1 and τ_2 , is only an approximation. A logical next step in the study of the influence of a hole size distribution on PAS results is the generation of spectra with calculated distributions, including assumptions for τ_1 and τ_2 , noise, a source term and a time resolution function, and the subsequent analysis of these spectra by the conventional PAS spectral analysis software²⁹. The results of this approach will be presented separately³⁵.

With regard to the distribution of holes the work reported by Rigby and Roe³⁶ has to be mentioned. In a molecular dynamics study the distribution of unoccupied space is analyzed using Voronoi tessellation. Comparing their distribution of holes with the completely differently obtained distribution from this chapter, remarkable agreement is found. Rigby and Roe find that in the melt the distribution shifts to higher volumes and also becomes broader. The closer to T_g , the more asymmetrical the distribution gets. And in principle, choosing the right value for the exclusion diameter, they can describe systems in which the number of holes exhibits a maximum with increasing temperature, and one in which also the difference between number and volume fraction distribution can become very large. This latter resembles percolation of a few very large holes. All these features can also be found in the distribution based on random filling of a lattice.

Qualitative agreement is obtained with hole size distributions based on the diffusion of low molar mass species³⁷. A comparison with the directly from PAS determined hole distribution²⁵ also shows similarities in the general temperature behaviour of the distribution. All these facts suggest that the hole distribution derived in this work on the basis of a lattice, may be of a more general nature. Thus the results of positron annihilation simulations presented in this chapter are probably at least partly independent of the choice of the particular model used to obtain a hole size distribution.

7.8 References

1. *Positrons in Solids*, P. Hautojarvi, ed., Springer, Berlin, 1979.
2. *Positron Solid-State Physics*, W. Brandt and A. Dupasquier, ed., North-Holland, Amsterdam, 1983.
3. S. J. Wang and Y. C. Jean in *Positron and Positronium Chemistry*, D. M. Schrader and Y. C. Jean, ed., Elsevier, Amsterdam, 1988, p. 255.
4. D. M. Schrader and Y. C. Jean in *Positron and Positronium Chemistry*, D. M. Schrader and Y. C. Jean, ed., Elsevier, Amsterdam, 1988, p. 19.
5. A. E. Ruark, *Phys. Rev.*, **68**, 278 (1945).
6. W. Brandt and N. Arista, *Phys. Rev. B.*, **26**, 4229 (1982).
7. R. M. Singru, K. B. Lal and S. J. Tao, *At. Data Nucl. Data Tables*, **17**, 271 (1976).
8. O. E. Mogensen, *J. Chem. Phys.*, **60**, 998 (1974).
9. L. J. Bartal and H. J. Ache, *Radiochim. Acta*, **19**, 49 (1973).
10. Y. Ito in *Positron and Positronium Chemistry*, D. M. Schrader and Y. C. Jean, ed., Elsevier, Amsterdam, 1988.
11. S. Vleeshouwers, *unpublished* (1991).
12. Y. C. Jean, T. C. Sandreczki and D.P. Ames, *J. Polym. Sci., Polym. Phys. Ed.*, **24**, 1247 (1986).

13. Y. Kobayashi, W. Zheng, E. F. Meyer, J. D. McGervey, A. M. Jamieson and R. Simha, *Macromolecules*, **22**, 2302 (1989).
14. J.-E. Kluin, Z. Yu, S. Vleeshouwers, J. D. McGervey, A. M. Jamieson and R. Simha, *Macromolecules*, **25**, 5089 (1992).
15. A. D. Kasbekar, P. L. Jones and A. Crowson in *Positron Annihilation*, proceedings of 8th International Conference on Positron Annihilation, Gent, 1988, L. Dorikens-Vanpraet, M. Dorikens and D. Segers, ed., World Scientific, Singapore, 1988, p. 799.
16. W. Brandt, S. Berko and W. W. Walker, *Phys. Rev.*, **120**, 1289 (1960).
Erratum, *ibid*, **121**, 1864 (1961).
17. H. Nakanishi and Y. C. Jean, in *Positron and Positronium Chemistry*, D. M. Schrader and Y. C. Jean, ed., Elsevier, Amsterdam, 1988, p. 159.
18. R. A. Ferrel, *Phys. Rev.*, **108**, 167 (1957).
19. Y. Ujihira, T. Ryno, Y. Kobayashi and T. Nomizo, *Appl. Phys.*, **16**, 71 (1978).
20. H. Nakanishi and Y. Ujihira, *J. Phys. Chem.*, **86**, 4446 (1982).
21. M. Eldrup, D. Lightbody and J. N. Sherwood, *Chem. Phys.*, **63**, 51 (1981).
22. S. J. Tao, *J. Chem. Phys.*, **56**, 5499 (1972).
23. K. Venkateswaran, K. L. Cheng and Y. C. Jean, *J. Phys. Chem.*, **88**, 2465 (1984).
24. J. D. Ferry, *Viscoelastic Properties of Polymers*, Wiley & Sons, New York, 1980.
25. Q. Deng, F. Zandiehnam and Y. C. Jean, *Macromolecules*, **25**, 1090 (1992).
26. E. Nies and A. Stroeks, *Macromolecules*, **23**, 4088 (1990).
27. D. Stauffer, *Introduction to Percolation Theory*, Taylor & Francis, London, 1985.

28. R. Zallen, *The Physics of Amorphous Solids*, Wiley & Sons, New York, 1983.
29. P. Kirkegaard, N. J. Pedersen and M. Eldrup, *PATFIT-88*, Risø National Laboratory, Denmark, 1989.
30. P. Zoller, *J. Polym. Sci., Polym. Phys. Ed.*, **20**, 1453 (1982).
31. A. Quach and R. Simha, *J. Appl. Phys.*, **42**, 4592 (1971).
32. J. E. McKinney and M. Goldstein, *J. Res. Nat. Bur. Stand.-A. Phys. Chem.*, **78A**, 331 (1974).
33. J.-E. Kluin, *unpublished* (1992).
34. H. Nakanishi, Y. Y. Wang, Y. C. Jean, T. C. Sandreczki and D. F. Ames, in *Positron Annihilation*, proceedings of 8th International Conference on Positron Annihilation, Gent, 1988, L. Dorikens-Vanpraet, M. Dorikens and D. Segers (ed), World Scientific, Singapore, 1988, p. 781.
35. J.-E. Kluin, Z. Yu, S. Vleeshouwers, J. D. McGervey, A. M. Jamieson and R. Simha, *submitted* (1992).
36. D. Rigby and R. J. Roe, *Macromolecules*, **23**, 5312 (1990).
37. L. G. F. Stuk, *J. Polym. Sci., Polym. Phys. Ed.*, **27**, 2561 (1989).

Chapter 8

Outstanding problems

In chapter 4 an empirical relation to describe the mobility of polymer melts was presented. This expression excellently describes both temperature and pressure dependence of e.g. viscosity (figures 4.2b and 4.4b). However, the temperature and pressure dependence for low molar mass liquids was shown to be different (figure 4.5). It has to be further investigated how the description of viscosity for both polymers and low molar mass liquids can be combined. Also for the description of more complicated systems (e.g. polymer blends) a good understanding of the viscosity and its dependence on for example temperature and local structure is necessary.

The explicit appearance of temperature in the expression for polymer viscosity causes a complete freeze in of the free volume at low temperatures in simulations of polymer glasses. This is in contrast with experimental data of e.g. physical aging of polystyrene at room temperature. To obtain optimal agreement with experimental data on e.g. the dimension (stability) of a polymer glass the expression can therefore not be used. Possibly relaxation mechanisms other than the combined relaxation of several chain segments, which is related to the glass transition, have to be taken into account. In the presented theory the relaxation mechanism which is important just above T_g is extrapolated to low temperatures. At these temperatures the relaxation of small chain parts or side groups attached to the polymer backbone might contribute significantly to the overall relaxation of the polymer.

The complete freeze in of the order parameter h in simulated polymer glasses reduces the thermal expansion to volume changes in the lattice cell. The

thermal expansion of the cell are determined by the averaging of the free volume over a gas and solid like component (chapter 2). A further contribution to the expansion of the glass could be given by the above indicated, but so far neglected relaxations of small parts of molecules.

Experimentally it is found that aging rates can differ significantly for different properties (e.g. volume, enthalpy and density fluctuations), whereas in the calculations they are fully correlated (paragraph 4.4). It must be further pursued whether the stochastic theory is capable of describing different aging rates for different properties, resulting from distinguishable contributions of parts of the free volume distribution to the different properties.

A logical extension of the presented theory (chapter 5) is the possible evaluation of the glass transition and physical aging of polymer blends. This brings up the issue of the influence of stresses on the free volume and the induced anisotropy of the cell. If immiscible blend systems are treated by the presented theory, possible stresses resulting from adhesion at interfaces have to be taken into account. Relaxation processes in the glass have to include relaxation of the anisotropy of the cell. In case of (partly) miscible blends the use of free volume fluctuations (a one dimensional distribution) has to be extended to include also concentration fluctuations (a two dimensional distribution). A start has been made along this line. Like in the one component case a canonical ensemble (N, V, T constant) was chosen. The advantage of choosing the number of particles of both types (N_1 and N_2) as variables that define a state, is that a transition to an adjacent state is related to changes in only one component, which enables definition of transition rates. However, the overall mass balance is not automatically fulfilled. Due to considerable correlations between N_1 and N_2 an inefficient use of the matrix was made, resulting in numerical problems. It is well worth to evaluate the distribution using other variables than N_1 and N_2 , more so to obey the overall mass balance. An assumption has to be made which parameters determine the

mobility of the components. The question arises if except the structure (h) and the temperature (T) also the composition of the surroundings of a segment is a determining factor. This of course brings up the question of determining these relations independently.

In the analysis of cluster distributions (chapter 7) connectivity of polymer segments and interaction between segments was not taken into account. Only the first moment of the theoretical free volume distribution (i.e. the average) was used. Neglecting connectivity and interactions will tend to scatter the segments over the lattice, thus also scattering the empty sites. Lattice simulations of polymer chains have been performed by dr. P. Cifra. Analysis of these results in terms of hole cluster distribution is presently being pursued. Preliminary results yield the expected trends, compared to the random cluster results. Further lattice simulations can possibly indicate a relation between the free volume distribution and a hole cluster size distribution. This can clarify if e.g. the presence of large hole clusters is related to a high local free volume.

Summary

Long term stability of dimensional and mechanical properties is important for applications of polymers. Often properties determined by conditions prevailing during the melt processing and product formation will be conserved in the final product which, commonly, is in the glassy state. The properties of the final product are not in equilibrium, and can thus change in time (this relaxation is often called physical aging). Knowledge of the relation between formation conditions and product properties, and also of physical aging processes, is therefore important. In this work the glassy polymer state is described starting from the melt situation. In the equilibrium melt, a free volume distribution (i.e. average and width) is assumed, which depends on pressure and temperature. In the glass this distribution is also determined by the formation process. It is assumed that due to the gradual freeze in during the formation of the glass the equilibrium distribution is partly arrested. Relaxation processes in the glass are interpreted as a relaxation of the non equilibrium free volume distribution towards the equilibrium situation. The rate of relaxation of the various parts of the distribution is determined by the local free volume.

To model the free volume the Holey-Huggins (HH) hole theory is used for description of the equilibrium equation of state behaviour of the polymer. The HH-theory is based on a lattice which allows for empty lattice sites and for variations in the cell size. The central quantity is the disorder parameter h , equal to the fraction empty lattice sites, which depends solely on pressure and temperature. Defining the free volume as being equal to the disorder parameter h , the free volume has been defined quantitatively and unambigu-

ously. The fluctuations in free volume are evaluated using fluctuation theory. The HH theory allows for evaluation of e.g. enthalpy and volume from the free volume.

In contrast to the melt, the free volume distribution in a polymer glass does not only depend on pressure and temperature. To evaluate the free volume distribution in the glass a stochastic transition theory is developed. The mobility in parts of the free volume distribution is related to the local free volume content. Thus, effectively a mobility distribution is obtained. A relational dependence of mobility on free volume is assumed. During formation of the glass (e.g. by cooling) mobility will become increasingly hampered and gradually the free volume distribution will become arrested, starting at the low free volume side (i.e. the low mobility side). In this way, the influence of formation conditions, such as pressure and cooling rate, on the free volume distribution in the glass is automatically incorporated.

Parameters needed in the theory are mainly based on equilibrium properties and are determined independently. One set is formed by the three scaling parameters in the HH theory. This set describes the equation of state behaviour of the polymer melt. Another set describes the equilibrium mobility versus free volume. For this description a Fulcher-Tammann-Hesse (FTH) type expression is used. Pressure dependence of mobility data seems to suggest the use of a more complex relation for mobility. An empirical modification of the FTH-expression is presented to describe this pressure dependence. Taking into account this pressure dependency in the stochastic theory, a good prediction of the pressure dependence in several applications is obtained. Mobility data are extracted from various experimental data such as viscosity, creep and dielectric relaxation. In general, so called shift factors can be used, because only the relative mobility has to be considered. To fix the mobility scale to an absolute value, a single adjustable parameter is used. This has to be extracted from non-equilibrium data (e.g. a relaxation

experiment). In good approximation, however, it probably can be given a universal value.

Successful predictions for different polymer glasses have been achieved. First of all, a glass transition is predicted for amorphous polymers. Also the location of the glass transition and its dependence on pressure and cooling rate are predicted well. Furthermore volumetric properties of the glass, such as the thermal expansion, the compressibility and relaxation effects are predicted. Predictions are not restricted to volumetric data, but have also been extended to enthalpy, entropy and density fluctuations.

From the basis of the stochastic theory it is clear that the free volume distribution plays an important role. The simulation of the polymer on a lattice, including the presence of empty lattice sites, will result in a quasi-random clustering of empty sites and therefore also in the presence of a cluster size distribution. To gain experimental support for this view, positron annihilation spectroscopy (PAS) is used. The two interesting quantities in this technique are the o-positronium lifetime and intensity, which are linked to the size and concentration of spots with low electron density, respectively. These spots can be compared to the hole clusters on the lattice. An explanation of the o-positronium lifetime and intensity data is presented, with the assumption of a randomly filled lattice and a correspondence between a spot of low electron density and empty lattice sites. In the melt the hole size distribution obtained from the lattice simulations is in close agreement with PAS data. In the glass deviations between theory and experiment can be related to the presence of a non equilibrium distribution. As pointed out before, this change in shape of the distribution finds its origin in the gradual freeze in of the polymer structure, which is comparable to the consequences of the mobility distribution in the stochastic theory.

Samenvatting

Lange termijn stabiliteit van dimensies en van mechanische eigenschappen is belangrijk voor toepassingen van polymeren. Vaak zijn in de eigenschappen van het eindprodukt, dat zich gewoonlijk in de glastoestand bevindt, de condities tijdens de verwerking van de smelt en de vorming van het produkt terug te vinden. De eigenschappen van het eindprodukt zijn niet in evenwicht en kunnen daarom veranderen in de tijd (deze relaxatie wordt vaak fysische veroudering genoemd). Kennis van de relatie tussen enerzijds vormingsgeschiedenis en anderzijds de eigenschappen van het produkt en fysische veroudering is daarom belangrijk. In dit werk wordt de glastoestand van het polymeer beschreven vanuit de smeltsituatie. In de evenwichtssmelt wordt er een vrij volume verdeling aangenomen (d.w.z. gemiddelde en breedte), die afhangt van druk en temperatuur. In het glas wordt de verdeling ook bepaald door het vormingsproces. Er wordt aangenomen dat door de geleidelijke verstarring tijdens de vorming van het glas de evenwichtsverdeling geleidelijk invriest. Relaxatieprocessen worden geïnterpreteerd als een relaxatie van de niet-evenwichts vrij-volume-verdeling naar de evenwichts-situatie. De snelheid van relaxatie wordt bepaald door het lokale vrij volume.

Om het vrij volume te modelleren is de Holey-Huggins (HH) celvloeistof theorie gebruikt voor de beschrijving van de evenwichtstoestandsvergelijking van het polymeer. De HH theorie is gebaseerd op een rooster met een fractie lege roosterplaatsen, waarin ook variaties in de grootte van een cel mogelijk zijn. De centrale grootte is de structuurparameter h , gelijk aan de fractie lege roosterplaatsen, die alleen afhangt van temperatuur en druk. Door het vrij volume gelijk te stellen aan de structuurparameter h is het vrij volume

kwantitatief en eenduidig gedefinieerd. De fluctuaties in vrij volume worden geëvalueerd met behulp van fluctuatietheorieën. De HH theorie maakt evaluatie mogelijk van bijvoorbeeld enthalpie en volume uit het vrij volume.

In tegenstelling tot de smelt hangt het vrij volume in een glas niet alleen af van druk en temperatuur. Om het vrij volume in een glas te evalueren is een stochastische transitietheorie ontwikkeld. De mobiliteit in delen van de vrij-volume-verdeling is gerelateerd aan het lokale vrij volume. Zo is er in feite een mobiliteitsverdeling verkregen. Een expliciete afhankelijkheid van de mobiliteit van het vrij volume wordt aangenomen. Tijdens vorming van het glas (door bijvoorbeeld afkoelen) zal de mobiliteit steeds verder afnemen en zal de vrij-volume-distributie geleidelijk verstarren, het eerst aan de lage vrij-volume kant (waar de laagste mobiliteit heerst). Zo wordt de invloed van de vormingsomstandigheden, zoals druk en koelsnelheid, op de vrij-volume-verdeling in het glas automatisch meegenomen.

De parameters in de theorie zijn voornamelijk gebaseerd op evenwichtseigenschappen en kunnen door onafhankelijke metingen bepaald worden. Een deel wordt gevormd door de drie schalingsparameters in de HH theorie. Deze set beschrijft de toestandsvergelijking van het polymeer in de smelt. Een ander deel beschrijft de evenwichtsmobiliteit als functie van vrij volume. Hiervoor wordt een Fulcher-Tammann-Hesse (FTH) uitdrukking gebruikt. Drukafhankelijkheid van mobiliteitsgegevens lijkt een complexere relatie te suggereren. Een empirische modificatie van de FTH vergelijking wordt gepresenteerd om deze drukafhankelijkheid te beschrijven. Als deze drukafhankelijkheid meegenomen wordt in de stochastische theorie, wordt ook een goede voorspelling van de drukafhankelijkheid in verschillende toepassingen bereikt. Mobiliteitsgegevens worden bepaald uit verschillende experimentele data, zoals viscositeit, kruip en dielectrische relaxatie. Algemeen gesproken kunnen zogenaamde verschuivings- (shift-) factoren gebruikt worden omdat slechts de relatieve mobiliteit van belang is. Om de mobiliteitsschaal vast te leggen, wordt een enkele aanpasbare parameter gebruikt. Deze moet bepaald worden

uit niet-evenwichts gegevens (b. v. een relaxatie-experiment). Mogelijk kan aan deze parameter in goede benadering een universele waarde toegekend worden.

Succesvolle beschrijving voor verschillende polymeerglazen is bereikt. Ten eerste wordt er een glasovergang voorspeld voor amorfe polymeren. Ook de plaats van de glasovergang en de afhankelijkheid van druk en koelsnelheid worden goed voorspeld. Verder worden volumetrische eigenschappen en relaxatieverschijnselen voorspeld. Voorspellingen zijn echter niet beperkt tot volumetrische eigenschappen, maar zijn ook uitgebreid tot enthalpie, entropie en dichtheidsfluctuaties.

Vanuit de uitgangspunten van de stochastische theorie is het duidelijk dat de vrij-volume-verdeling een belangrijke rol speelt. De simulatie van een polymeer op een rooster, met de aanwezigheid van lege roosterplaatsen, zal resulteren in een quasi-willekeurige clustering van lege plaatsen en daarom ook in de aanwezigheid van een clustergrootte-verdeling. Om experimentele ondersteuning van dit gezichtspunt te krijgen wordt positron-annihilatiespectroscopie (PAS) gebruikt. De twee interessante grootheden in deze techniek zijn de o-positronium-levensduur en -intensiteit, gerelateerd aan respectievelijk de grootte en concentratie van gebieden met lage elektronendichtheid. Deze gebieden kunnen vergeleken worden met de clusters van gaten op het rooster. Een analyse van de o-positronium-levensduur en -intensiteit wordt gepresenteerd, met als aannames een willekeurig gevuld rooster en de overeenkomst tussen gebieden met lage elektronendichtheid en clusters van lege roosterplaatsen. In de smelt komt de gatgrootte verdeling verkregen met de roostersimulaties goed overeen met PAS-metingen. Afwijkingen in het glas tussen theorie en experiment kunnen gerelateerd worden aan de aanwezigheid van een niet-evenwichts-verdeling. Zoals al eerder uitgelegd wordt deze verandering van de vorm van de verdeling veroorzaakt door de geleidelijke verstarring van de polymeerstructuur. Dit is vergelijkbaar met de gevolgen van een mobiliteitsverdeling in de stochastische theorie.

Nawoord

In de eerste plaats wil ik Erik Nies bedanken voor zijn uitstekende, vriendelijke en motiverende begeleiding.

Verder hebben ook alle andere personen die ooit een kamer met mij hebben gedeeld ertoe bijgedragen dat ik met plezier aan dit onderzoek gewerkt heb.

I want to thank prof. R. Simha for all our (as extensive as necessary or possible) discussions. It was always a pleasure to be offered a chair in his room, or to offer him a chair in my room.

I also want to thank all other people in Cleveland who made the positron annihilation experiments possible.

Tenslotte is de belangstelling en aanmoediging van collega's, vrienden en familie belangrijk voor mij geweest. Ik wil met name mijn broers en zus noemen die altijd hebben meegeleefd met mijn werk, en vooral ook mijn ouders voor al hun steun en hun interesse in mijn studie en promotie.

Curriculum Vitae

De auteur van dit proefschrift werd op 22 mei 1962 geboren te Schaesberg. Hij doorliep van 1974 tot 1980 het gymnasium β aan het Coriovallum College te Heerlen. Hierop aansluitend, in september 1980, begon hij met de studie Scheikundige Technologie aan de Technische Universiteit Eindhoven. Zijn propaedeutisch examen behaalde hij in juni 1981, zijn kandidaatsexamen in november 1984. Als 'research scholar' was de auteur van november 1986 tot april 1987 werkzaam op het Department of Macromolecular Science van de Case Western Reserve University, Cleveland, Ohio (USA). Na het afronden van de eerstegraads-lerarenopleiding in het vak scheikunde, begon hij in december 1987 aan een afstudeerproject binnen de vakgroep der kunststof-technologie, uitmondend in het behalen van het ingenieursdiploma in augustus 1988. In december 1988 begon de auteur aan zijn promotieonderzoek binnen dezelfde vakgroep, onder leiding van dr. E. Nies. Het promotieonderzoek werd gesponsord door de Stichting Polymer Blends. Een deel van het promotieonderzoek werd uitgevoerd in het Physics Department, Case Western Reserve University.

Stellingen

bij het proefschrift van Servaas Vleeshouwers

1. De schijnbare afwezigheid van veroudering van dichtheidsfluctuaties bij lage temperaturen in bijvoorbeeld polystyreen is een gevolg van de definitie van deze fluctuaties. Als in plaats van $I(0)$, de verstrooiing in doorgaande richting, $\overline{(N-\bar{N})^2}/\bar{N} = \psi(\infty)$ wordt beschouwd, kan men concluderen dat bij lage temperatuur dichtheidsfluctuaties en volume dezelfde veroudering vertonen.
R.-J. Roe and J. J. Curro, Macromolecules, 16, 428 (1983); J. J. Curro and R.-J. Roe, J. Polym. Sci.: Polym. Phys., 21, 1785 (1983); Polymer, 25, 1424 (1984).
2. De conclusie van Cowie en Ferguson dat in een poly(vinyl methyl ether) (PVME)-polystyreen (PS) blend de veroudering gedomineerd wordt door PVME maar PS de kinetiek bepaalt, valt niet af te leiden uit hun experimentele resultaten.
J. M. G. Cowie en R. Ferguson, Macromolecules, 22, 2312 (1989).
3. Roe en Millman's conclusie dat de endotherme piek in een DSC experiment het gevolg is van 'enhanced mobility' ten gevolge van veroudering is niet te verdedigen.
R.-J. Roe en G. M. Millman, Polym. Eng. Sci., 23, 318 (1983).
4. Bij de gelijkstelling door McKenna en medewerkers van de tijd t^* waarbij de shiftfactor een andere tijdsafhankelijkheid gaat vertonen met de tijd benodigd om mechanisch evenwicht te bereiken, moeten vraagtekens worden gezet.
A. Lee en G. B. McKenna, Polymer, 29, 1812 (1988); Polym. Eng. Sci., 30, 431 (1990); M. M. Santore, R. S. Duran en G. B. McKenna, Polymer, 32, 2377 (1991).
5. De gelijkstelling van vrij volume met $(V-V_\infty)/V_\infty$ leidt tot verkeerde conclusies en een onterechte afwijzing van het vrij volume concept.
H. H. D. Lee en F. J. McGarry, J. Macromol. Sci.-Phys., B29, 237 (1990).

6. Het gebruik van polynomen voor het beschrijven van experimentele gegevens kan aanleiding geven tot artefacten als ze gebruikt worden om afgeleiden te bepalen.
J. E. McKinney en M. Goldstein, J. Res. Nat. Bur. Stand., 78A, 331 (1974).
7. Het verschil in volumetrische eigenschappen dat Lee en McGarry vinden tussen twee verschillende polystyreen monsters is te groot om volledig verklaard te worden door het verschil in molmassa.
H. H. D. Lee en F. J. McGarry, J. Macromol. Sci.-Phys., B29, 185 (1990).
8. De opsplitsing van de invloed van temperatuur op relaxatie tijden in een thermisch geactiveerd deel en een deel dat afhangt van de structuur kan vastgesteld worden door bestudering van de drukafhankelijkheid.
Dit proefschrift, hoofdstukken 3 en 4.
9. Het is curieus om te refereren naar een niet bestaand boek, waarnaar al eerder gerefereerd is.
W. H. Stockmayer, R. Koningsveld en E. Nies, in 'Equilibrium Thermodynamics of Polymer Systems, vol 1: Polymer Phase Diagrams', Oxford Univ., 1988.
10. Het onder druk zetten van mensen kan het beoogde resultaat opleveren. Bij polymeren is dit niet te verwachten.
Dit proefschrift, hoofdstuk 4.
11. Volgens de Alliant computer is (1.or.2) gelijk aan 3.
12. Omdat verslaggevers en presentatoren zo vaak over zichzelf praten verdient het aanbeveling om hen behalve op welbespraaktheid te selecteren op hun avontuurlijkheid en persoonlijkheid.
13. Het handen wassen met warm water zal iemand niet snel laten wennen aan koud weer, zodat nog bij temperaturen ver boven het vriespunt handschoenen gedragen moeten worden.